MASTER THESIS

ENERGY TECHNOLOGIES FOR SUSTAINABLE DEVELOPMENT

COMPARATIVE ANALYSIS OF MODERN ENERGY SYSTEMS FOR ICE RINKS

AUTHOR: **PENDAR HEMATI**

TUTOR: CARLA ISABEL MONTAGUD-MONTALVÁ

EXTERNAL TUTOR: SAMER SAWALHA

EXTERNAL TUTOR: JÖRGEN ROGSTAM

Academic Year: 2022-23

September 2023

ABSTRACT

Ice rinks are highly energy-intensive commercial buildings with an average annual energy consumption of 1,000 MWh, most of it being used to cover the simultaneous heating and cooling demands. The aim of this thesis is to find the most energy efficient energy system for ice rinks by evaluating different system modifications and refrigerants. A comparative analysis of ammonia, CO_2 and propane energy systems based on a representative ice rink for northern climates has been conducted.

A traditional integrated ammonia ice rink consumes about 340 MWh per year to cover the thermal demands. The most promising energy efficiency measures for ammonia are using aqua ammonia as the secondary fluid and using an auxiliary heat pump to aid with covering heating demands. Thanks to these measures, energy savings of 12.9% can be achieved.

A state-of-the-art trans-critical CO_2 system using parallel compression consumes approximately 42.6% less energy than a conventional ammonia system, making it the most energy efficient solution for ice rinks with an SPF of 7.5. The good performance is largely linked to the possibility of operating CO_2 systems as direct systems, eliminating the need for indirect heat transfer and minimizing auxiliary equipment energy consumption.

Propane, which has not been investigated as a refrigerant in ice rinks yet, was evaluated and compared against ammonia and CO_2. A modern integrated propane system using parallel compression and an auxiliary heat pump is more energy efficient than a traditional ammonia system but requires more energy than modern ammonia or CO_2 systems. Propane proved to be feasible and represents a potential alternative solution in ice rinks.

Waste heat recovery is beneficial in every system and should be a key feature in ice rink energy systems. All systems use environmentally friendly refrigerants and their environmental impact is almost exclusively indirect and caused by electricity consumption.

Keywords: Ice rinks, refrigeration, heat recovery, CO2, ammonia, propane

RESUMEN

Las pistas de hielo son edificios comerciales que consumen mucha energía, con un consumo medio anual de 1,000 MWh, la mayor parte de la cual se utiliza para cubrir las demandas simultáneas de calefacción y refrigeración. El objetivo de esta tesis es encontrar el sistema energético más eficiente para las pistas de hielo evaluando diferentes modificaciones del sistema y refrigerantes. Se ha realizado un análisis comparativo de los sistemas energéticos de amoníaco, CO_2 y propano basado en una pista de hielo representativa de los climas nórdicos.

Una pista de hielo de amoníaco integrada tradicional consume unos 340 MWh al año para cubrir las demandas térmicas. Las medidas de eficiencia energética más prometedoras para el amoníaco son el uso de aqua amoníaco como fluido secundario y la utilización de una bomba de calor auxiliar para ayudar a cubrir las demandas de calefacción. Gracias a estas medidas, se puede conseguir un ahorro energético del 12.9%.

Un sistema de CO_2 transcrítico de última generación que utiliza compresión paralela consume aproximadamente un 42.6% menos de energía que un sistema de amoníaco convencional, lo que lo convierte en la solución más eficiente desde el punto de vista energético para pistas de hielo con un SPF de 7.5. El buen rendimiento está ligado en gran medida a la posibilidad de operar los sistemas de CO_2 como sistemas directos, eliminando la necesidad de transferencia indirecta de calor y minimizando el consumo de energía de los equipos auxiliares.

El propano, que aún no se ha investigado como refrigerante en pistas de hielo, se evaluó y comparó con el amoníaco y el CO_2. Un sistema moderno integrado de propano que utiliza compresión paralela y una bomba de calor auxiliar es más eficiente energéticamente que un sistema tradicional de amoníaco, pero requiere más energía que los sistemas modernos de amoníaco o CO_2. El propano demostró ser viable y representa una posible solución alternativa en las pistas de hielo.

La recuperación del calor residual es beneficiosa en todos los sistemas y debería ser una característica clave en los sistemas energéticos de las pistas de hielo. Todos los sistemas utilizan refrigerantes respetuosos con el medio ambiente y su impacto ambiental es casi exclusivamente indirecto y causado por el consumo de electricidad.

Palabras Clave: Pistas de hielo, refrigeración, recuperación de calor, CO2, amoníaco, propano

RESUM

Les pistes de gel són edificis comercials que consumeixen molta energia, amb un consum mig anual de 1,000 MWh, la major part de la qual s'utilitza per a cobrir les demandes simultànies de calefacció i refrigeració. L'objectiu d'aquesta tesi és trobar el sistema energètic més eficient per a les pistes de gel avaluant diferents modificacions del sistema i refrigerants. S'ha realitzat una anàlisi comparativa dels sistemes energètics d'amoníac, CO_2 i propà basat en una pista de gel representativa dels climes nòrdics.

Una pista de gel d'amoníac integrada tradicional consumeix uns 340 MWh a l'any per a cobrir les demandes tèrmiques. Les mesures d'eficiència energètica més prometedores per a l'amoníac són l'ús de aqua amoníac com a fluid secundari i la utilització d'una bomba de calor auxiliar per a ajudar a cobrir les demandes de calefacció. Gràcies a aquestes mesures, es pot aconseguir un estalvi energètic del 12.9%.

Un sistema de CO_2 transcrític d'última generació que utilitza compressió paral·lela consumeix aproximadament un 42.6% menys d'energia que un sistema d'amoníac convencional, la qual cosa el converteix en la solució més eficient des del punt de vista energètic per a pistes de gel amb un SPF de 7.5. El bon rendiment està lligat en gran manera a la possibilitat d'operar els sistemes de CO_2 com a sistemes directes, eliminant la necessitat de transferència indirecta de calor i minimitzant el consum d'energia dels equips auxiliars.

El propà, que encara no s'ha investigat com a refrigerant en pistes de gel, es va avaluar i va comparar amb l'amoníac i el CO_2. Un sistema modern integrat de propà que utilitza compressió paral·lela i una bomba de calor auxiliar és més eficient energèticament que un sistema tradicional d'amoníac, però requereix més energia que els sistemes moderns d'amoníac o CO_2. El propà va demostrar ser viable i representa una possible solució alternativa en les pistes de gel.

La recuperació de la calor residual és beneficiosa en tots els sistemes i hauria de ser una característica clau en els sistemes energètics de les pistes de gel. Tots els sistemes utilitzen refrigerants respectuosos amb el medi ambient i el seu impacte ambiental és quasi exclusivament indirecte i causat pel consum d'electricitat.

Paraules clau: Pistes de gel, refrigeració, recuperació de calor, CO2, amoníac, propà

CONTENTS

LIST OF FIGURES

LIST OF TABLES

LIST OF ABBREVIATIONS

AC	Air conditioning
AEU	Annual energy use
AOC	Annual operation cost
$CaCl_2$	Calcium chloride
CO_2	Carbon dioxide
COP	Coefficient of performance
DHW	Domestic hot water
DSH	De-superheater
DX	Direct expansion
EES	Engineering Equation Solver
F-gas	Fluorinated gas
FC	Floating condensing
FGB	Flash-gas bypass
GHG	Greenhouse gas
GWP	Global warming potential
HP	Heat pump
HR	Heat recovery

HT	High temperature
HRHE	Heat recovery heat exchanger
IHX	Internal heat exchanger
JC	Justified costs
LT	Low temperature
NH_3	Ammonia
PC	Parallel Compression
ppm	Parts per million
R1234ya	Tetrafluoropropene
R152a	Difluoroethane
R290	Propane
R717	Ammonia
R744	Carbon Dioxide
RH	Relative humidity
SC	Subcooling
SPF	Seasonal Performance Factor
SotA	State-of-the-Art
TEWI	Total Equivalent Warming Impact

NOMENCLATURE

Latin letters

ACH	$1/h$	Air Changes per Hour
c_p	J/kgK	Specific heat capacity
d	m	Diameter
d	%	Discount rate
dh	$€/kWh$	District heating price
e	$€/kWh$	Electricity price
f_1	-	Friction factor
h	kJ/kg	Enthalpy
i	%	Interest rate
k	W/mK	Thermal conductivity
L	m	Length
$\dot{m}$	kg/s	Mass flow rate
M	kg/mol	Molar mass
n	-	Number
P	kW	Power
p	bar	Pressure
Pr	-	Prandtl number

$\dot{Q}$	kW	Heating/cooling rate
RC	$kg\ CO_2 - eq/kWh_{el}$	Regional conversion factor
RH	%	Relative Humidity
$\dot{V}$	m^3/s	Volumetric flowrate
V	m^3	Volume
v	m/s	Velocity

Greek letters

ΔAOC	€	Annual operation cost difference
Δh	J/kg	Enthalpy difference
Δp	bar	Pressure difference
ρ	kg/m^3	Density
η	%	Efficiency
κ	-	Recycling factor
ν	m^2/s	Kinematic viscosity
ω	g_{H2O}/kg_{air}	Humidity ratio
ω	-	Mass entrainment ratio

Subscripts

amb	Ambient
atm	Atmospheric
aux	Auxiliary

c, out	Condenser/Gas cooler outlet
$circ$	Circuit
$cool$	Cooling
dh	Dehumidification
dis	Discharge
ej, e	Ejector primary inlet
ej, out	Ejector outlet
ej, s	Ejector suction
el	Electrical
$evap_{in}$	Evaporator inlet
$evap_{out}$	Evaporator outlet
exp	Expansion
is	Isentropic
$leak$	Leakage
opt, gc	Optimum gas cooler
p	Pump
pre	Preheating
ref	Refrigeration
sat	Saturation
suc	Suction
tot	Total

1 INTRODUCTION

1.1 Background

Unsustainable energy use is among the main factors contributing to greenhouse gas (GHG) emissions and consequently to global warming. Global surface temperatures today are approximately 1.1°C higher than in pre-industrial years and the consequences of anthropogenic climate change are already affecting many parts of the world: rising sea levels, an increased likelihood of heatwaves, droughts and floods, loss of biodiversity or glacier melting, to name a few. Both adaptation and mitigation measures are needed to reduce climate risks. Mitigation measures include (inter)national policies and agreements such as the Paris Agreement, and the implementation of sustainable technological advances such as renewable energies and energy efficiency measures to limit global warming below 1.5°C. [1]

With the energy sector contributing to 75% of global emissions, energy efficiency is one of the key measures to tackle climate change. According to the International Energy Agency (IEA), energy efficiency measures alone can contribute to more than 40% of the required emission savings to reach its Sustainable Development Scenario targets. Energy efficiency measures are especially critical for the decarbonization of heating and cooling systems, which account for 50% of the EU's energy consumption. [2], [3]

Fluorinated gases, or F-gases, are synthetic industrial gases used in a variety of applications such as in the manufacturing of electronics, as insulating gases for electricity emissions and most significantly as refrigerants in refrigeration and air-conditioning applications in the form of hydrofluorocarbons (HFCs). F-gases are sometimes also referred to as "super-pollutants" due to their severe impact on the environment. According to the International Panel on Climate Change (IPCC), F-gases are responsible for 13% of global warming. 43% of F-gas emissions can be linked to the cooling industry alone, with cooling demands projected to increase in the future. Energy efficiency, design improvements and substitution of F-gases with low-/no-GWP and natural refrigerants are among the most efficient measures to abate F-gas related emissions and reach climate targets. HFCs can be substituted in most applications by environmentally friendly refrigerants such as ammonia, carbon dioxide, propane, butane, or other natural refrigerants. [4]

Ice rinks belong to the most energy intensive commercial buildings due to their simultaneous demand for large amounts of heating and cooling. An average Swedish ice rink consumes about 1,000 MWh of energy per year, of which about 43% can be attributed to the refrigeration system. The ice sheet is usually cooled by a vapor compression system and the heating demands are met by district heating, or in more modern systems, to a large extent by heat recovery from the refrigeration system. In 2010, the average age of a Swedish ice rink was 19.4 years, which is most likely even higher today. [5], [6]

Their age and high energy requirements make ice rinks ideal to implement energy efficiency measures and prove the relevance of natural refrigerants in modern refrigeration and heating applications.

1.2 Objective

The objective of this work is to evaluate and compare different refrigerants and energy systems in ice rinks to find the most promising solution in terms of energy, economic and environmental performance. In addition to evaluating and proposing improvements for ammonia and CO_2 systems which are already in use today, the suitability of propane as a potential refrigerant in ice rinks is investigated for the first time.

1.3 Scope and Limitations

This thesis focuses on indoor ice rinks in northern climates, specifically in Sweden. The performance is largely dependent on ambient conditions and moderate/warm climates are outside the scope of this thesis.

Based on the premise of finding sustainable and long-term solutions, the investigated refrigerants are limited to natural refrigerants, i.e. ammonia, CO_2 and propane.

Certain assumptions and simplifications are necessary to not go beyond the scope of a master thesis. Consequently, the results are accompanied by uncertainty, especially regarding the control strategy.

1.4 Methodology

First, a literature review is conducted to compile the latest findings in refrigeration/heating technologies and find suitable measures to improve the energy efficiency in ice rinks. Based on field data and literature, a reference ice rink together with its heating and cooling demands is defined, which serves as the baseline for all systems.

Reference systems for ammonia and CO_2 as they are found today, and a propane system that is similar to the ammonia one are modelled for fixed operating conditions and different modifications to enhance energy efficiency are evaluated. A simplified and individual control strategy is applied to the most promising design for each system and they are compared against each other based on energy efficiency, operation costs and CO_2-equivalent emissions.

1.5 Document Structure

Chapter 2 provides technical background information on ice rinks and their energy systems, including recent state-of-the-art modifications of vapor compression cycles for increasing their energy efficiency. **Chapter 3** introduces the case study and the ice rink systems, which will be used as references. The methodology of this work is elaborated in **Chapter 4**. First, a typical reference ice rink in a northern climate is defined, which will be used for all investigated energy systems. Second, the modelling of the systems is presented, including the used boundary conditions, assumptions and evaluation methods. In **Chapter 5**, the results are presented and discussed, and the most promising ice rink energy system is defined. **Chapter 6** summarizes the main results in the form of a conclusion and **Chapter 7** gives an outlook on future works on this subject.

2 LITERATURE REVIEW

2.1 Introduction to Ice Rinks

Long before the construction of artificial ice rinks, natural ice rinks were used as a means of transportation and for outdoor activities. The oldest known ice skates, made from animal bones, have been found in Switzerland and are roughly 5,000 years old. In the 14th century, metal components were added to the skates in the Netherlands and in 1850, ice skates with steel blades were invented by the American E.W. Bushnell. The first modern, mechanically refrigerated ice rink, called “The Glaciarium”, was opened in 1876 by Prof. John Gamgee in London. The technology behind the refrigeration system was similar to modern indirect systems and involved copper tubes, through which a pre-cooled mixture of water and glycerin was circulated. Given the success of the Chelsea ice rink in 1876 and the rising popularity ice skating/hockey as recreational and competitive activities, the number of ice rinks consistently increased in Europe and worldwide. [7]

Nowadays, ice rinks are mainly used for sport activities like ice hockey, curling, figure skating, or recreational skating. Their size can vary from small patches of ice with a size of about 60 m^2 used for figure skating training, to public arenas that are used for ice sports spectator events, up to Olympic sized bobsleigh tracks that require refrigerated ice surfaces of up to 10,000 m^2. [8]

2.2 Energy Demands

Today, there are about 365 ice rinks in operation in Sweden [9] with an annual average energy consumption of about 1,000 MWh (electricity and heat) [5]. The five main technical subsystems and simultaneously biggest energy consumers are the lighting, heating, refrigeration, dehumidification and ventilation systems, which are illustrated in a scheme of a typical ice rink in Figure 1. Together, they account for 95% of the energy consumption [9].

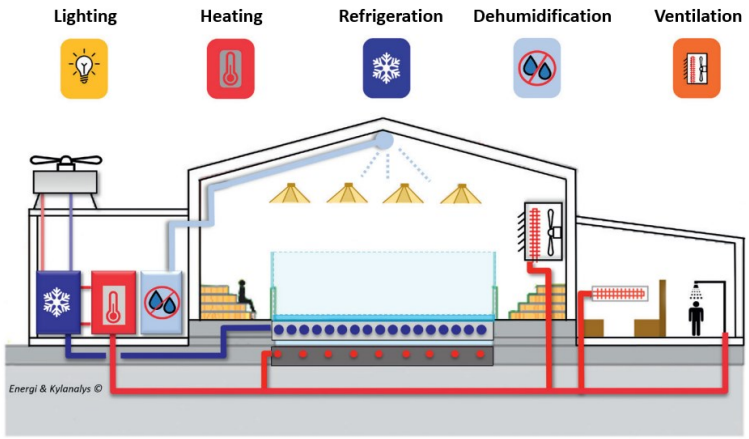

Figure 1: Ice rink layout [9]

Figure 2 shows the energy distribution of the main technical systems. The refrigeration system is responsible for the largest share of energy consumption with about 43%, followed by the heating system with 26%. Lighting, ventilation and dehumidification account for 10%; 9% and 6% of the energy consumption respectively, while the remaining 6% are attributed to miscellaneous energy consumers. [6]

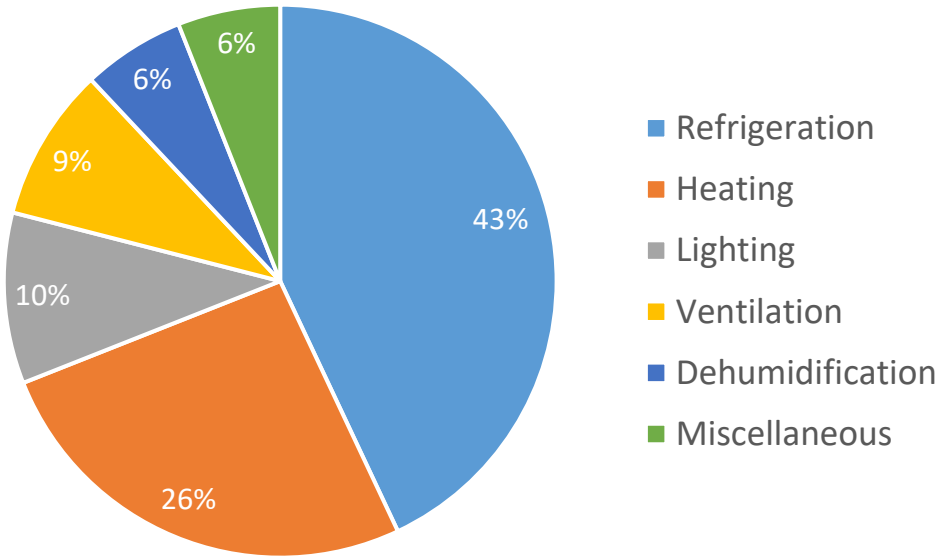

Figure 2: Ice rink energy distribution [6]

2.2.1 Lighting

Lighting in ice rinks is required to ensure a pleasant and functional indoor environment. Depending on the area in the building and what activity is being performed on the ice, different lighting levels are necessary. Table 1 shows the amount of required lighting in different ice ink areas/during different ice rink activities. [10]

Table 1: Typical lighting levels in ice rinks [10]

Area/Activity	Required lighting
Recreational Hockey	500 lx
Recreational Skating	300 lx
Dressing Rooms	300 lx
Common Areas	300 lx

2.2.2 Heating

Ice rinks require heating for various processes, mainly space heating, water heating, dehumidification, melting of waste ice and ground frost protection. The space heating system is necessary to provide thermal comfort to both the spectators and the ice skaters, and to prevent fog and condensation by maintaining appropriate air temperatures to control humidity levels of the ice rink. Table 2 shows recommended temperatures for different parts of the rink and during different activities. [10]

Table 2: Recommended ice rink air temperatures [10]

Activity	Rink (at 1.5 m height)	Tribune
Hockey		
Game	6°C	10°C – 15°C
Training	6°C	6°C – 15°C
Figure Skating		
Competition	12°C	10°C – 15°C
Training	6°C	6°C – 15°C

Water temperatures of at least 55°C are required to prevent legionella growth and produce domestic hot water (DHW). It is predominantly needed for tap water and showers in locker rooms, but also for cleaning and facilities such as cafeterias and restaurants. [10]

Part of an ice pad structure, as seen in Figure 3, is the ground frost protection. Below an insulation layer, a subfloor heating system is required to prevent the formation of permafrost and heaving. Heaving worsens the quality of the ice, causes uneven ice surfaces and damages the floor. Heating pipe temperatures are in the range of 4.4°C to 5.6°C [8]

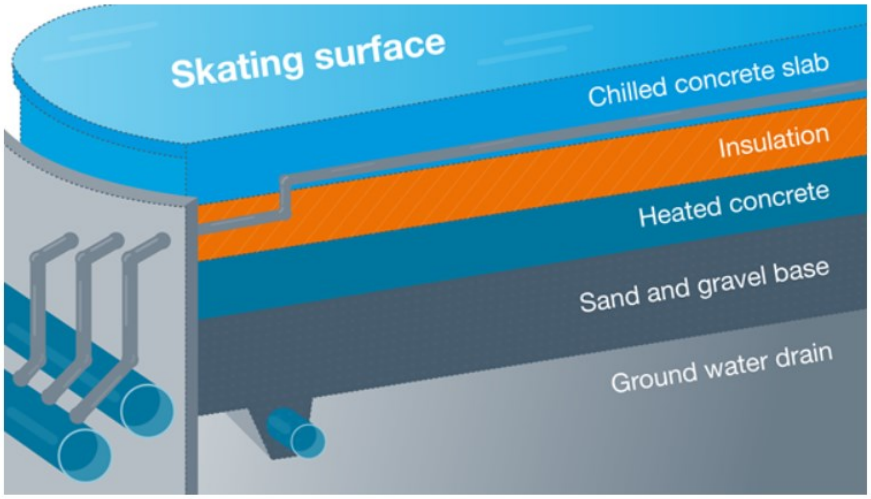

Figure 3: Cross-section of an ice pad [11]

Regular ice resurfacing is required to maintain a good quality ice surface. It is usually done by resurfacing machines, which plane the ice and pick up the created waste snow. On average, 0.4 m^3 to 0.8 m^3 of flood water with a temperature of 30°C to 60°C is then poured over the ice sheet, freezing and smoothing the ice surface. [8], [10]

During the ice resurfacing process, a thin layer of the ice surface is removed as snow. When it cannot be disposed outside to melt, the waste ice is disposed in melting pits. The required heating for melting the ice can come from different sources such as DHW, however, ideally it comes from the waste heat of the refrigeration system. [8]

2.2.3 Refrigeration

The refrigeration plant is the central unit in an ice rink and provides cooling for the ice sheet to freeze and, if equipped with a heat recovery system, it can also provide heating to the facility. The refrigeration capacity for single sheet ice rinks is typically in the range of 300-350 kW [10]. The refrigeration system is normally based on the vapor compression cycle, of which the main components are illustrated in Figure 4. The four main components of the vapor compression cycle are the evaporator, compressor, condenser, and expansion valve. A working fluid (refrigerant) is circulated in the system and undergoing phase changes. In an ideal cycle, low-pressure saturated vapor enters the compressor, where it is compressed to a higher pressure and lifted to a higher temperature level. Superheated vapor is passed through the condenser, where it condenses, and heat is rejected at constant pressure until the refrigerant reaches saturated liquid form. The condensed liquid then enters the throttling device, where it is expanded and its pressure reduced, resulting in the working fluid entering a two-phase state. The liquid/vapor mixture is routed through the evaporator, usually in the form of coils, where it absorbs heat from a heat source and evaporates until reaching a state of saturated vapor, ready to enter the compressor again and completing the cycle. [12]

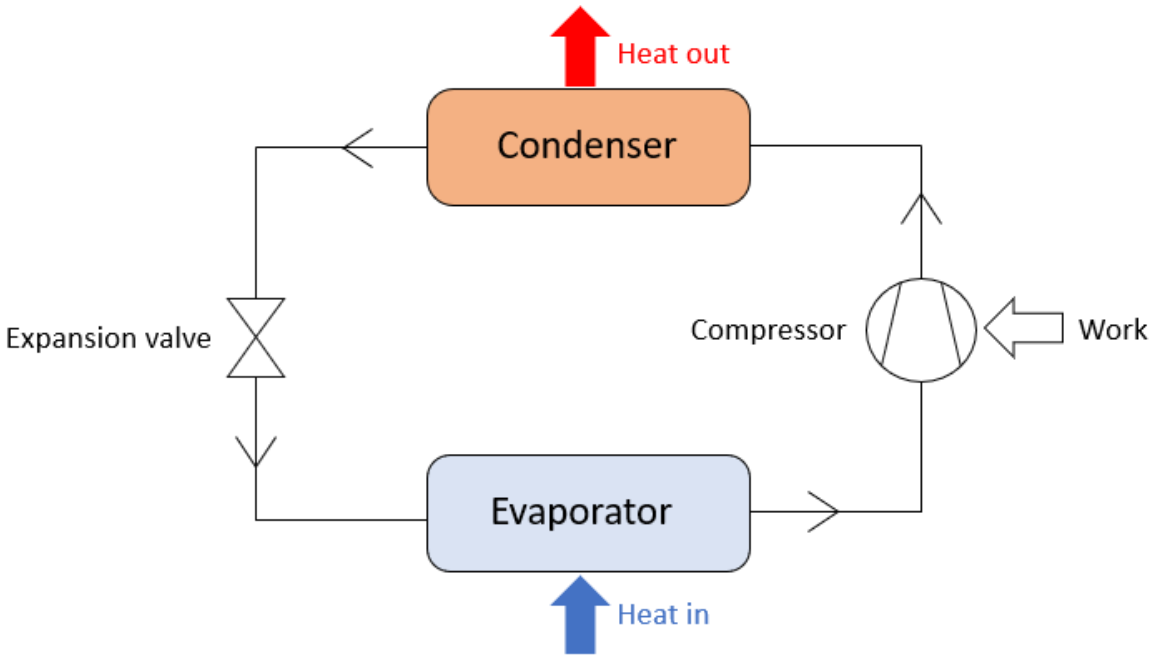

Figure 4: Basic vapor compression cycle, based on [12]

Figure 5 shows a fully indirect refrigeration system with an integrated heat recovery system. On the evaporator side, it is used to cool down the ice sheet while the heat from the condensing level is used to cover the heating demands of the arena.

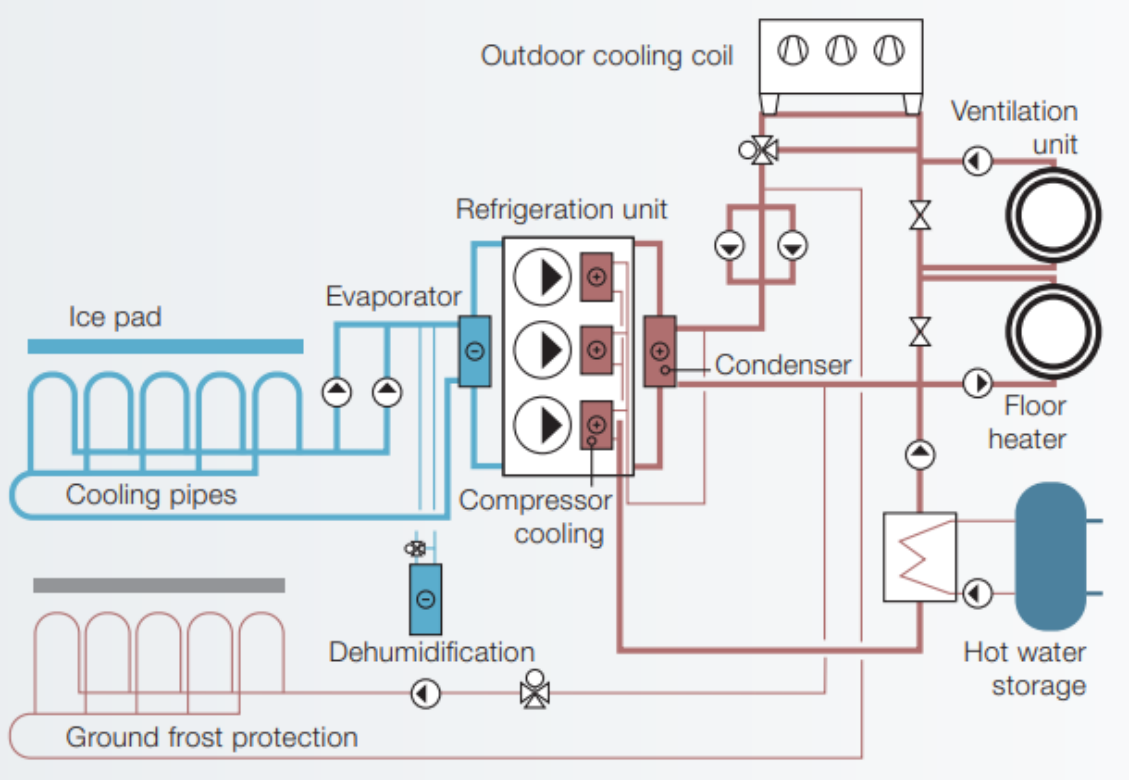

Figure 5: Ice rink energy system [10]

Depending on the ice rink activity, different ice temperatures are required. Ice hockey requires harder ice and therefore lower ice temperatures, while figure skating generally requires softer ice and therefore slightly higher ice temperatures. Table 3 shows recommended ice sheet temperatures during different activities. [10]

Table 3: Desired ice sheet temperatures [10]

Activity	Ice temperature
Hockey	
Game	-5°C
Training	-3°C
Figure Skating	
Competition	-4°C
Training	-3°C

2.2.4 Dehumidification

Dehumidification of the air in ice rinks is necessary to avoid moisture related issues and maintain a pleasant indoor climate. Moisture is mainly introduced by infiltration of outside air into the ice rink caused by air leakages and by internal loads of the people in the building (sweating, breathing). An insignificant part of moisture is also introduced by diffusion of water vapor through the building envelope. Moisture related problems can cause long-term issues like metal corrosion, rotting of wood and fungi/bacteria growth. Further, moisture removal is necessary to ensure a satisfactory experience for the athletes and spectators. Moisture mishandling can cause the ice surface to soften, and the viewing experience of spectators can be negatively affected by water dripping from the ceiling and/or condensation/fog on the protective ice rink glass. Finally, dehumidification also has a direct impact on the energy consumption of the ice rink. Unwanted condensation of water on the ice due to non-optimal humidity levels leads to an increase in the refrigeration demand, while the dehumidification system itself is responsible for a non-negligible part the energy consumption of an ice rink. [13]

There are two main dehumidification methods utilized in ice rinks to remove moisture: condensing and desiccant dehumidification. The processes are shown in Figure 6. Condensing dehumidification is based on mechanical refrigeration and aims at lowering the temperature of the humid air coming from the ice rink below the dew point with the help of a cooling coil. This results in condensation of the moisture in the air, which is removed, and dry air can be supplied back to the rink. On the other hand, desiccant dehumidification is based upon adsorption or absorption. Humid air is passed through a rotating desiccant wheel, which is coated with an absorbent such as silica gel, which absorbs moisture from the air. The desiccant wheel is reactivated when hot air passes through it, releasing the previously absorbed moisture. The resulting hot and moist air is then exhausted from the building. Modern adsorption type dehumidifiers require temperatures of about 55°C to regenerate the desiccant, which allows for the operation with waste heat from the refrigeration system. [14], [15]

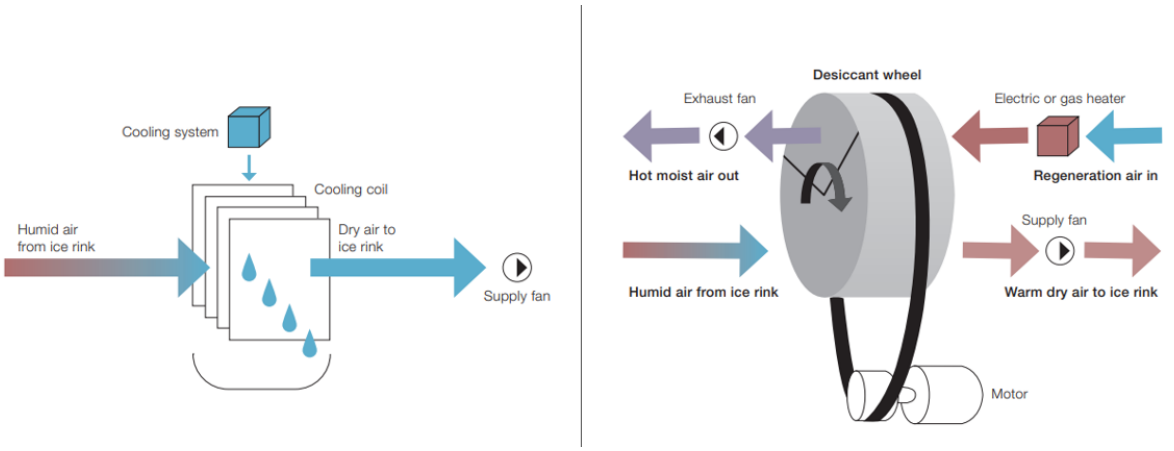

Figure 6: Condensing dehumidification (left) and desiccant dehumidification (right) [10]

2.2.5 Ventilation

Supply of fresh outdoor air by means of a ventilation system is necessary to maintain good indoor air quality and to ensure comfortable and healthy conditions for the users inside. In ice rinks, ventilation

and supply of fresh air is especially important to control the indoor humidity levels and reduce the dehumidification loads. The ventilation system in ice rinks is often linked together with the heating and dehumidification systems in the form of a mechanical air handling unit, as illustrated in Figure 7. [16]

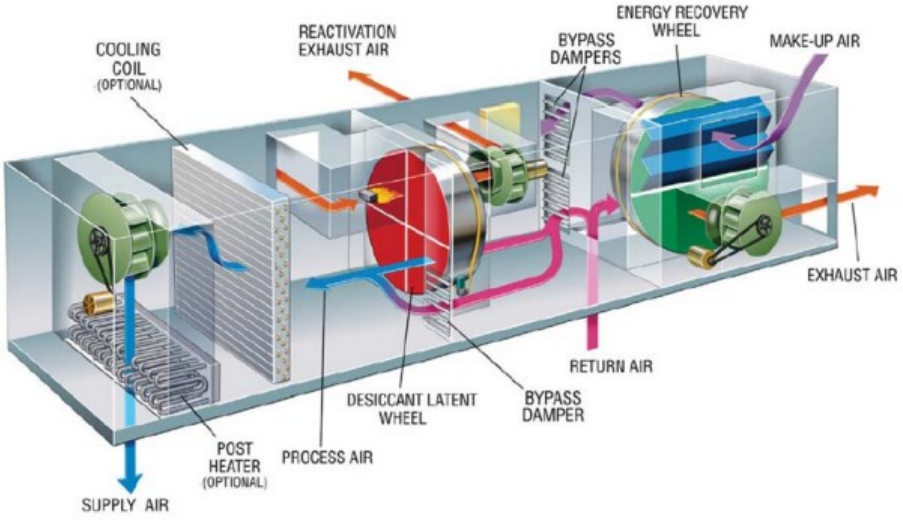

Figure 7: Air handling unit for ventilation, heating and dehumidification [17]

2.3 Heat loads

Heat loads that act on ice rinks are made up of convective, conductive and radiative components. Convective loads constitute a major share of the heat loads on ice rinks and are caused by sensible heat transfer between the ice and the air due to difference in temperature, as well as by latent heat transfer due to condensation of moisture on the ice. Conductive heat loads compromise heat gains from the warmer ground below the ice sheet, heat gains to the piping/headers, ice resurfacing and in the case of indirect systems, heat gains from circulation pumps. Radiative heat loads stem from radiation on the ice sheet by the ceiling and by the lighting. Ice skaters also cause heat loads on the ice, which are made up of various different loads such as friction from ice skates, body radiation or respiration. [8] Figure 8 shows the share of various heat loads in a typical Swedish ice rink.

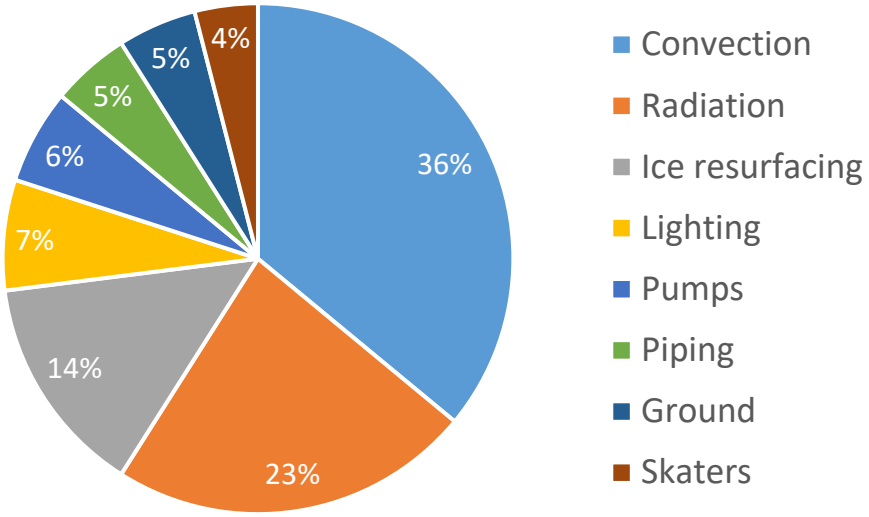

Figure 8: Heat loads in ice rinks [18]

2.4 Refrigeration System

Refrigeration systems in ice rinks can be classified into indirect, partially indirect or direct system solutions. In 2011, 97% of Swedish ice rinks were fully indirect or partially indirect systems and 3% were direct systems [19]. However, given the great heat recovery potential of direct CO_2 systems and their proven success in supermarket applications, which are comparable to ice rinks due to also having simultaneous heating and cooling demands, direct refrigeration systems in ice rinks are becoming more widespread [20].

2.4.1 Indirect

In indirect refrigeration systems, a primary refrigerant is circulated in a vapor compression cycle and connected to one (partially indirect) or two (fully indirect) secondary circuits, that transport heat to the evaporator and/or from the condenser via heat exchangers [21]. Figure 9 shows the basic layout of a fully indirect refrigerated ice rink system. The working fluid, often ammonia, is undergoing phase-changes in the primary refrigeration cycle. It absorbs heat in the evaporator from a secondary heat transfer fluid, which is usually a brine like calcium chloride ($CaCl_2$). The brine is circulated through a pipe network below the ice rink with the help of a secondary fluid pump, where it freezes the ice sheet and maintains it at the desired temperature. In the condenser, the primary refrigerant rejects heat to a secondary coolant such as glycol, which is also circulated by means of a circulating pump and releases the absorbed heat by rejecting it to the ambient via a dry cooler. [8]

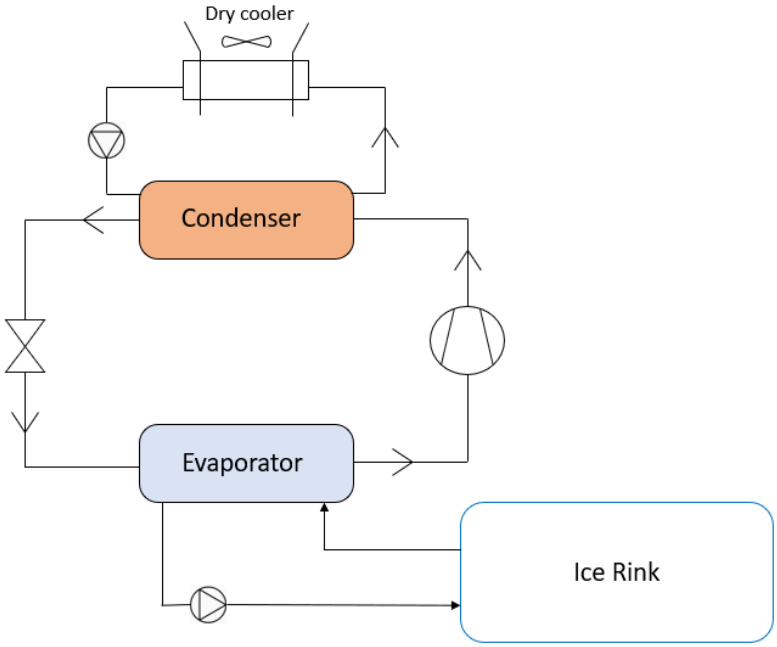

Figure 9: Fully indirect system, based on [22]

A major advantage of indirect systems is that they can reduce the charge of the main refrigerant down to 5-15% of the charge of a direct system. Low refrigerant charges are desirable for various reasons such as safer operating conditions, a reduction in their environmental impact and requiring smaller and more compact refrigeration units. Furthermore, indirect systems offer more flexibility in making adjustments to the system design. [21]

On the other hand, indirect systems require more components and equipment in the form of additional heat exchangers, secondary fluids, piping and pumps, leading to increased costs and energy consumption. Figure 10 illustrates the electricity consumption of components from a study of 19 indirect ice rinks. The necessary auxiliary equipment to run indirect systems is responsible for about 20% of the total energy consumption of the refrigeration system. In addition to the extra pump work needed to circulate the secondary fluids, indirect systems require lower evaporation temperatures due to the additional temperature difference between the refrigerant and secondary fluid, lowering the energy efficiency of the system. [21], [23]

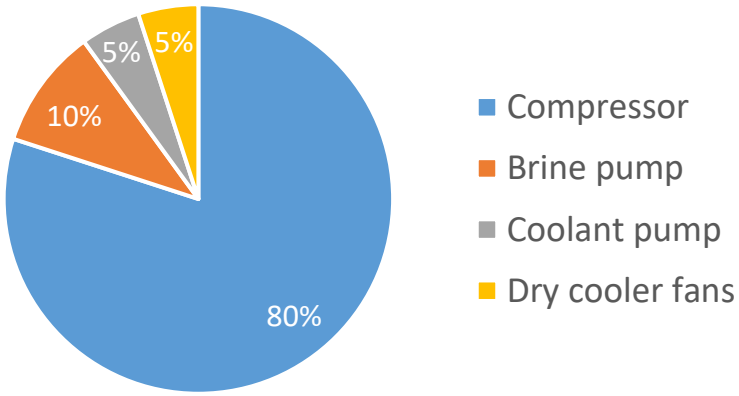

Figure 10: Energy distribution in indirect ice rinks [23]

2.4.2 Direct

Direct refrigeration systems use direct expansion or flooded evaporators where the refrigerant itself cools down the ice sheet and rejects heat to the heat sink. Examples of a direct ice rink refrigeration systems are illustrated in Figure 11. The refrigerant, in recent cases CO_2, is directed/circulated under the ice sheet and evaporates. The vapor either first re-enters the flooded evaporator or alternatively is directly compressed and releases heat in a condenser/gas cooler to the ambient before it is expanded and ready to cool down the ice sheet again. [8]

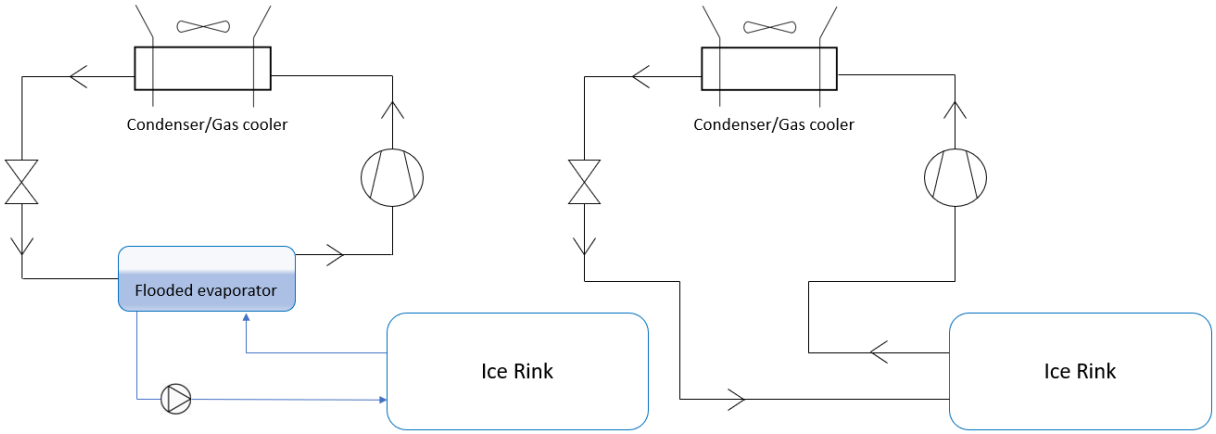

Figure 11: Direct system with flooded evaporator (left) and direct expansion (right), based on [22]

Some advantages of direct systems are higher energy efficiencies and simpler system designs, while disadvantages include the need for high refrigerant volumes and large refrigeration units requiring professional expertise in design and installation. [10]

2.4.3 Refrigerants

Fluorinated gases (F-gases) have favorable refrigeration properties and are therefore widely used in refrigeration applications as synthetic refrigerants. They are energy efficient, not harmful to the ozone layer, relatively safe due to their low toxicity and flammability, and cheap. On the other hand, F-gases are highly polluting with global warming potentials (GWP) up to 23,500 higher than that of CO_2. Owing to their extremely harmful impacts on the environment, several international agreements and regulations have been established to regulate, restrict or reduce the use of F-gases. The most significant of these agreements are the Montreal Protocol together with the Kigali Amendment, the Kyoto Protocol, the Paris Agreement and, within the European Union, the F-gas Regulation. Environmentally friendly substitutes include natural refrigerants such as hydrocarbons (propane, isobutane), ammonia or CO_2, and synthetic refrigerants such as R152a or R1234yf. [4]

Ammonia (NH_3, R717) is the most commonly used refrigerant in Swedish ice rinks with a share of 85% in all ice rink refrigeration systems [19]. It is well-known and has been used as a refrigerant for over 100 years. It has very good thermodynamic properties and is environmentally friendly with an ozone depletion potential (ODP) and GWP of 0, while being abundant and cheap. [24] One of the main advantageous thermo-physical properties of ammonia is seen in Figure 12. It has extremely high values for the latent heat of vaporization/condensation, which is a very beneficial property for refrigerants. [25]

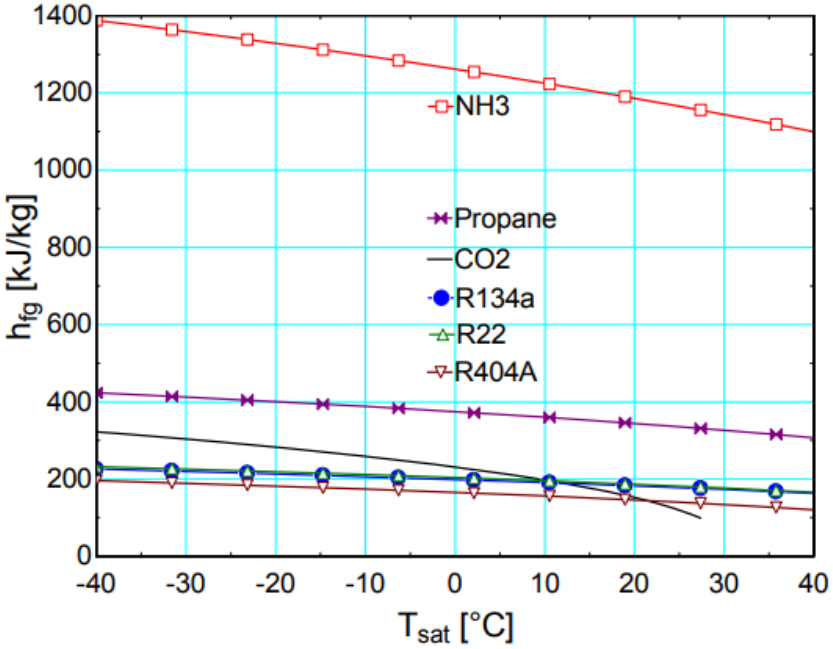

Figure 12: Latent heat of vaporization/condensation [25]

Carbon dioxide (CO_2, R744) is non-toxic, non-flammable, low-cost, abundant, has zero-ODP and a GWP of 1. Its most defining characteristic is its low critical point temperature at 31°C, corresponding to a pressure of 74 bar (a). Especially in trans-critical operation, i.e., operation above and below the critical point, CO_2 shows excellent heat transfer properties and great potential for heat recovery. Figure 13 depicts one of the unique characteristics of CO_2: its high volumetric refrigeration capacity which is owed to the high operating pressure and therefore high vapor density. As a result, CO_2 requires a lower volumetric flowrate to achieve the same cooling capacity as other refrigerants. At the end of 2016, six CO_2 ice rink systems were in operation in Sweden, and the number is expected to grow. [25]–[27]

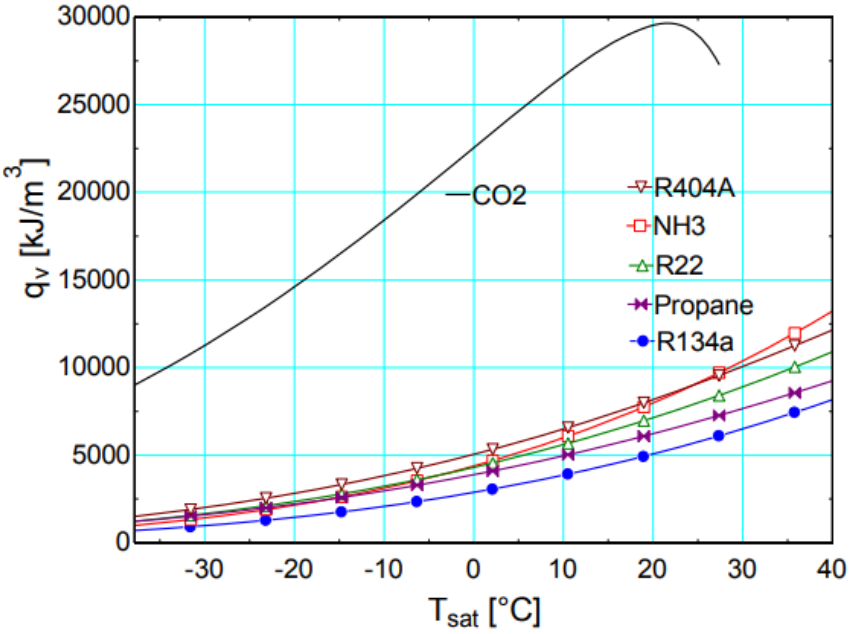

Figure 13: Volumetric refrigeration capacity [25]

Propane (C_3H_8, R290) is an environmentally friendly natural refrigerant with an ODP of 0 and a GWP of 3. Its energy efficiency, ease of transport and good heat transfer properties make it a popular refrigerant choice that is used in many applications such as domestic appliances (fridges, freezers, air conditioning (AC)), low- and medium-temperature commercial equipment, and large industrial refrigeration systems. [24] The suitability of propane for ice rink applications has yet to be investigated.

2.4.4 Safety and Practical Aspects

Aspects that need to be considered when using ammonia as a refrigerant are that it is flammable, toxic and has a pungent smell. Even though the toxicity only starts to become a concern at concentrations above 2,500 parts per million (ppm), the smell can already be noticed at concentrations as low as 5 ppm and it starts to become intolerable at 500 ppm. The pungent smell is a safety concern for use in public areas since even small leakages can be perceived and might evoke panic. Due to its toxicity and flammability, it is normally not allowed in closed spaces where people are present, such as ice rinks or supermarkets. It is therefore mainly used in indirect systems and placed in an isolated machine room to reduce the refrigerant charge and supply the heating/cooling via a secondary fluid. In contrast to CO_2 and propane, which are compatible with all commonly used refrigerant materials, ammonia has corrosive effects on certain materials such as copper, non-ferrous metals and some plastics. [24], [28], [29]

CO_2 occurs in the natural atmosphere at concentrations around 350 ppm and is relatively safe compared to other refrigerants. At CO_2 concentrations above 1000 ppm, a deterioration in air quality becomes noticeable. At higher concentrations, caused for instance by refrigerant leakages, CO_2 imposes serious health risks such as breathing problems, unconsciousness or even suffocation. In contrast to ammonia, CO_2 is not detectable by odor or any other property, which is why it is recommended to place CO_2 sensors in the machine room/usage site and ensure proper ventilation. CO_2 is heavier than air, so the sensors should be placed close to the floor. Another main drawback of CO_2 as a refrigerant lies in the high operating pressure, which requires higher safety precautions and costs. When using CO_2 in a direct system, copper or steel pipes are needed to withstand the high operating pressure, as opposed to plastic pipes which can be used for secondary fluids in indirect ammonia systems. [25], [28]

The most relevant concern with regards to propane and other hydrocarbons is their high flammability and the subsequent necessity of safety procedures and standards when handling them. Propane and hydrocarbons in general require significantly less energy and lower concentrations to ignite than other flammable refrigerants. Additionally, should it come to an explosion after refrigerant leakage and ignition, the damage caused by hydrocarbons is higher than that of other refrigerants due to their high heat of combustion and combustion speed. Safety standards such as the EN 378 standard restrict the maximum allowable charge and impose other safety requirements. [30]

2.5 Review of State-of-the-Art Features

In 2010, the average age of a Swedish ice rink was 19.4 years [6]. Today, this number is most likely even higher, which leaves a lot of room for implementing the latest findings to improve system

performance. Research in all areas of the refrigeration cycle is continuously being conducted, ranging from a system perspective down to individual components, including research on ice rinks specifically. The most relevant features and improvements are presented in the following sections.

2.5.1 Heat Recovery

The simultaneous heating and cooling demand of ice rinks makes them very suitable for waste heat recovery. Instead of rejecting the heat at high pressure levels, it can be recovered and used for covering the heating demands of ice rinks, which in certain cases can be enough to cover all the heating needs and thus, make the ice rinks self-sufficient. [20]

Because of their high heat recovery potential, CO_2 systems are especially well-suited for ice rink applications, which have both high- and low-grade heat demands. The graph in Figure 14 depicts a comparison of available heat between CO_2 at a discharge pressure of 80 bar (a) and NH_3 at a condensing temperature of 35°C, both being cooled down to 20°C. It shows that approximately 60% of the heat in CO_2 systems is available at high temperature levels that can be used for hot water heating or dehumidification, as opposed to only roughly 20% in NH_3 systems. [26]

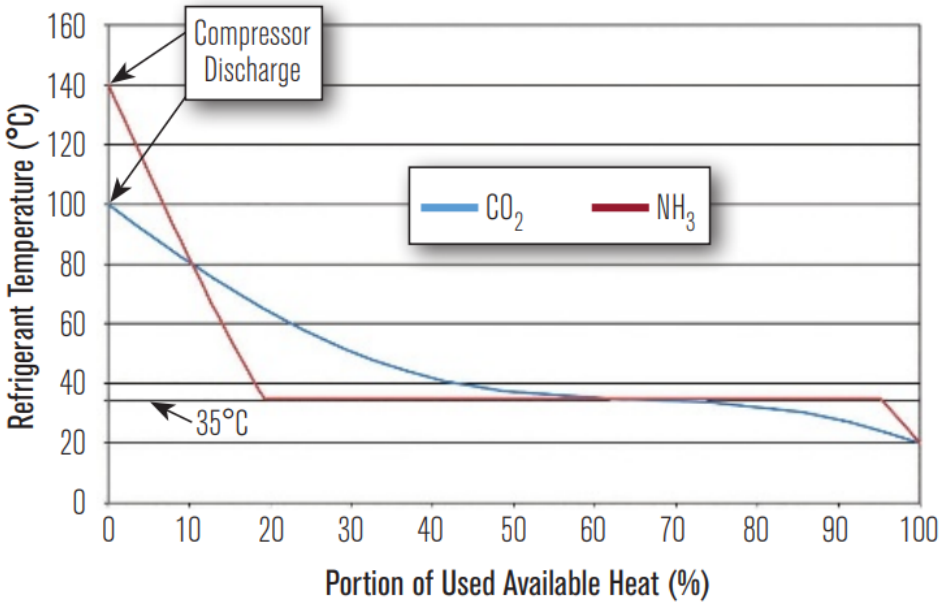

Figure 14: Heat recovery comparison between CO_2 and NH_3 [26]

Figure 15 depicts standard system configurations for ice rinks with integrated heat recovery. In CO_2 systems, heat is typically recovered with one or two de-superheaters in trans-critical operation, supplying heat at different temperature levels. In indirect NH_3 systems, one heat exchanger is used to recover the high-grade temperature during the de-superheating process, while a second heat exchanger is used to cool down the coolant fluid and recover low-grade heat from condensation. [31]

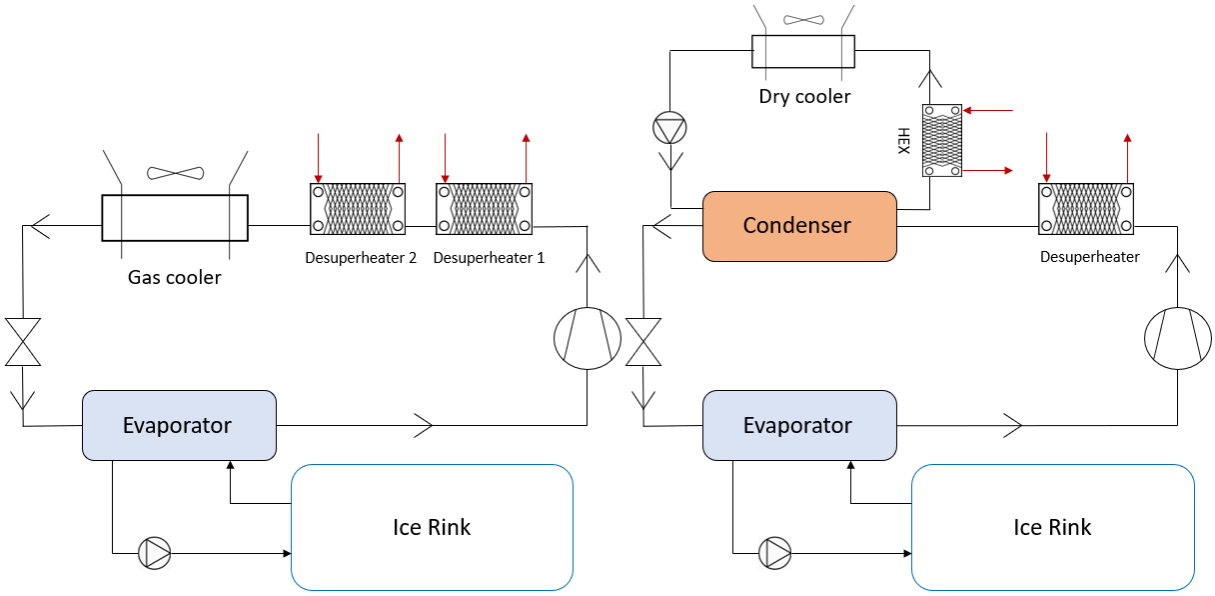

Figure 15: Standard CO_2 (left) and NH_3 (right) ice rink refrigeration systems with integrated heat recovery, based on [31]

A simulation study based on field measurements by Rogstam et al. [31] showed that both ammonia and carbon dioxide heat recovery systems are feasible, whereas CO_2 proved to be more efficient with heat recovery COPs of 4 and higher. Bolteau et al. [20] evaluated the performance of the first fully trans-critical CO_2 ice rink in Europe and showed that the waste heat can cover 100% of the heating demands. Thanasoulas [32] investigated two-stage heat recovery in CO_2 ice rinks, finding that two de-superheaters can help avoid pinch-point occurrences, deliver water at levels of up to 10°C higher than single-stage heat recovery systems, increasing the global COP by up to 10%. Pomerancevs et al. [33] compared an indirect ammonia system with an integrated propane heat pump for additional heat recovery and a trans-critical carbon dioxide system. The CO_2 system proved to be more efficient, consuming about 16% less energy than the ammonia system.

2.5.2 Internal Heat Exchanger

An internal heat exchanger (IHX) transfers heat within a vapor compression cycle. The most common position of an IHX is seen in Figure 16, which is after the condenser/gas cooler and before the expansion valve, and at the outlet of the evaporator and before the compressor inlet. Heat is transferred from the high-pressure level to the low-pressure level, lowering the evaporator inlet quality and thus increasing the cooling capacity. Further, it increases superheat and therefore compressor work. This trade-off between increased capacity and increased compressor work can improve or worsen the energy performance of the cycle. [34]

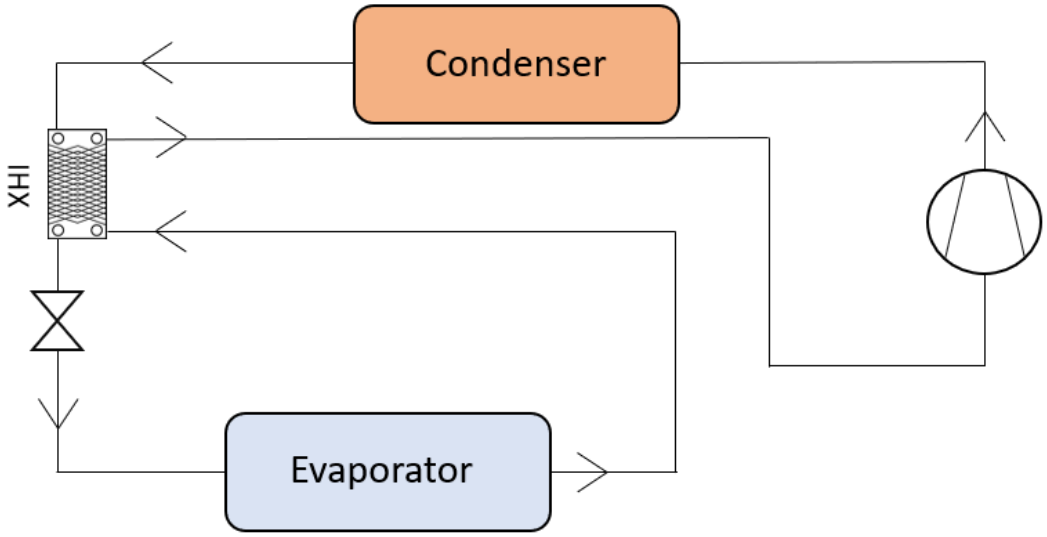

Figure 16: Basic vapor compression cycle with internal heat exchanger, based on [34]

In a combined numerical and experimental study by Cao et al. [35], a theoretical model of a trans-critical CO_2 heat pump cycle with IHX was developed and validated with a test-rig. It was found that the IHX allowed for a lower discharge pressure while achieving a COP improvement of around 12%. Cabello et al. [36] investigated the impact of IHXs in freezing cabinets using low-GWP refrigerants. In the case of propane, energy savings of up to 6% were achieved.

2.5.3 Flash Gas Bypass

After the isenthalpic expansion process in a direct expansion (DX) vapor compression cycle, flash gas is produced and the refrigerant enters a two-phase state of liquid and vapor. Both liquid and vapor enter the evaporator, even though the vapor does not have a considerable cooling effect. By using a flash tank, which collects the refrigerant in two-phase condition, and a flash gas bypass (FGB) valve, the vapor can be forwarded directly to the compressor. Saturated refrigerant in liquid phase and only very small amounts of vapor enter the evaporator. A scheme of a basic vapor compression cycle with a flash gas bypass configuration is found in Figure 17. The main advantages are an improved refrigerant distribution in the evaporator, a reduction in the pressure drop of the low-pressure side and an improvement of the refrigerant heat transfer coefficient. [37]

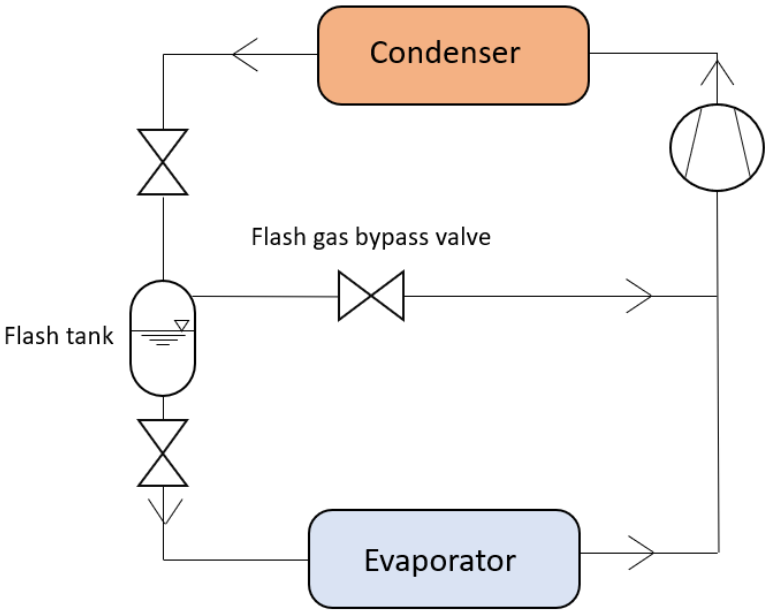

Figure 17: Basic vapor compression cycle with flash gas bypass, based on [34]

In an experimental study by Elbel and Hrnjak [37], the COP of a conventional DX CO_2 system could be improved by 7% by adding a FGB configuration. Tuo and Hrnjak [38] investigated the implementation of a flash gas bypass in a mobile air conditioning system with R134a, yielding a COP increase in the range of 4%-7%. Wang et al. [39] conducted a numerical study on a basic DX CO_2 system and found that the addition of a FGB increases the COP by 7%.

2.5.4 Parallel Compression

Parallel compression (PC) is similar to a flash gas bypass configuration where a flash tank is used to direct vapor that is formed after the expansion process to the high-pressure side without it passing through the evaporator. In contrast to the flash gas bypass system, where the vapor is expanded to evaporator pressure and one compressor is used to compress all the refrigerant flow, parallel compression systems utilize an auxiliary compressor that directly compresses the vapor from the flash tank. By compressing the vapor from a higher pressure level than the evaporator pressure, less compressor work is required due to the lower compression ratio, improving the efficiency of the system. The layout of a system using parallel compression is shown in Figure 18. [34]

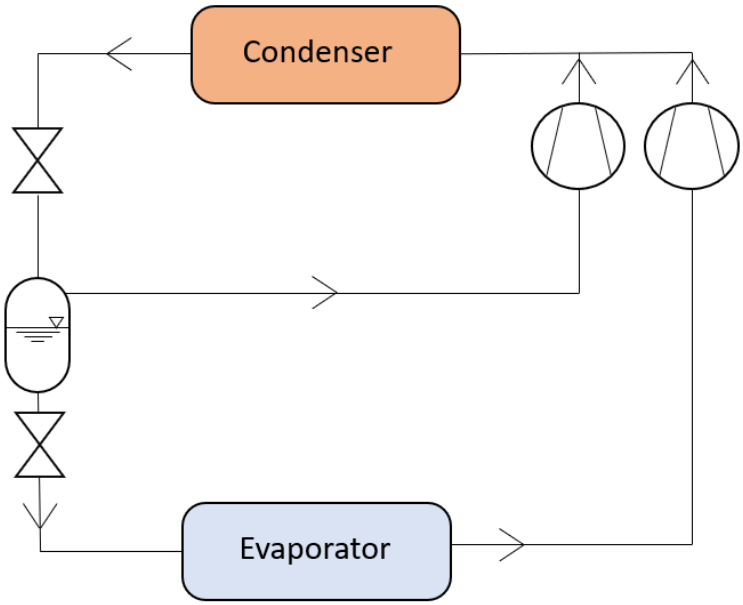

Figure 18: Basic vapor compression cycle with parallel compression, based on [34]

Chesi et al. [40] investigated the performance of a CO_2 refrigeration cycle with PC compared to one without. While the theoretical analysis showed COP improvements of 30%, experimental data yielded a COP improvement of 10%, given to limitations real systems such as the flash tank not being a perfect liquid-vapor separator and pressure losses. Karampour and Sawalha [41] numerically evaluated parallel compression in supermarket applications with CO_2 refrigeration in warm (Barcelona) and cold (Stockholm) climates, leading to 7% and 3% savings in the annual energy use (AEU) compared to a CO_2 system with a flash gas bypass, respectively. Torrella et al. [42] evaluated the performance of a trans-critical CO_2 refrigeration plant at different evaporation temperatures and gas cooler operating conditions based on experimental data of the system with and without IHX. The implementation of an IHX increased the COP and cooling capacity by up to 12%.

2.5.5 Ejector

The working principle of an ejector is illustrated in Figure 19. A high-pressure fluid enters the ejector nozzle (P_H), accelerating in the converging section of the nozzle to sonic flow at the throat, after which the fluid enters the diverging section of the nozzle where it accelerates further to supersonic velocity. The increase in velocity leads to a reduction in pressure, creating a low-pressure zone at the exit of the nozzle (P_S). The pressure at the low-pressure zone is lower than that of the low-pressure fluid at the secondary inlet (P_L), creating a pressure differential and sucking the fluid into the ejector. The two streams are mixed in the mixing chamber and decelerated in the diffuser, which increases the pressure to an intermediate pressure level (P_D). [43]

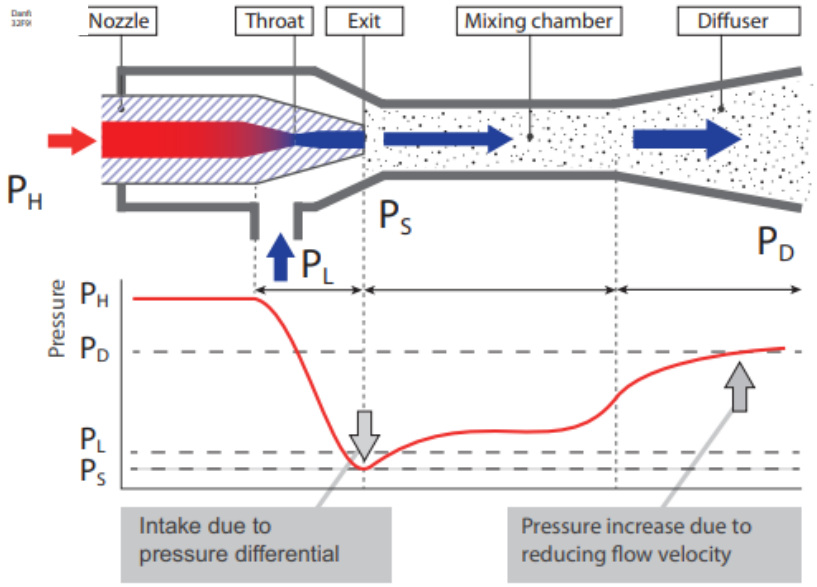

Figure 19: Ejector working principle [43]

In vapor compression systems, high-pressure fluid (refrigerant) enters the ejector at condensing pressure level and the ejector outlet leads to a receiver at intermediate pressure, where refrigerant in two-phase condition is collected. The refrigerant in liquid phase is expanded to evaporation pressure level, passing through the evaporator and evaporating, after which it enters the ejector at the secondary inlet. The refrigerant vapor in the intermediate pressure receiver is fed to the compressor. Ejectors are advantageous in vapor compression cycles for two reasons: the throttling losses during the expansion process can be reduced and the recovered energy is used to increase the pressure of the suction flow, reducing the energy consumption of the compressor, and lower quality/enthalpy refrigerant enters the evaporator, increasing the refrigeration capacity. The key parameters of ejectors are the entrainment ratio, the pressure lift, the ejector efficiency and the suction pressure ratio. [44]

Hafner et al. [45] investigated the use of ejectors in supermarkets operating with CO_2 refrigeration systems in combination with heat recovery in different climates. Compared to a CO_2 system without ejectors, COP improvements in summer operation mode were found to range from 5% in cold climates (Trondheim) to 17 % in warm climates (Athens), while typical COP improvements of 20 – 30% were achieved in winter operation mode. In a study of two ice rinks by Fehling [46], ejectors lead to energy savings of 7% in a direct refrigeration ice rink and negligible effects on the system performance in an indirect refrigeration ice rink, given too low evaporation temperatures. Ejector efficiencies reached up to 40%.

2.5.6 Subcooling

There are several ways to achieve subcooling (SC) or further cooling in refrigeration cycles, such as economizer arrangements, heat storage, integrated mechanical subcooling or dedicated thermoelectrical/mechanical subcooling systems, as seen in Figure 20. The focus of this work lies on mechanical subcooling in CO_2 systems. An additional vapor compression cycle is added to the exit of the gas cooler to further cool the refrigerant. As a result, the quality at the evaporator inlet is reduced,

increasing the cooling capacity of the refrigeration cycle. The subcooling cycle usually works with a different refrigerant and requires an additional energy input. When designed correctly, the COP of the main cycle can be substantially increased, outweighing the additional energy costs of the subcooling cycle and improving the performance of the entire system. [47]

In ice rinks, the condenser of the subcooling system could be coupled to the heat recovery system, providing useful heating and cooling at the same time.

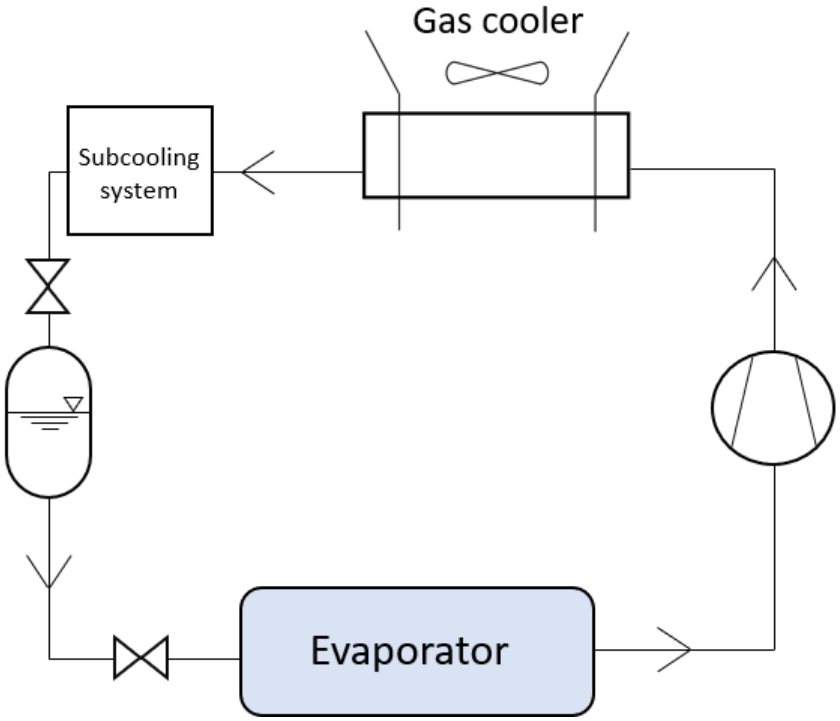

Figure 20: Basic vapor compression cycle with dedicated subcooling, based on [47]

Llopis et al. [48] theoretically analyzed the energy performance of a trans-critical CO_2 system using dedicated mechanical subcooling. Different evaporation and condensing temperatures were investigated, as well as different refrigerants for the subcooling cycle. While the refrigerant choice was insignificant for the system performance, COP improvements reached up to 20%. Nebot-Andrés et al. [49] experimentally compared integrated and dedicated mechanical subcooling in trans-critical CO_2 refrigeration systems against parallel compression at different heat rejection levels. It was found that both subcooling systems outperformed the reference PC system, with COP improvements ranging from 4.1% at 25°C to 9.5% at 35.1°C rejection temperature for the integrated and 7.8% at 25°C to 17.5% at 35.1°C rejection temperature for the dedicated mechanical subcooling system.

2.5.7 Flooded Evaporation with Pump Circulation

Flooded evaporation makes use of the higher heat transfer coefficient of two-phase flow compared to single-phase flow. After exiting the expansion device in two-state condition, the refrigerant enters a liquid accumulator. In the case of ice rinks, liquid refrigerant is drawn from the accumulator and circulated in the ice rink floor, where it partly evaporates and reenters the liquid accumulator. As opposed to direct expansion, where the refrigerant fully evaporates and passes through the superheater section of the evaporator in single-phase as vapor, flooded evaporation allows the

refrigerant to stay in two-phase condition throughout the entire evaporator, leading to a higher heat transfer coefficient. The increased heat transfer and no need for superheat enables higher evaporation temperatures which decreases the compressor work and thus improve the efficiency of the system. Saturated vapor leaves the liquid accumulator and enters the compressor, eliminating the need for superheating. The layout of a direct CO_2 ice rink system using flooded evaporation with pump circulation is illustrated in Figure 21. [41]

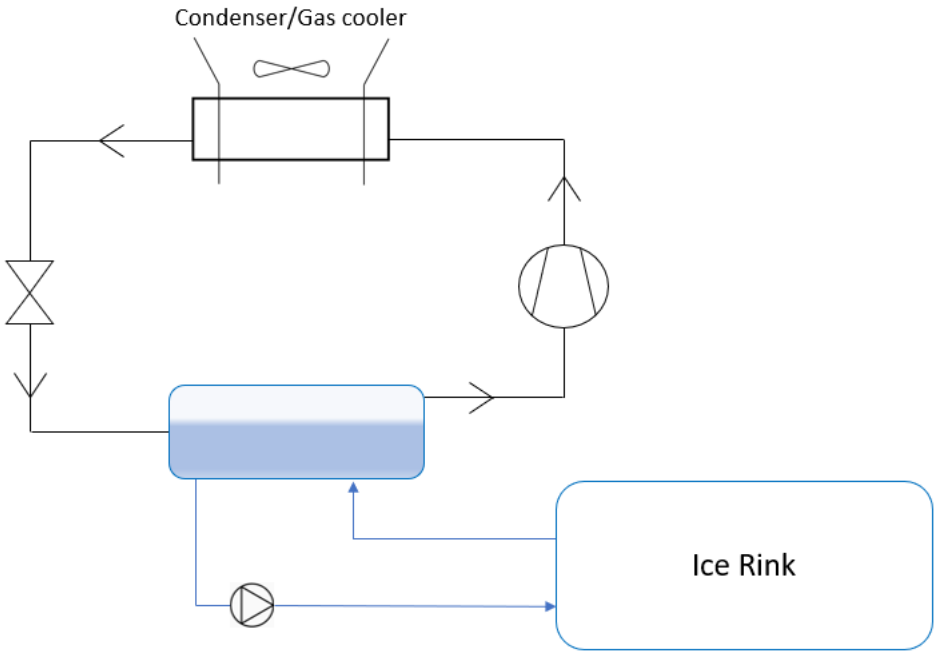

Figure 21: Ice rink with flooded evaporation, based on [20]

In an experimental study by Minetto et al. [50], a 13% reduction in the compressor energy consumption of a CO_2 refrigeration system could be achieved by using flooded evaporation. Karampour and Sawalha [41] analyzed the performance of flooded evaporation in supermarket applications using CO_2 as the refrigerant, resulting in 12% AEU savings compared to a standard CO_2 system with direct expansion.

2.5.8 Secondary Fluids

With indirect systems making up most of the ice rinks in Sweden and auxiliary pumps accounting for a large part of the energy consumption, the choice of the secondary fluid has a significant effect on the performance of the whole refrigeration system. The most commonly used secondary fluid in Swedish ice rinks is $CaCl_2$ [19]. However, recent research has shown that alternative secondary fluids can lead to lower pumping power requirements and thus, energy savings. A secondary fluid that has gained attention in recent years is aqua ammonia. It has low viscosity, good heat transfer properties and requires a low pumping power. One advantage of the lower pumping power requirements can be seen in Figure 22, which shows pump sizes for $CaCl_2$ and ammonia water for the same refrigeration capacity. [28]

Figure 22: Comparison secondary fluid pump sizes [28]

Rogstam [23] investigated the use of CO_2 as a secondary fluid in ice rinks, showing that it could reduce the pumping power by 90% compared to a fixed-speed $CaCl_2$ system and by 50% compared to a capacity-controlled system. In a theoretical study applicable to ice rink conditions, Ignatowicz et al. [51] found that aqua ammonia and potassium formate yielded 5% and 3% higher coefficients of performance (COP) than $CaCl_2$. In a recent study by Kilberg [52], the use of aqua ammonia as a secondary fluid has been investigated. Compared to a conventional $CaCl_2$ ice rink system, Kilberg showed that aqua ammonia had 45% lower pumping power requirements, leading to a COP increase of 4.7%.

3 CASE STUDY DEFINITION

3.1 Ammonia

Figure 23 shows a standard ammonia system for ice rinks. It is a fully indirect NH_3 system with brine ($CaCl_2$) as the secondary fluid and the evaporator is a flooded type evaporator. A circulation pump circulates the brine between the evaporator and the cooling pipes below the ice sheet. Heat is recovered in two heat exchangers: the first acts as a desuperheater and is used for high-temperature demands such as hot tap water, while the second is used to cool down the coolant (ethylene glycol) and supply heat for low-temperature demands such as space heating. Extra heat is rejected via a fan to the ambient air. The main drawbacks/areas of improvement are high condensing temperatures that are required to recover heat, leading to high discharge temperatures and energy consumption, and the low amount of superheat of ammonia that limits the heat recovery of high-grade heat.

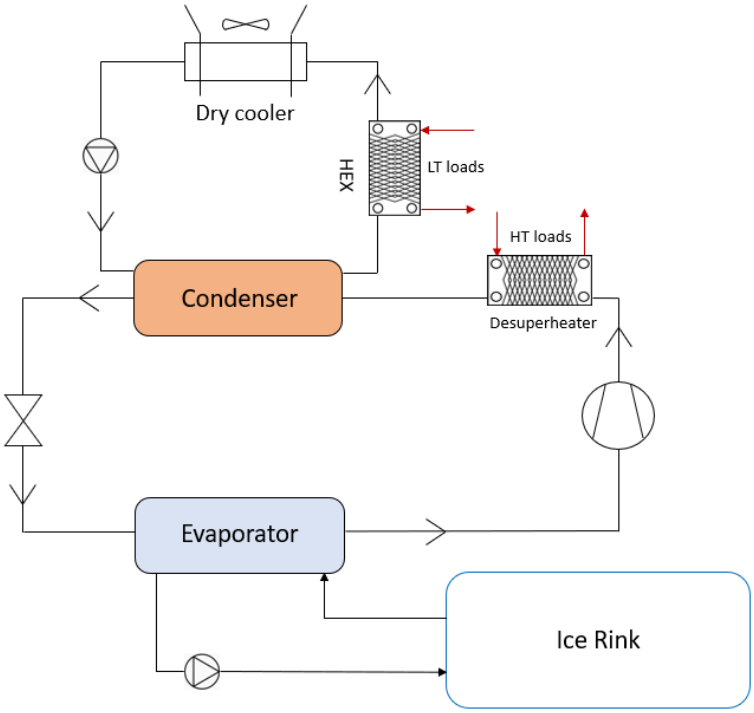

Figure 23: Ammonia reference system

3.2 Carbon Dioxide

A standard CO_2 ice rink system that has emerged in recent years is depicted in Figure 24. It is a partially indirect refrigeration system that uses a secondary fluid to cool the ice sheet and two heat exchangers in series to recover heat. It is usually run in trans-critical conditions and additional heat is rejected via a gas cooler to the ambience. Due to being relatively new, there are still areas of improvement in CO_2

ice rinks, mainly with regards to system efficiency. Several advancements and modifications of CO_2 systems have been achieved in recent years, which have not been implemented in ice rinks yet.

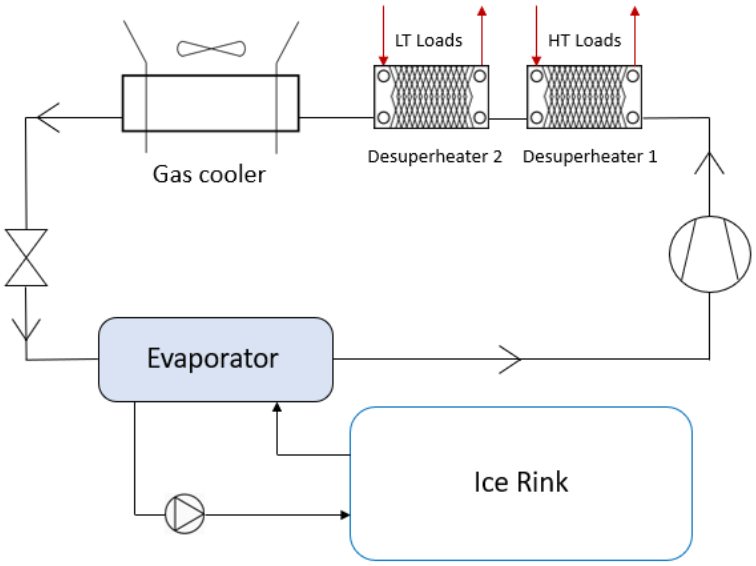

Figure 24: CO_2 reference system

3.3 Propane

The suitability of propane in ice rink applications has not been investigated yet. Due to similar safety requirements as ammonia with regards to limits to the refrigerant charge, the baseline propane system is also an indirect system and follows the same system layout, as seen in Figure 25. Propane has only little superheat available, which means that heat recovery of high-grade heat most likely cannot be achieved with this layout and a different system configuration is needed.

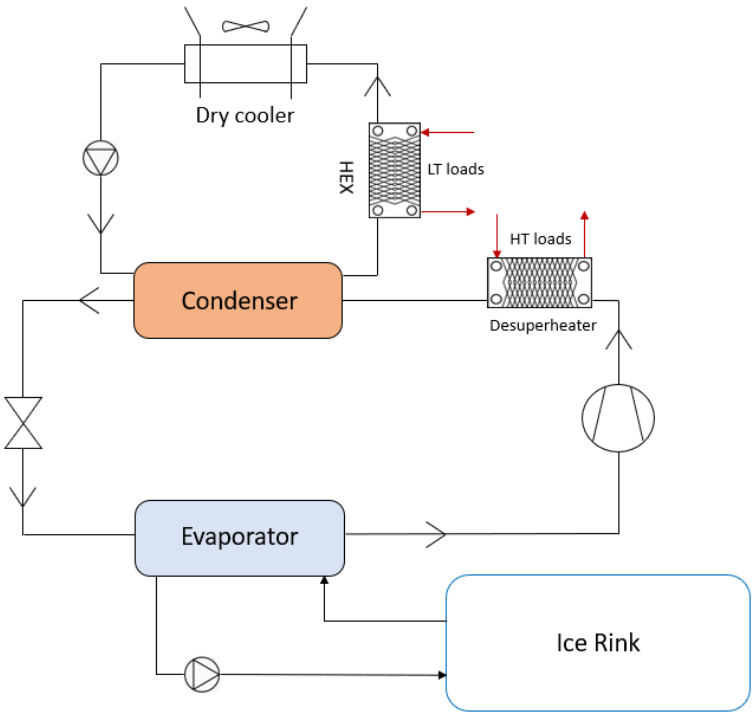

Figure 25: Propane reference system

4 METHODOLOGY

4.1 Field Measurement Analysis

Field data from real ice rink installations is acquired through the online monitoring platforms IWMAC and ClimaCheck Online. IWMAC's energy management software allows the operation, data collection, and visualization of technical installations and facilities in the fields of refrigeration, freezing, heating and ventilation. ClimaCheck Online is an online monitoring tool that measures system parameters and evaluates the performance of air-conditioning, heat pump and refrigeration systems. [53], [54]

The field data will provide necessary data to define the heating and cooling loads for the reference ice rink, as well as boundary conditions and assumptions for the simulation models.

4.2 Reference Ice Rink

In order to evaluate and compare the different system solutions, a reference ice rink with typical heating and cooling loads for an ice rink in a northern climate is defined. The characteristics are found in Table 4.

Table 4: Reference ice rink characteristics

Ice sheet size	30 m x 60 m (1,800 m^2)
Type	Indoor ice rink
Season length	August – March
Design cooling capacity	250 kW
Heating system	Waste heat recovery + district heating

4.2.1 Cooling Demand

The cooling profile is based on the Gimo ice rink, an ice rink in Sweden's municipality of Östhammar and located about 100 km north of Stockholm. It is a well monitored system and as an average sized indoor ice rink with a refrigeration capacity of 250 kW and a single ice sheet with a size of 1,800 m^2, its cooling profile is used as a reference for this work.

The capacity profile is calculated using the ClimaCheck method [55], which uses temperature, pressure and electrical power measurements to calculate the performance of the refrigeration cycle. Temperature sensors are located at the condenser/evaporator inlets/outlets, before the expansion valve and together with pressure sensors, before and after the compressor. Additionally, the electrical power consumption of the compressor is measured. The arrangement of the sensors is found in Figure 26.

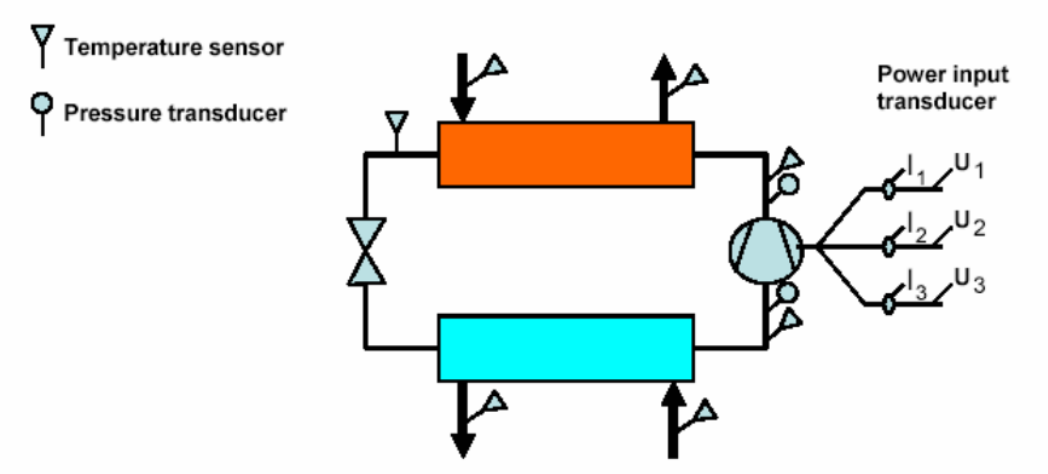

Figure 26: ClimaCheck sensor placement [55]

The ClimaCheck method allows the calculation of the refrigerant mass flow without needing to install expensive mass flow meters through thermodynamic calculations. An energy balance over the compressor yields:

$$\dot{m} * (h_{dis} - h_{suc}) = P_{el} - \dot{Q}_{loss} \quad (1)$$

which can be rewritten as:

$$\dot{m} = \frac{P_{el} - \dot{Q}_{loss}}{h_{dis} - h_{suc}} \quad (2)$$

where $\dot{m}$ is the refrigerant mass flow rate, P_{el} is the power consumption of the compressor, $\dot{Q}_{loss}$ is the heat loss of the compressor, and $h_{discharge}$ and $h_{suction}$ are the discharge and suction enthalpies of the refrigerant, respectively. The compressor heat loss is assumed to be 7% of the electrical power consumption [55]. The enthalpies can be calculated from the refrigerant properties since the pressures and temperatures are known. Finally, the cooling capacity can be calculated according to:

$$\dot{Q}_{cool} = \dot{m} * (h_{evap_{out}} - h_{evap_{out}}) \quad (3)$$

with $\dot{Q}_{cool}$ being the cooling capacity, $h_{evap_{out}}$ being the evaporator outlet enthalpy and $h_{evap_{out}}$ being the inlet enthalpy.

4.2.2 Heating Demand

The heating demands are estimated to complete the definition of the reference ice rink for the simulation models. Where needed, field data is taken from the Gimo ice rink for the season August 2022 to March 2023.

Subfloor heating for ground frost protection is calculated based on a standard rink floor design. The cooling pipes are embedded in a concrete base slab below the ice sheet, lying on top of an insulation layer. The heating pipes are embedded below the insulation layer in a concrete base layer [8]. The basic layout of the floor design is illustrated in Figure 27 together with the relevant geometries for the calculation.

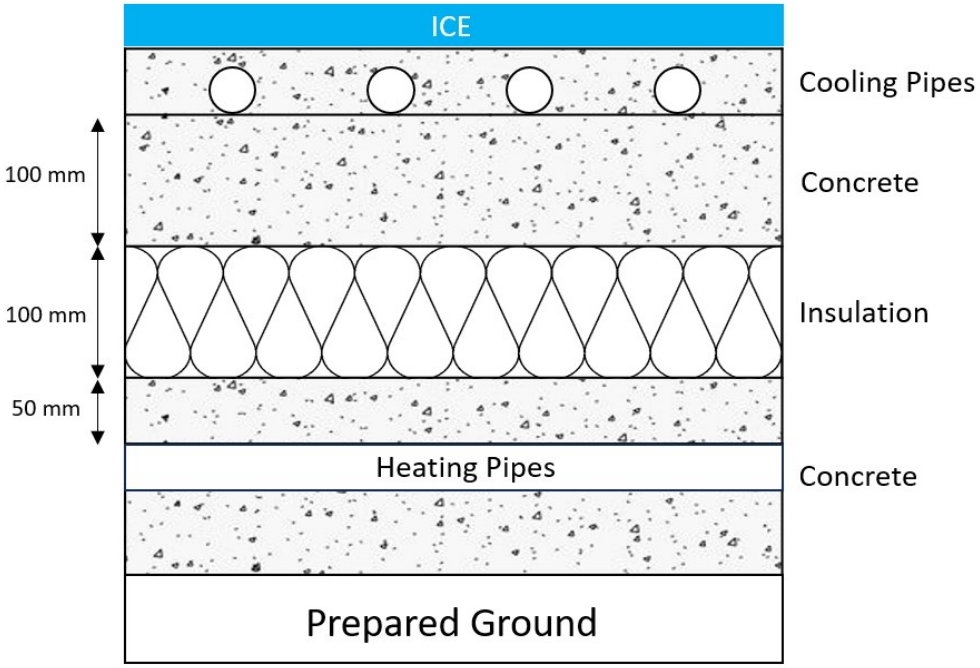

Figure 27: Ice rink floor, based on [8]

With thermal conductivities of 1.7 $\mathrm{W/m \cdot K}$ for concrete and 0.04 $\mathrm{W/m \cdot K}$ for the insulation (polystyrene), the overall heat transfer coefficient can be calculated:

$$U = \frac{1}{\frac{d_{concrete,top}}{k_{concrete}} + \frac{d_{insulation}}{k_{insulation}} + \frac{d_{concrete,bottom}}{k_{concrete}}} \quad (4)$$

where U is the overall heat transfer coefficient, $d_{concrete,top}$, $d_{concrete,bottom}$ and $d_{insulation}$ are the thicknesses of the materials and $k_{concrete}$ and $k_{insulation}$ are the thermal conductivities of the materials. Finally, assuming that the concrete layers surrounding the cooling and heating pipes have a temperature of -5°C and +5°C respectively [17], the heating demand for subfloor heating can be estimated:

$$\dot{Q}_{floor} = U * A_{ice} * \left(t_{pipes,heat} - t_{pipes,cool}\right) \quad (5)$$

where $\dot{Q}_{floor}$ is the subfloor heating demand, A_{ice} the area of the ice sheet, $t_{pipes,heat}$ the temperature of the heating pipes and $t_{pipes,cool}$ the temperature of the cooling piptes. This yields a heating demand for ground frost protection of 7 kW, which is constant throughout the entire operating season.

Space heating demand is based on a previous study of the of the Gimo ice rink by Pomerancevs [56], which resulted in the following correlation to keep the indoor temperature at 8°C:

$$\dot{Q}_{sh} = -2.0819 * t_{amb} + 91.551 \text{ [kW]} \quad (6)$$

where $\dot{Q}_{sh}$ is the space heating demand and t_{amb} the ambient temperature.

Melting pit heating demand is estimated as the amount of energy required to melt the ice that is transported away during the resurfacing process:

$$Q_{melting} = m_{ice} * (\Delta h_{fusion} + c_{p,water} * (t_{water} - 0°C) + c_{p,ice} * (0°C - t_{ice})) \quad (7)$$

where m_{ice} is the amount of removed snow, Δh_{fusion} the latent heat of fusion of water, $c_{p,water}$ and $c_{p,ice}$ the specific heat of water and ice, t_{water} the water temperature the ice is heated to and t_{ice} the temperature of the removed ice. The parameter values are found in Table 5. The heating demand per melting process amounts to 51.5 kWh.

Table 5: Melting pit heating demand assumptions

Parameter	Value	Unit
$\boldsymbol{m_{ice}}$	500	kg
$\boldsymbol{\Delta h_{fusion}}$	334	kJ/kg
$\boldsymbol{c_{p,water}}$	4.18	kJ/kg · K
$\boldsymbol{c_{p,ice}}$	2.03	kJ/kg · K
$\boldsymbol{t_{water}}$	10	°C
$\boldsymbol{t_{ice}}$	-2	°C

Dehumidification heating demand is based on a study of multiple ice rinks in Sweden by Pomerancevs et al. [13], which found the heating demand for dehumidification in ice rinks to follow the correlation:

$$\dot{Q}_{dh} = 1.7947 * \dot{m}_{dh} * V_{rink} \quad (8)$$

where $\dot{m}_{dh}$ is the flowrate of dehumidification air and V_{rink} the volume of the ice rink arena. $\dot{m}_{dh}$ is found with the equation:

$$\dot{m}_{dh} = \rho_{air} * ACH * \omega/1000 \quad (9)$$

where ρ_{air} is the density of air, ACH the Air Changes per Hour $[\frac{1}{h}]$ of the building due to infiltration of outdoor air and ω the humidity ratio of the wet air $[\frac{g_{H2O}}{kg_{air}}]$. The humidity ratio is calculated using the following equation:

$$\omega = \frac{M_w}{M_{air}} * \frac{p_{sat} * RH}{p_{atm} - p_{sat} * RH} \quad (10)$$

where M_w and M_{air} are the molar mass of water and air, respectively, p_{sat} the saturation pressure of the water vapor, p_{atm} the atmospheric pressure and RH the relative humidity of the air. The saturation vapor pressure is calculated according to the Buck equation:

$$p_{sat} = 0.61121 * e^{\left(18.678 - \frac{t_{amb}}{234.5}\right) * \left(\frac{t_{amb}}{257.14 - t_{amb}}\right)} \quad (11)$$

It is assumed that the number of ACH is 0.1 $\frac{1}{h}$ and that the dehumidification system turns on when the humidity ratio inside the rink surpasses 4.3 $\frac{g_{H2O}}{kg_{air}}$, corresponding to a dewpoint of 2°C, which is the recommended upper limit to prevent condensation on ice and other surfaces [13]. The temperature and relative humidity profiles are found in Appendix a and Appendix b.

Preheating is based on the assumption that multiple water storage tanks are used and that high temperature water demands, i.e. resurfacing and hot tap water, are preheated in a first and second tank together with the low and medium temperature demands, and then further heated in a next step after exiting the medium temperature storage tank (see Figure 28). The preheating temperature is set to 35°C.

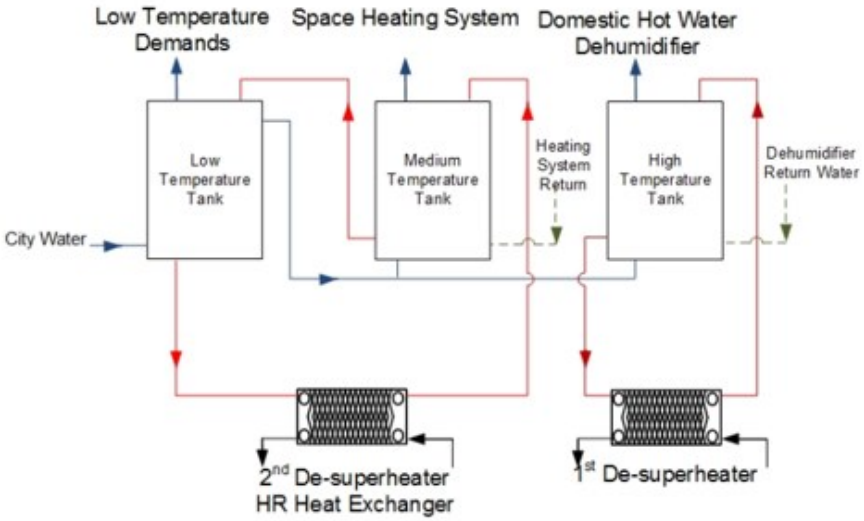

Figure 28: Heat Recovery and Water Storage Tank Configuration [31]

Resurfacing heating demand is the energy required to heat cold city water (8°C) up to the resurfacing temperature, which is assumed to be 60 °C and the amount of water per flooding is equal to 0.5 m^3, i.e. 500 kg [8]. The heating process for resurfacing water is split into two steps: 1) cold city water is preheated to 35°C and 2) preheated water is heated to the required 60°C flood water.

$$Q_{resurf,pre} = m_{flood} * c_{p,water} * (t_{pre} - t_{cold}) \quad (12)$$

$$Q_{resurf} = m_{flood} * c_{p,water} * (t_{flood} - t_{pre}) \quad (13)$$

where m_{flood} is the amount of flood water, t_{pre} is the preheating temperature, t_{cold} the temperature of the cold city water and t_{flood} the resurfacing water temperature.

Hot tap water heating demand is calculated similarly to the resurfacing water in two steps and the required water demand is calculated based on the assumption that hot tap water is mainly used for showering. Shower water is supplied by mixing hot tap water and cold city water. The water flowrates are calculated based on the equations [56]:

$$\dot{m}_{shower} * t_{shower} = \dot{m}_{hot} * t_{hot} + \dot{m}_{cold} * t_{cold} \quad (14)$$

$$\dot{m}_{shower} = \dot{m}_{hot} + \dot{m}_{cold} \quad (15)$$

where $\dot{m}_{shower}$ is the shower flow rate, t_{shower} the shower water temperature, $\dot{m}_{hot}$ is the flow rate of hot tap water, t_{hot} the temperature of hot tap water and $\dot{m}_{cold}$ the flow rate of the cold city water. The values that are used for the calculation are found in Table 6 [57]:

Table 6: Hot water heating demand assumptions

Parameter	Value	Unit
$\dot{m}_{shower}$	13	l/min
t_{shower}	43	°C
t_{hot}	65	°C
Showers per hour	20	-
Time per shower	5	min
Number of activity hours	7	h

4.3 Modelling

Steady-state conditions are assumed for all models. Wherever possible, field data from real installations is used as inputs to the simulation models. If it is not available, data is taken from existing literature or assumed. A comprehensive table with all the used assumptions, boundary conditions and input parameters is found in Appendix f.

4.3.1 Tools

The primary tool for modelling, simulation and system analysis is EES (Engineering Equation Solver). It is a commercial software program used for numerically solving non-linear algebraic and differential equations, and has an extensive in-built library for thermodynamic and transport properties of a multitude of working fluids. [58]

4.3.2 Boundary Conditions and Assumptions

To maintain the desired ice sheet quality, the evaporation temperature of the indirect ammonia, and CO_2 systems is fixed at -11°C. No superheat is assumed in any of the systems. The ammonia system uses open type reciprocating compressors, while the CO_2 and propane systems use semi-hermetic reciprocating compressors. The overall efficiencies from the compressors η_{tot} are extracted from manufacturer data and found in Appendix c, Appendix d and Appendix e. In the case of ammonia, which uses an open-type reciprocating compressor, the total calculated efficiency from the manufacturer data only refers to the shaft power and not the total power input. The electrical motor efficiency is not included and must be accounted for in the energy consumption calculation. It is assumed that a permanent magnet motor with an efficiency η_{motor} of 95% [59] is used.

Every system is equipped with heat recovery heat exchangers (HRHE), that are connected to hot water storage tanks. The water return and supply temperatures are 35°C/65°C and 20°C/35°C for the first and second HRHE, respectively. Heating demands that cannot be covered by heat recovery are covered by district heating. The water storage tanks are assumed to be perfectly insulated, i.e. there are no heat losses.

Heat that is not recovered is rejected to the ambient via a gas cooler in the CO_2 system, which has an approach temperature difference of 3 K in trans-critical operation and 7 K in sub-critical operation. In floating condensing (FC) mode, the gas cooler pressure follows the saturation pressure of CO_2 in sub-critical operation, and the optimum gas cooler pressure $P_{opt,gc}$ equation by Sawalha [31] in trans-critical operation, which starts at 22°C ambient temperature:

$$P_{opt,gc} = 2.7 * T_{gc,exit} - 6 \quad (16)$$

where $T_{gc,exit}$ is the gas cooler exit temperature. In the ammonia and propane systems, waste heat is rejected to the ambience by fans via the coolant with an approach temperature difference of 5 K. No subcooling is assumed. To avoid frost formation and keep the minimum exit temperatures at the condenser/gas cooler at 5°C, the minimum condensation temperature is fixed at 10°C for air cooled condensers/gas coolers and at 15°C for condensers cooled with a coolant.

4.4 Modifications

The system modifications are modelled and evaluated to find the most efficient system design for each refrigerant. After implementing the modifications individually, combinations of different features are evaluated to define state-of-the-art solutions.

4.4.1 Heat Recovery

Heat recovery is evaluated by first running the systems in floating condensing mode to find the minimum energy consumption to only provide cooling. Afterwards, the systems are run in heat recovery mode to cover the heating demands as well. Heat recovery mode means increasing the condensing temperatures/discharge pressure and therefore additional energy consumption. The feasibility of heat recovery is assessed by the heat recovery COP, which is explained in more detail in Section 4.6.2.

4.4.2 Direct System

A direct CO_2 system is implemented by changing the indirect reference system to a direct one with flooded evaporation and CO_2 as the heat transfer fluid. By eliminating the temperature difference between the refrigerant and the secondary fluid, the evaporation temperature can be increased. Further, the circulation pump for CO_2 requires considerably less energy than the circulation pump for regular secondary fluid brines. Field data of direct CO_2 ice rinks operating with flooded evaporation is available, which provide the data.

4.4.3 Internal Heat Exchanger

IHXs are modelled using a simple energy balance over the heat exchanger. The IHX is positioned as seen in Figure 16, so after the condenser/gas cooler and before the compressor.

$$\dot{Q}_{ihx} = \dot{m}_{ref} * (h_{evap,out} - h_{suct}) = \dot{m}_{ref} * (h_{c,out} - h_{exp}) \quad (17)$$

where $\dot{m}_{ref}$ is the refrigerant mass flow rate, $h_{evap,out}$ the evaporator outlet enthalpy, h_{suct} the suction enthalpy, $h_{c,out}$ the condenser/gas cooler outlet enthalpy and h_{exp} the expansion enthalpy. The efficiency of the IHX is defined as:

$$\eta_{ihx} = \frac{T_{1,} - T_1}{T_3 - T_1} \quad (18)$$

where $T_{1,}$ is the suction temperature, T_1 the evaporator outlet and T_3 the gas cooler/condenser outlet temperature. A reasonable efficiency for ice rink applications is 30%, which is the assumed efficiency in this work. Figure 29 shows the log(p)-h-diagram of a trans-critical R744 cycle with and without IHX.

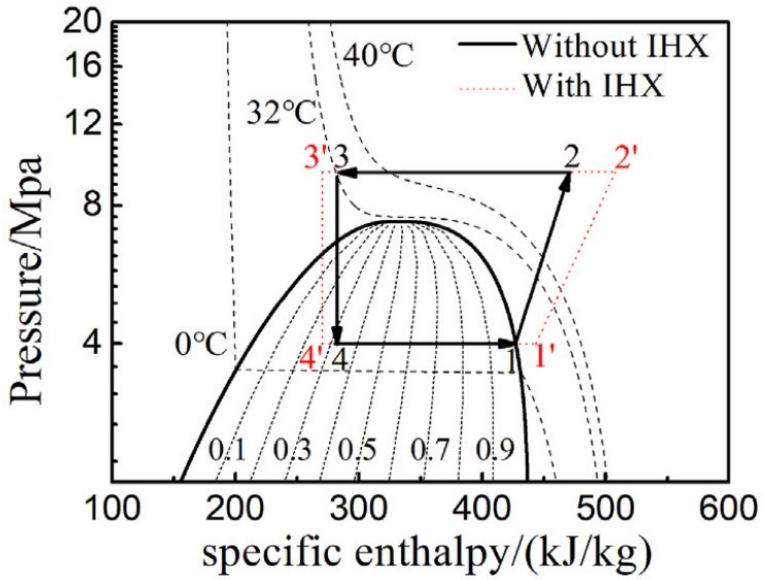

Figure 29: log(p)-h diagram with and without internal heat exchanger [34]

4.4.4 Flash-gas bypass

Flash-gas bypass will be implemented together with an IHX. Since the systems run in flooded evaporation, the reduced outlet quality due to the FGB bypass will lead to unsaturated vapor leaving the evaporator. Therefore, an IHX is used to ensure saturated/superheated conditions at the compressor suction inlet.

4.4.5 Parallel Compression

Parallel Compression is assumed to be constantly in operation. The auxiliary compressor is the same as the main one but operating with a different pressure ratio, The most efficient intermediate pressure level for the system performance is found iteratively.

4.4.6 Ejector

Ejector modelling is based on a few key ejector parameters. The first one is the mass entrainment ratio ω, which is the mass flow ratio between the suction inlet of the ejector $\dot{m}_{ej,s}$ and the primary inlet mass flow $\dot{m}_{ej,e}$:

$$\omega = \frac{\dot{m}_{ej,s}}{\dot{m}_{ej,e}} \quad (19)$$

The pressure lift Δp_{lift} describes the pressure difference between the lifted pressure at the ejector outlet $p_{ej,out}$ and the ejector suction pressure $p_{ej,s}$:

$$\Delta p_{lift} = p_{ej,out} - p_{ej,s} \quad (20)$$

Finally, the ejector efficiency η_{ej} describes the ratio between the maximum amount of recoverable work and the real amount of recovered work:

$$\eta_{ej} = \omega * \frac{h_{ej,comp,is} - h_{ej,s}}{h_{ej,e} - h_{ej,exp,is}} \quad (21)$$

where $h_{ej,s}$ is the ejector suction enthalpy, $h_{ej,e}$ is the enthalpy at the primary ejector inlet, $h_{ej,comp,is}$ is the enthalpy after isentropic compression from the suction pressure to the ejector outlet pressure and $h_{ej,exp,is}$ the enthalpy after an isentropic expansion from the ejector inlet to the ejector outlet pressure. [46]

Figure 30 and Figure 31 visualize the key ejector parameters in P-h-diagrams. Ejector modelling will only be evaluated in CO_2 systems since ammonia and propane operate at lower pressures and have lower work recovery potential.

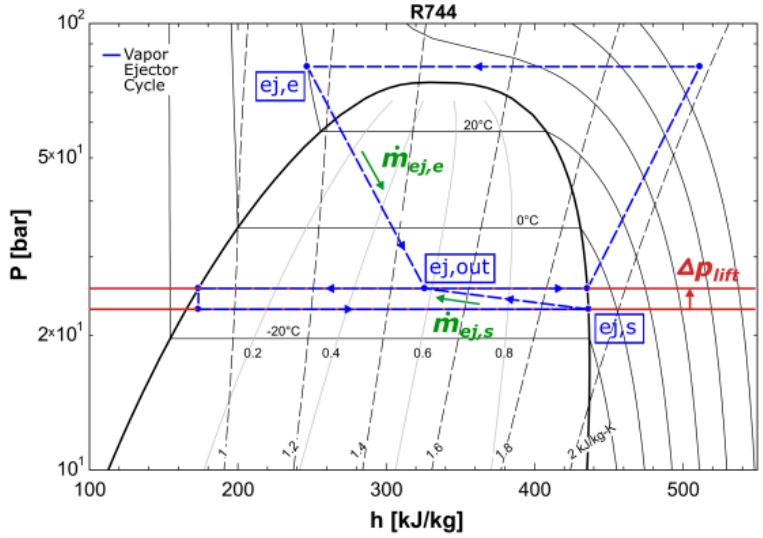

Figure 30: Ejector cycle in with R744 [46]

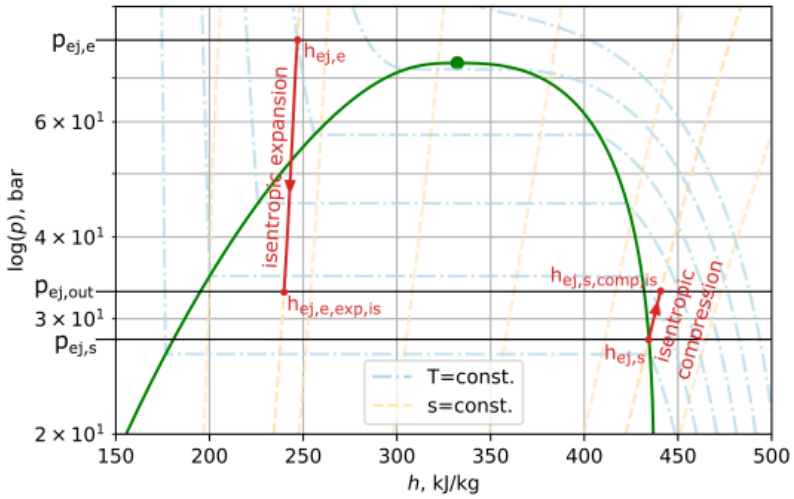

Figure 31: Relevant ejector enthalpies [46]

4.4.7 Subcooling

Subcooling is implemented in the form of dedicated mechanical subcooling (see Figure 32). A heat pump is added to the gas cooler exit of the CO_2 system and two operation strategies are evaluated. First, subcooling is run with a minimum temperature lift to only provide subcooling and heat is rejected to the ambient. Second, the subcooling heat pump is connected to the heat recovery system and provides low-grade heat to ensure a water supply temperature of 35°C. R290 and R717 are evaluated as refrigerants.

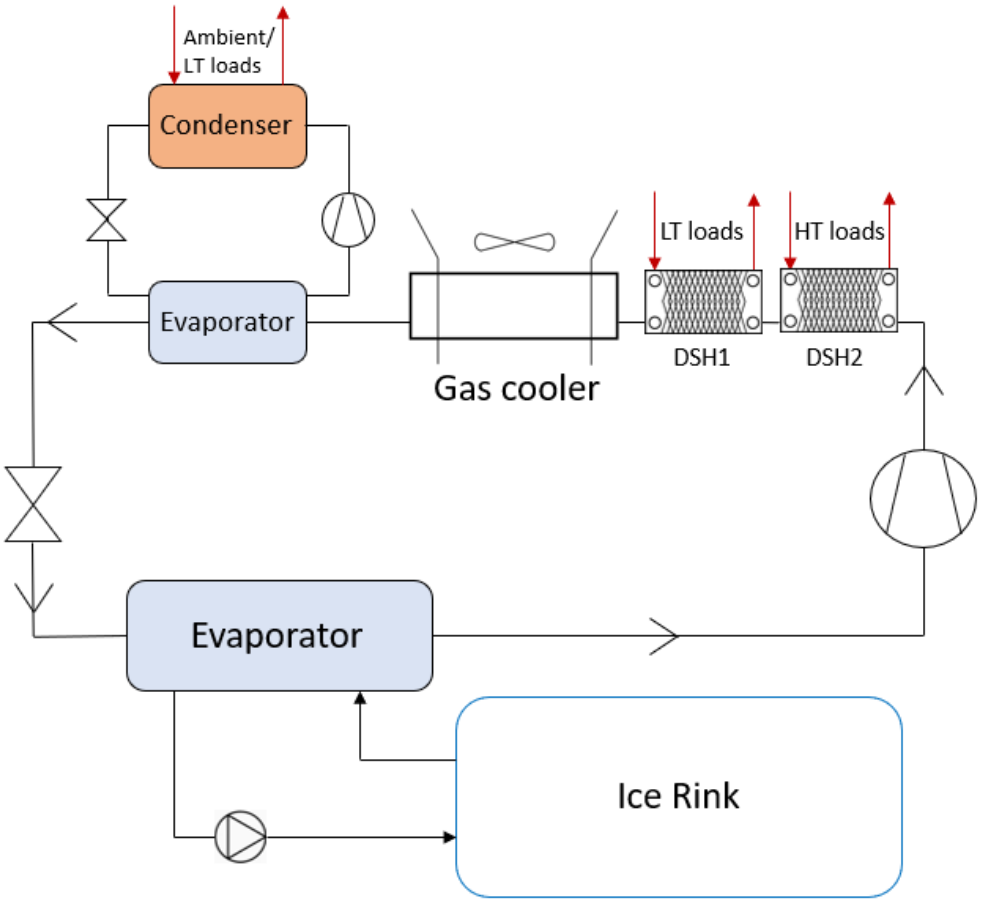

Figure 32: CO_2 system with dedicated mechanical subcooling

4.4.8 Auxiliary Heat Pumps

There are a variety of possible configurations that utilize auxiliary heat pumps to cover the heating demands and improve the performance of the systems. One of them can be seen in Figure 33 (LT HP). In order to cover the low-grade heating demands in the ammonia system, the condensation temperature is fixed at 40°C to achieve a supply temperature of 35°C of the HRHE in the coolant cycle which requires a high temperature lift and therefore a high amount of energy. By connecting a heat pump to the coolant cycle and the water storage tanks, the auxiliary heat pump can provide low-grade heat by using the heat of condensation and lifting it to the higher temperature level, thus allowing for lower condensation temperatures in the main ammonia cycle and increasing the efficiency. R290 and R717 are evaluated as refrigerants.

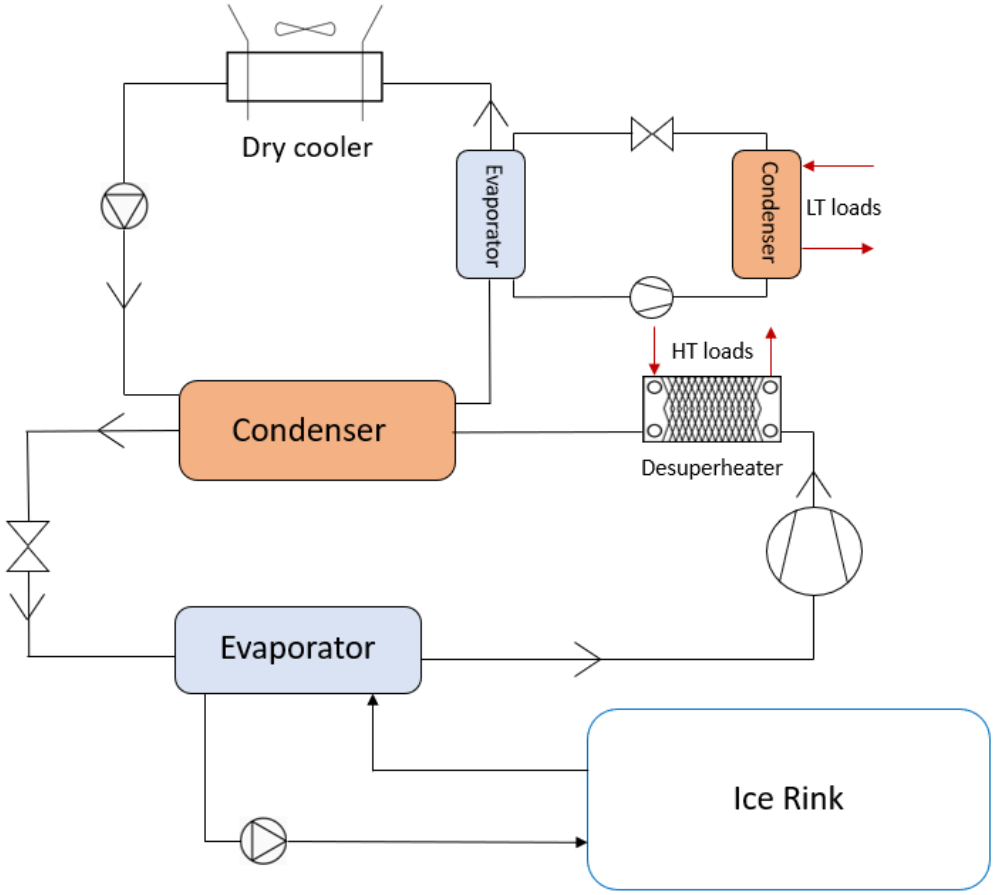

Figure 33: Ammonia system with auxiliary low temperature heat pump (LT HP configuration)

Another possible heat pump configuration for ammonia is seen in Figure 34 (HT HP). A heat pump is added to the coolant cycle to aid with both high- and low-grade heating demands. The condensing temperature is lowered to 35°C, which improves the COP on the one hand, while on the other hand less high-grade heat is available in the desuperheater and the HRHE can only provide water at 30°C and not the required 35°C. The auxiliary heat pump operates with R290 as the refrigerant and is controlled to provide high-grade heat from the condensing heat and higher temperature low-grade heat from the sub-cooler, which ensures a supply temperature of 35°C.

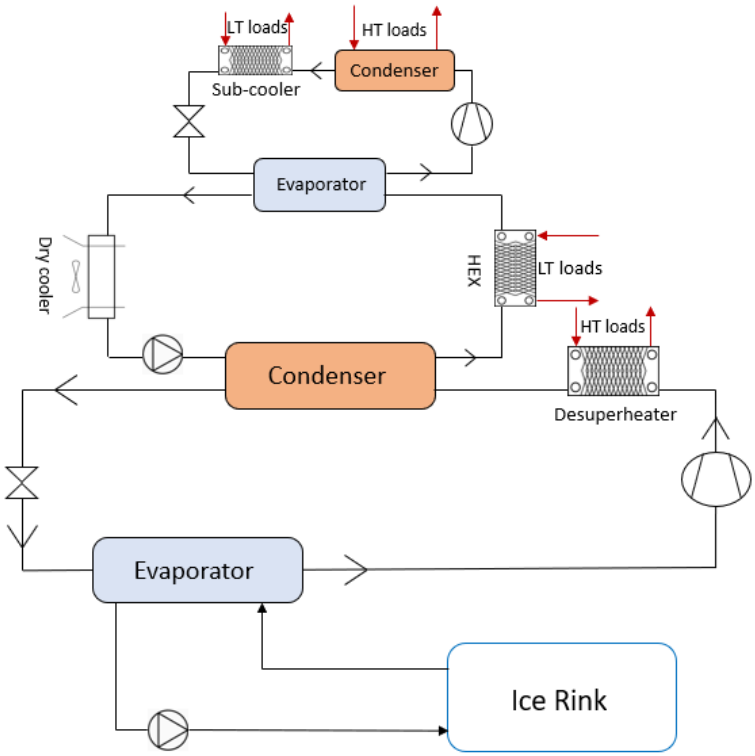

Figure 34: Ammonia system with auxiliary high temperature heat pump (HT HP configuration)

The addition of an auxiliary heat pump for the propane system is similar to the ones for ammonia. The heat pump will be used to supply high-grade heat, while the heat of condensation will be used to supply low-grade heat, reducing the condensation temperature of the reference operating conditions. The system layout is found in Figure 35 (HT HP). Again, R290 and R717 are used in the auxiliary cycle.

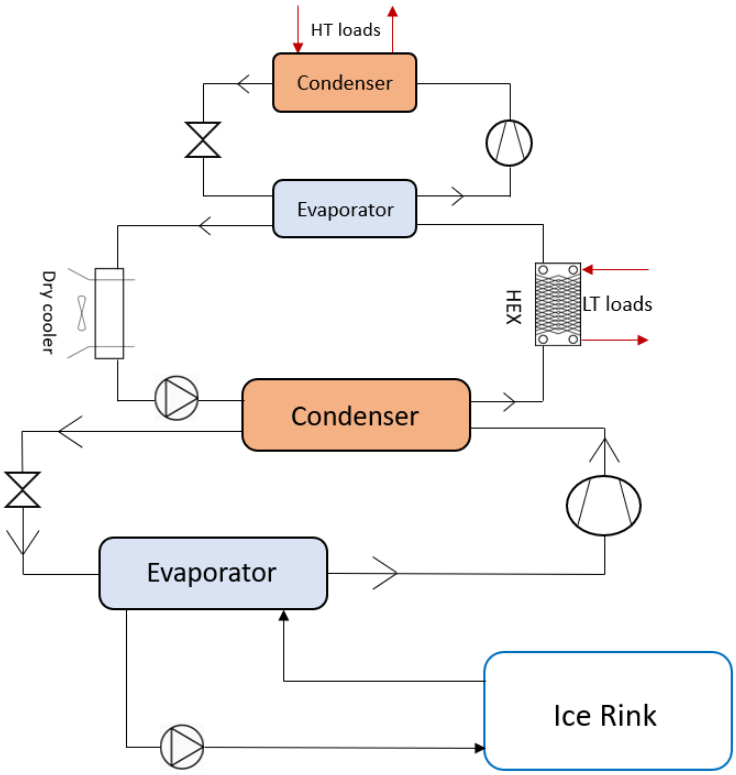

Figure 35: Propane system with auxiliary high temperature heat pump (HT HP configuration)

A final configuration that is evaluated for both ammonia and propane is seen in Figure 36 (CO2 HP). In the form of a cascade system, a trans-critical CO_2 heat pump is added on top of the main cycle. The systems are connected via a cascade heat exchanger, which acts as the condenser for the lower and as an evaporator for the upper cycle. The CO_2 heat pump is used to supply both high- and low-grade heating demands and eliminates the need for the coolant cycle.

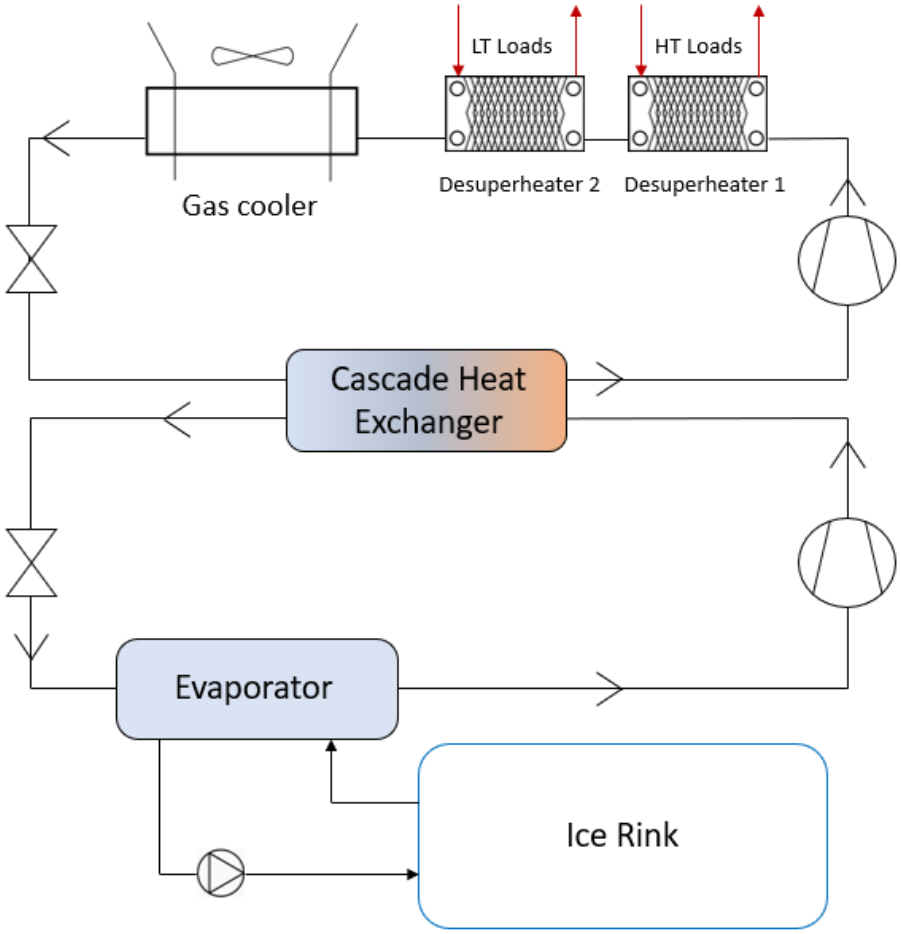

Figure 36: Indirect system with cascade configuration (CO_2 HP configuration)

4.4.9 Secondary Fluid

The effect of the secondary fluid choice on the system is evaluated based on the circulation pump power requirements, which are calculated based on the pressure drop. The pumping power is calculated using the following equation:

$$E_{pump} = \Delta p * \frac{\dot{V}}{\eta_p} * n_{circ} \quad (22)$$

where Δp is the pressure drop, $\dot{V}$ the flow rate of the secondary fluid, η_p the pump efficiency and n_{circ} the number of pipe circuits. The pressure drop is found using:

$$\Delta p = f_1 * \frac{L_{circ}}{d_i} * \frac{\rho}{2} * v^2 \quad (23)$$

where f_1 is the friction factor, L_{circ} the length of a secondary fluid pipe circuit, d_i the inner diameter of a pipe, ρ the density of the secondary fluid and v its velocity. The friction factor is calculated using the Gnielinski equation valid for transient/turbulent flows with a Reynolds number >2300:

$$f_1 = (0.79 * \ln(Re) - 1.64)^{-2} \quad (24)$$

where Re is the Reynolds number. The underlying assumptions and secondary fluid properties are presented in Table 7 and Table 8. Calcium chloride as the most common secondary fluid is utilized in the indirect reference systems, and aqua ammonia will be evaluated for use in state-of-the art systems.

Table 7: Secondary fluid properties

	Calcium Chloride	**Aqua Ammonia**
Concentration (≙ freezing temperature of -20°C) [%]	21	13.5
$\boldsymbol{\rho}$ $[\boldsymbol{kg/m^3}]$	1199	948
$\boldsymbol{c_p}$ $[\boldsymbol{J/kgK}]$	2985	4190
$\boldsymbol{\nu}$ $[\boldsymbol{m^2/s}]$	$3.8 * 10^{-6}$	$3.32 * 10^{-6}$
$\boldsymbol{Pr}$ [-]	25	33
$\boldsymbol{\lambda}$ $[\boldsymbol{W/mK}]$	0.629	0.492

Table 8: Assumptions pressure drop calculation

Parameter	**Value**	**Unit**
$\boldsymbol{d_i}$	0.015	m
$\boldsymbol{\eta_p}$	70	%
$\boldsymbol{L_{circ}}$	60	m
$\boldsymbol{n_{circ}}$	300	-

4.5 Control Strategy

The systems are run with fixed operating conditions for the evaluation of features and to define state-of-the-art systems, on which control strategies will be applied. The control strategies are individual for each system and aim at maximizing the efficiency of the systems.

4.6 Energy Analysis

The energy analysis of the systems is done by evaluating the performance of the systems against each other based on predefined performance indicators, focusing on the energy efficiency of the systems.

4.6.1 Governing Equations

Transferred energy over heat exchangers, evaporators, condensers, etc. is calculated using the enthalpy difference over the component Δh and the mass flow rate of the refrigerant:

$$\dot{Q} = \dot{m}_{ref} * \Delta h \quad (25)$$

The compressor work $\dot{E}_{comp}$ is found by using the overall efficiency of the compressors η_{tot}, and the isentropic expansion enthalpy over the compressor Δh_{is} for R290 and R744:

$$\dot{E}_{comp} = \dot{m}_{ref} * \Delta h_{is}/\eta_{tot} \quad (26)$$

and for R717:

$$\dot{E}_{comp} = \dot{m}_{ref} * \Delta h_{is}/(\eta_{tot} * \eta_{motor}) \quad (27)$$

The total electricity input $\dot{E}_{tot}$ in the systems is made up of the compressor work and of that of the auxiliary equipment, i.e. circulation pumps $\dot{E}_{pump}$ and dry cooler/gas cooler fans $\dot{E}_{fan}$:

$$\dot{E}_{tot} = \dot{E}_{comp} + \dot{E}_{pump} + \dot{E}_{fan} \quad (28)$$

4.6.2 Performance indicators

The annual energy use *AEU* is the sum of all consumed energy of the systems to cover all the demands over the operating season:

$$AEU = \sum E_{tot} + E_{aux} \quad (29)$$

where E_{tot} is the energy consumption of the refrigeration plant and E_{aux} the required energy to cover the heating demands that are not covered by the heat recovery system. To only have electricity as the energy input into the systems, it is assumed that an electric boiler with an efficiency of 100% is used as the auxiliary heat source. However, district heating is the most common heating method in Sweden and will be used in the economic evaluation.

The coefficient of performance (COP) is an indicator of the energy efficiency of the systems. It is the ratio of useful heat/cold and consumed energy. Different COPs are defined to have a clearer assessment of the system performance. The refrigeration COP COP_{ref} is an indicator of the cooling performance of system when running in floating condensing mode.

$$COP_{ref} = \frac{\dot{Q}_{ref}}{\dot{E}_{tot,ref}} \quad (30)$$

where $\dot{E}_{tot,ref}$ is the total energy consumption of the system to cover the cooling demands in floating condensing mode without heat recovery. To assess the performance of heat recovery and the additional energy consumption that comes with it, a heat recovery COP COP_{hr} is defined:

$$COP_{hr} = \frac{\dot{Q}_{heat,cov}}{\dot{E}_{tot} - \dot{E}_{tot,ref}} \quad (31)$$

where $\dot{Q}_{heat,cov}$ is the covered heat by the system running in heat recovery mode. Lastly, a COP is defined that considers all energy demands, the total COP COP_{total}:

$$COP_{total} = \frac{\dot{Q}_{ref} + \dot{Q}_{heat}}{\dot{E}_{tot} + \dot{E}_{aux}} \quad (32)$$

Where $\dot{Q}_{heat}$ is the total heating demand and $\dot{E}_{aux}$ is the auxiliary energy needed to cover the heating demand if the heat recovery is not able to do so. The total COP allows for a holistic comparison between all the systems.

The Seasonal Performance Factor SPF is a measure to assess the performance over the whole operating season, taking into account different operating conditions. It is the ratio of all covered demands over the consumed energy:

$$SPF = \sum \frac{Q_{ref} + Q_{heat}}{E_{tot} + E_{aux}} \quad (33)$$

4.7 Economic Analysis

The economic analysis will be conducted using different means of evaluation to assess the feasibility of individual features for retrofits. Table 9 shows the assumptions that are used in this work for the economic evaluation.

Table 9: Economic assumptions

Parameter	Value	Unit	Source
Electricity price	0.1	€/kWh	[60]
District heating price	0.086	€/kWh	[61]
Inflation rate	3	%	[62]
Discount rate	2	%	[62]
$\boldsymbol{N}$	20	years	Assumed

4.7.1 Annual Operation Cost

The annual operation cost AOC is the operational cost of each system to cover all the heating and cooling demands:

$$AOC = E_{tot} * e + E_{aux} * dh \quad (34)$$

where E_{tot} is the total energy consumption of the refrigeration system over the year, e the electricity price, E_{aux} the required auxiliary heat and dh the cost of district heating. The refrigeration systems and all auxiliary equipment use electricity, while heating needs that are not met are covered by district heating.

4.7.2 Justified Costs

The justified costs JC are the maximum investment costs that the individual modifications are worth investing into to achieve higher system efficiency and therefore lower energy costs. The justified costs are an investment and therefore calculated according to:

$$JC = \Delta AOC * \frac{1}{d - i} * \left(1 - \left(\frac{1 + i}{1 + d}\right)^{N}\right) \quad (35)$$

where ΔAOC is the difference in annual operation costs between the reference system and the system including the modification and equal to the energy cost savings, i the inflation rate which is used for estimating the annual increase of electricity and district heating prices and d the discount rate. If the investment cost for the modification is lower than the calculated JC, it is worth making. It is assumed that no equipment has any residual value after the lifetime for any of the systems/modifications. The justified costs are only calculated for ammonia and CO_2, since these are the systems that are already in use today and where retrofits in the form of modifications are worth considering.

4.8 Environmental Analysis

The environmental impact of the systems is assessed using the *Total Equivalent Warming Impact* (TEWI). It is a measure to assess the global warming impact of the refrigeration systems caused by their direct and indirect emissions. Direct emissions refer to emissions caused by refrigerant leakage and the disposal of the refrigerant after its lifetime. Indirect emissions refer to emissions caused by the electricity consumption of the system, i.e. emissions that are related to the production of the electricity. The TEWI is calculated according to the following equation [41]:

$$TEWI = (M_{leak} * N + M_{ref} * (1 - \kappa)) * GWP_{ref} + RC * AEU * N \quad (36)$$

where M_{leak} is the annual refrigerant leakage, N the number of operation years, M_{ref} the refrigerant charge of the system, κ the recycling factor, GWP_{ref} the Global Warming Potential of the refrigerants and RC the regional conversion factor, corresponding to the carbon intensity of the

power sector in CO_2 equivalent (CO_2-eq) per unit of electricity. The assumptions for the calculation are found in Table 10.

Table 10: TEWI assumptions

Parameter	Value	Unit	Source
$\boldsymbol{M_{leak}}$	Direct systems: 10 Indirect systems: 5	% of M_{ref}	[41]
$\boldsymbol{N}$	20	years	Assumed
$\boldsymbol{M_{ref}}$	Direct systems: 3 Indirect systems: 1	kg/kW	[41]
$\boldsymbol{\kappa}$	0.95	-	[41]
$\boldsymbol{GWP_{ref}}$	R717: 0 R744: 1 R290: 3 R404A: 3,922	$CO_2 - eq$	[24]
$\boldsymbol{RC}$	0.045	$kgCO_2 - eq/kWh_{el}$	[63] (2022 Average)

5 RESULTS AND DISCUSSION

5.1 Reference Ice Rink

The cooling demand of the reference ice rink is based on field data from August 2022 to March 2023. It is evaluated with a 5-minute resolution and calculated according to the ClimaCheck method. The cooling profile of ice rinks is not significantly dependent on the ambient temperature and stays mostly constant throughout the year, which is why the profile of a typical week is chosen to serve as the cooling profile of the reference ice rink. The selected profile can be seen in Figure 37.

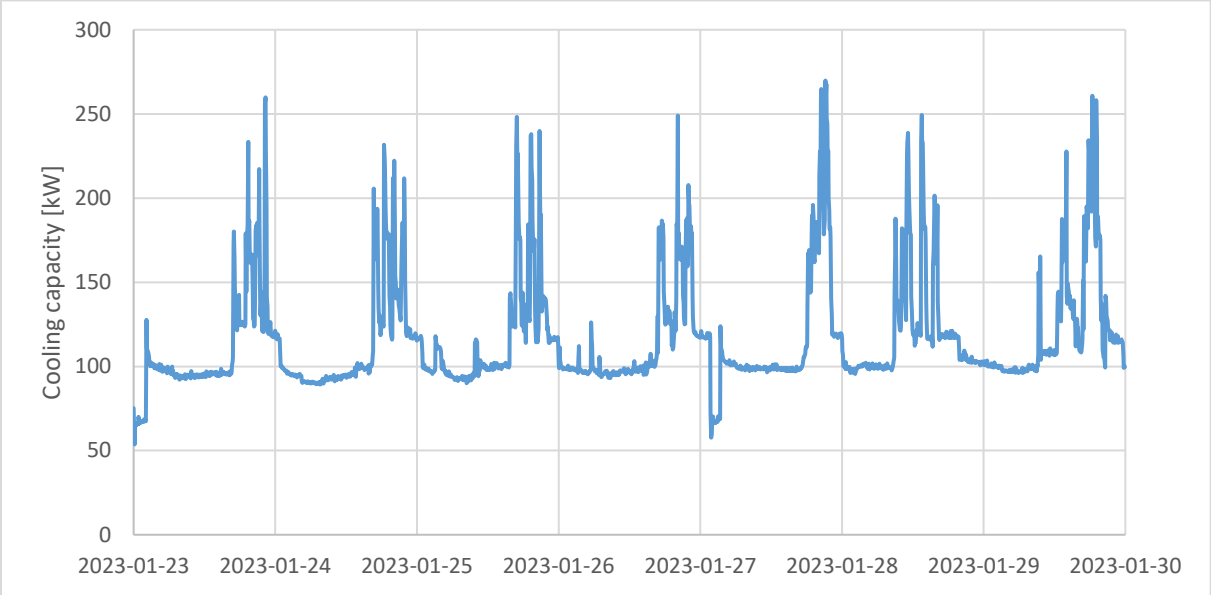

Figure 37: Gimo ice rink refrigeration profile 23.01.23-30.01.23

At night and in the morning hours, a cooling capacity of about 100 kW is needed to maintain the quality of the ice sheet. In the afternoon, when the skating activity begins, capacity peaks occur in regular intervals due to large heat loads caused by resurfacing processes, which require the refrigeration system to run at full capacity. Occasionally at night, the cooling capacity may drop down to 50 kW for short periods of time when the ice is found to be very cold.

The heating demand of the reference ice rink is made up of the sum of all the individual heating demands, which can be found in Figure 38 from August to March. Despite varying ambient temperatures, the total heating demand is relatively constant throughout the year, which is a defining characteristic of ice rinks. In the beginning of the season during the warmer months where the absolute humidity is at its highest, dehumidification contributes significantly to the heating demand. Space heating is constantly the biggest heating demand, peaking in December due to it being the month with the lowest temperatures. On the other hand, subfloor heating, melting pit heating, preheating, resurfacing and hot tap water demands are constant throughout the season.

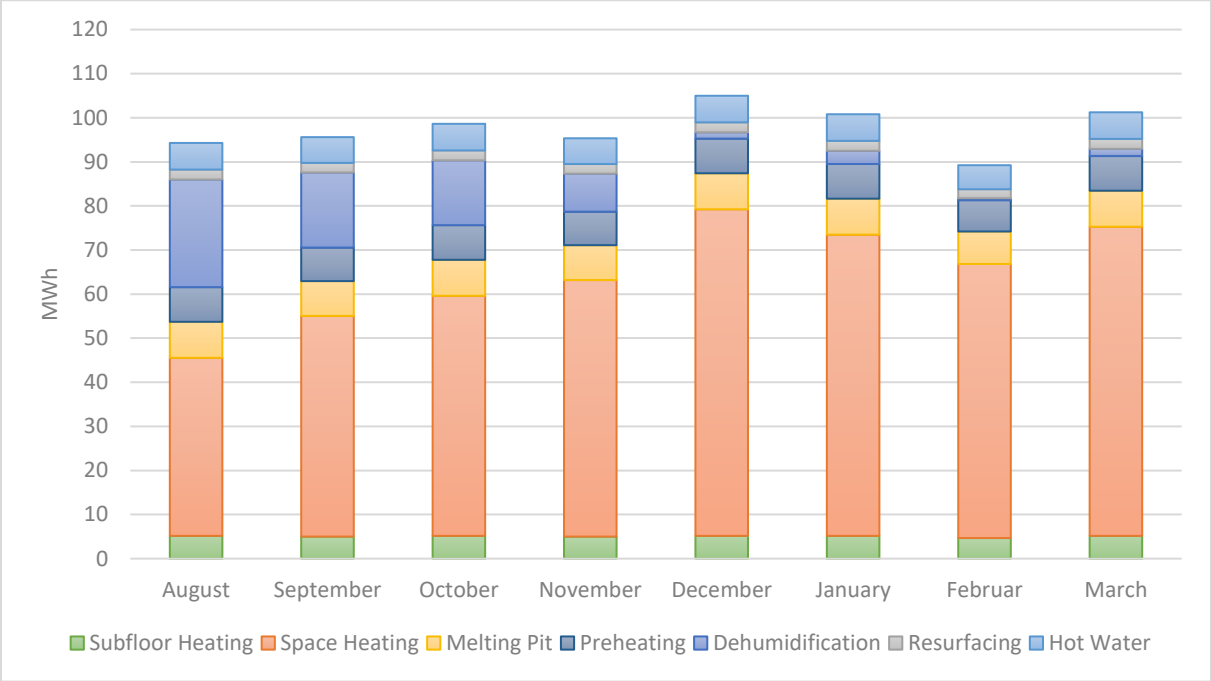

Figure 38: Monthly heating demand of the reference ice rink

Figure 39 shows the heating demand depending on the ambient temperature. The heating demands range from 113 kW at 30°C to 172 kW at -20°C ambient. Space heating demand declines, while dehumidification heating demand increases with increasing ambient temperatures. The remaining demands are not dependent on the ambient temperature.

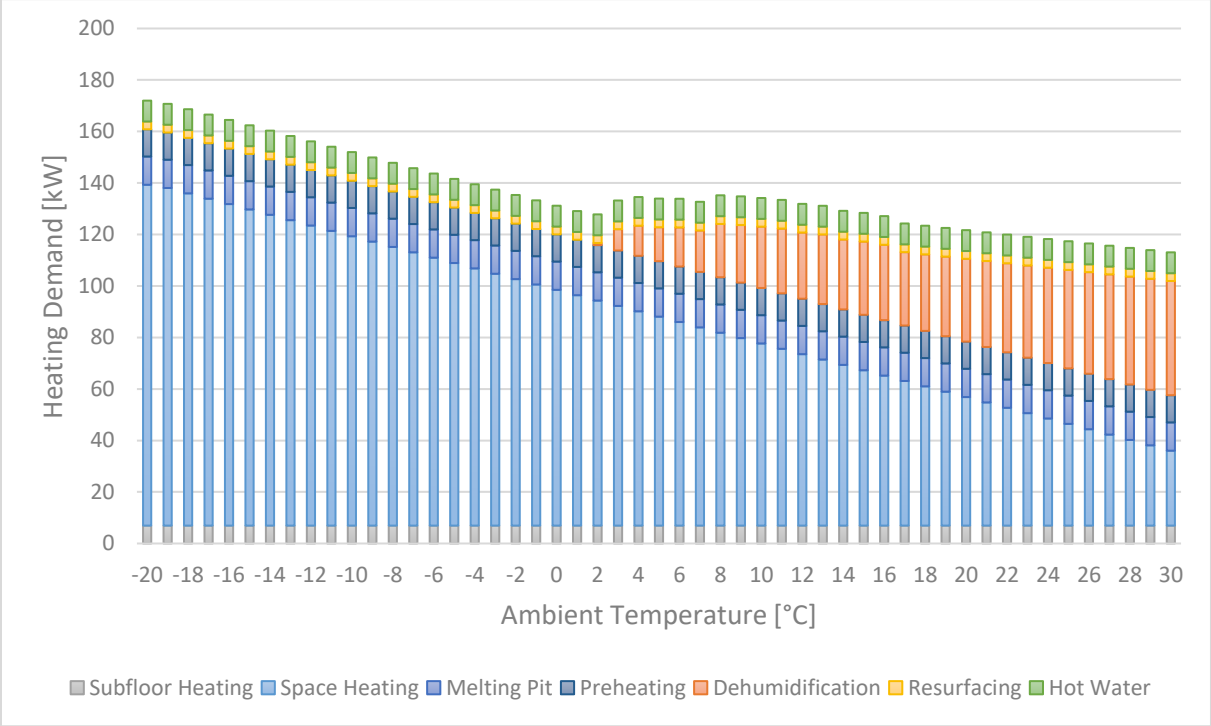

Figure 39: Heating demand against ambient temperature

5.2 Energy Performance

The first step for evaluating the different configurations is running the systems in floating condensing mode to see how much energy is needed to cover the cooling demands. Figure 40 shows the AEU of the reference systems defined in Chapter 3 for one operating season, without heat recovery. Ammonia requires about 193 MWh, carbon dioxide about 179 MWh and propane about 218 MWh of electricity to cover the cooling demands for one season, making CO_2 the most energy efficient solution and propane the least energy efficient solution. No heat rejection takes place, so all the heat needs to be rejected by the auxiliary equipment, i.e. dry coolers and gas coolers, which amount for a significant part of the energy consumption of the systems, in addition to the brine pumps in the secondary circuit to cool down the ice sheet. The auxiliaries account for roughly 35% of the total required energy in the propane and ammonia systems, and for about 26% in the CO_2 system. A gas cooler requires less energy than the coolant pump and dry cooler of the fully indirect systems, which explains the difference.

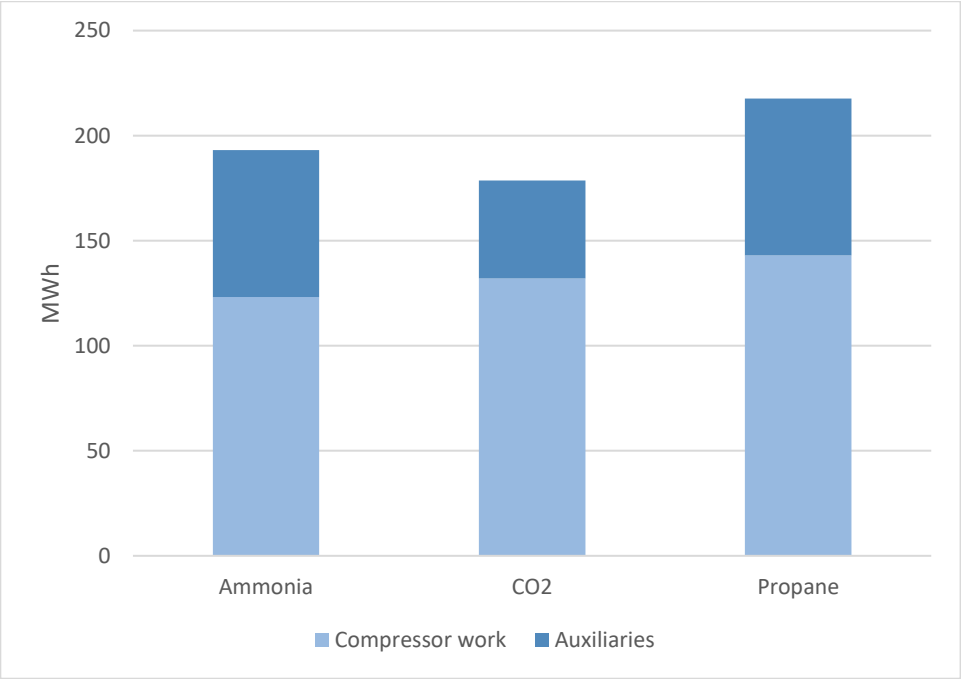

Figure 40: Annual energy use in floating condensing mode

Figure 41 shows the refrigeration COP and the number of operation hours against the ambient temperature. The refrigeration COPs are constant from -20°C to 3°C for all systems since they operate at their respective minimum condensing temperature. At 3°C ambient temperature, the systems raise the condensing temperature depending on the ambient temperature, increasing the pressure lift and thus compressor work, which reduces the COP. CO_2 is the most efficient solution for low ambient temperatures up until 18°C, followed by ammonia. At 18°C, ammonia starts to become more efficient than CO_2, indicating that it is a more suitable solution for warmer climates. Propane is constantly the worst performing refrigerant, however, it also starts to become more efficient than CO_2 at 22°C ambient temperature. For the reference location Gimo, a representative northern climate, the ambient temperatures are displayed using the temperature-bin method. The average ambient temperature is 4.6°C and the temperatures are below 18°C for most of the season, which makes CO_2 the best performing solution.

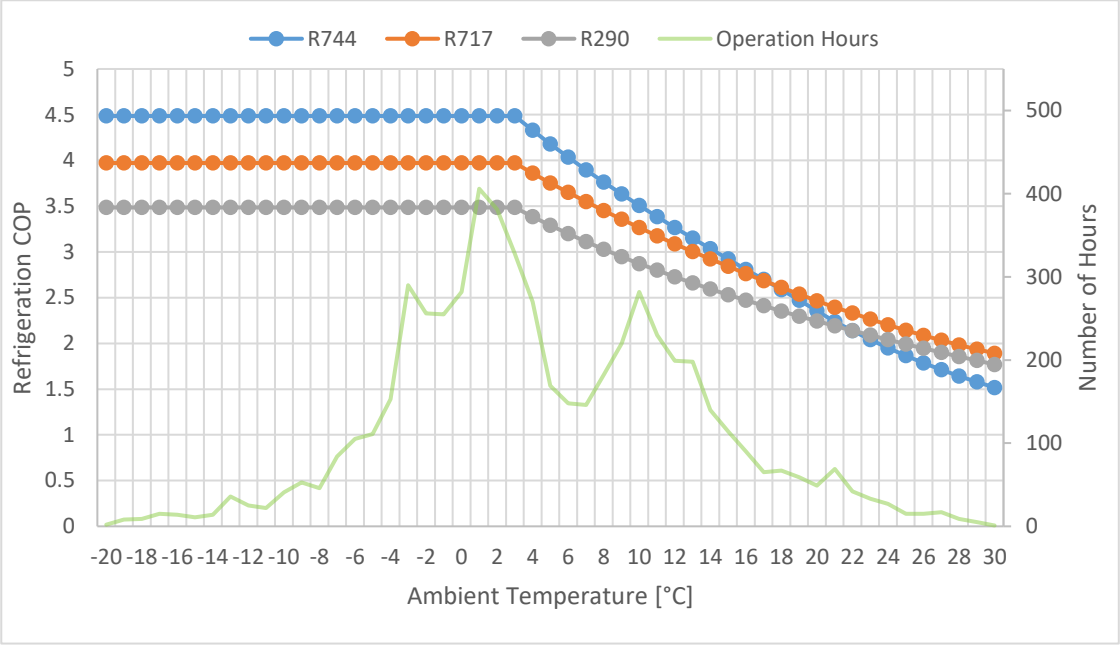

Figure 41: Refrigeration COP against ambient temperature

5.2.1 Heat Recovery

After evaluating the systems in floating condensing mode, heat recovery is evaluated by running them in heat recovery mode and taking into account the heating demands. The condensing temperature for ammonia is fixed at 40°C, which is required to ensure supply temperatures of 65°C/35°C for the high- and low-grade heat demands. However, it must be mentioned that a condensing temperature of 40°C for ammonia is the highest allowable condensing temperature for the selected compressor and leads to very high discharge temperatures, which are detrimental for the equipment and therefore it is one of the main goals of this work to find solutions that lower the condensing temperature, while still meeting the heating and cooling demands efficiently. The CO_2 system operates at a fixed discharge pressure of 80 bar, which is a common operating pressure for CO_2 systems. Propane operates at a condensing temperature of 50°C to ensure the discharge temperature is high enough to provide supply temperatures of 65°C for high-grade heating demands. The here defined operating conditions serve as the operating conditions for the reference systems (Chapter 3) for evaluating the state-of-the-art modifications. The ammonia system serves as the reference system against which the final systems are evaluated.

Figure 42 shows the AEU for the systems in heat recovery mode, covering all the heating demands. The additional energy consumption that is needed to lift the condensing temperatures/discharge pressures in the systems compared to operation in floating condensing mode is about 126 MWh for ammonia, 84 MWh for CO_2 and 215 MWh for propane. The energy increase for propane is exceptionally high and shows that heat recovery in this form is inefficient. Only CO_2 is able to cover all the heating demands solely with heat recovery, while the ammonia and propane systems need 20 and 27.5 MWh of additional heating to do so, respectively.

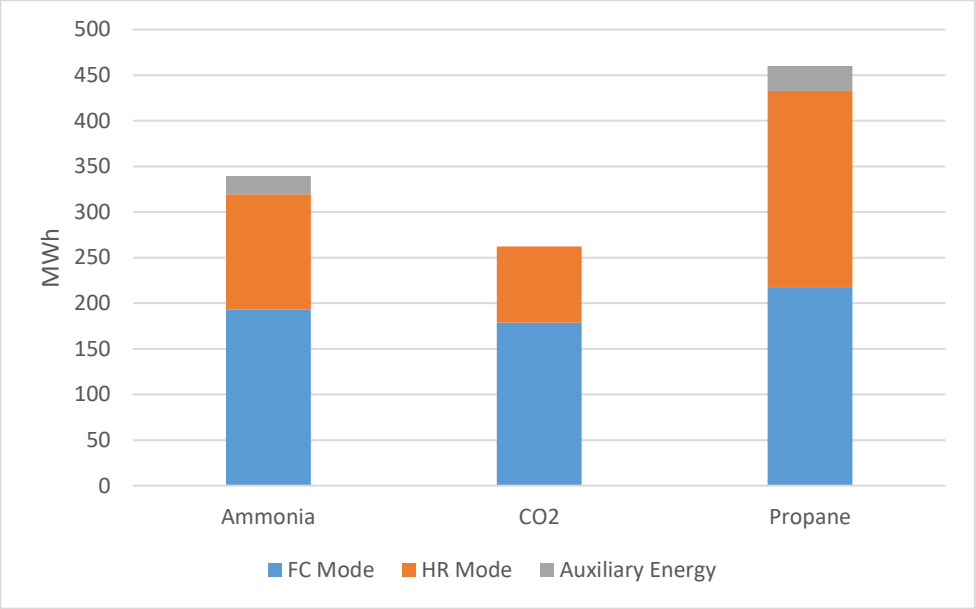

Figure 42: Annual energy use in heat recovery mode, cumulative

The available heat from heat recovery and heating demands over a season are shown in Figure 43, Figure 44 and Figure 45 for all systems. Ammonia can cover most of the heating demands with the exception of high-grade heat in the warmest months August and September and low-grade heat in coldest months of December and January, where a supplemental heating source is needed. A surplus of high-grade heat is available in the winter months due to lower needs for dehumidification.

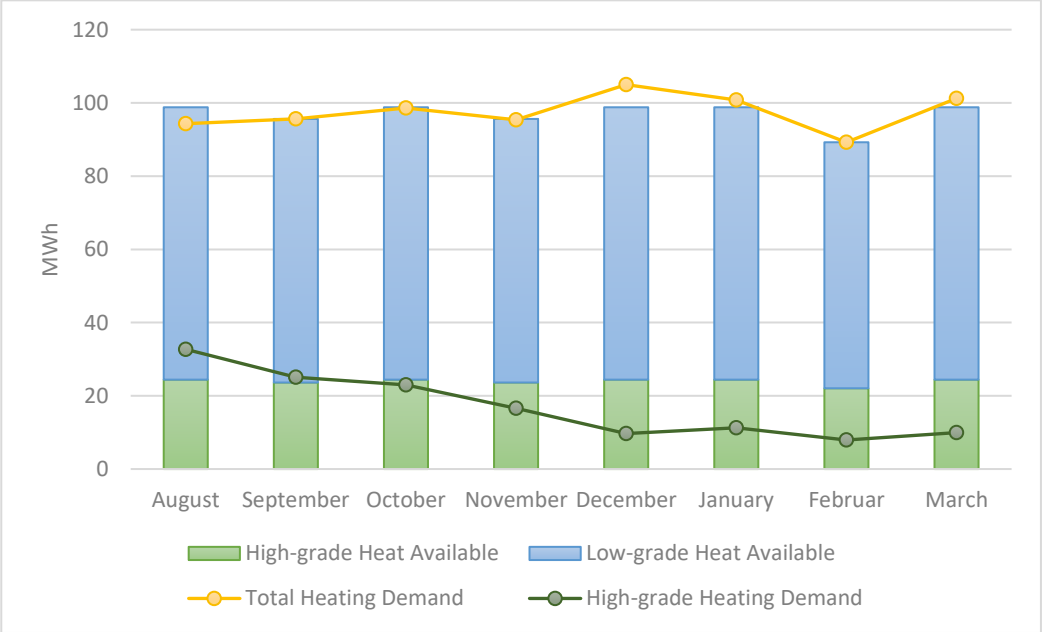

Figure 43: Ammonia reference system heat recovery performance for one operating season

CO_2 manages to cover all the heating demands, both high-grade and low-grade. Compared to the ammonia system, CO_2 has more high-temperature heat available thanks to the trans-critical operation. Similarly, to the ammonia system, there is a surplus of high-grade heat every month, and especially during the colder months.

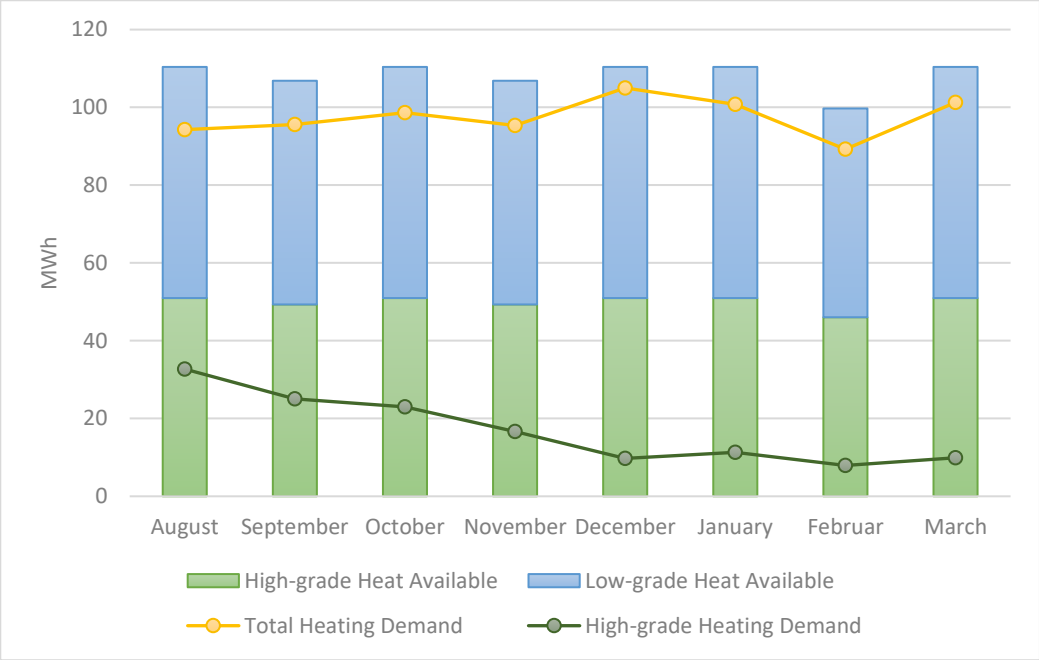

Figure 44: CO_2 reference system heat recovery performance for one operating season

The propane system is able to cover all the low-grade heating demands, but does not manage to cover the high-grade heating demands during the warmer months. The available superheat is not sufficient, which is why auxiliary heat is needed and different system configurations need to be investigated to improve the performance of the system.

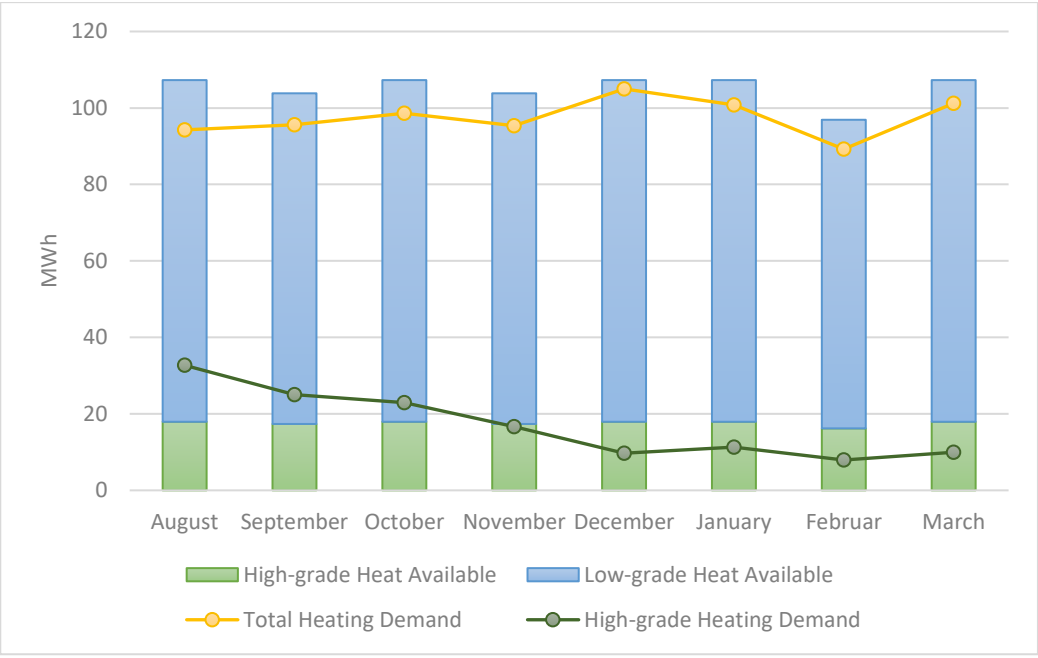

Figure 45: Propane reference system heat recovery performance for one operating season

The refrigeration COP for operation in floating condensing mode over one season, the heat recovery COP and total COP of the systems are presented in Figure 46. The performance of CO_2 is the highest for every COP, followed by ammonia and finally propane. The heat recovery COPs for ammonia and CO_2 are 6 and 9.3 respectively, which are significantly higher than that of an average heat pump. It must be mentioned that these high values are based on the underlying assumption that no heat

recovery takes place in floating condensing operation. Normally, ice rinks recover heat at least to some extent and do not reject all the heat to the ambient, as it is done here. Further, thanks to low-temperature heating demands such as subfloor heating and the melting pit the return temperatures are low, which allows for recovering great amounts of heat and a reduction of the auxiliary equipment energy consumption. Consequently, the heat recovery COPs for ammonia and especially CO_2 are exceptionally high. The global COP which includes both heating and cooling is higher than the COP for cooling alone, which shows that heat recovery improves the overall efficiency of the system. Therefore, it is concluded that heat recovery is feasible and efficient for both ammonia and CO_2. The heat recovery COP for propane is 3.5, which is comparable to a regular heat pump. Heat recovery slightly improves the energy efficiency of the system and is a favorable heating solution since it is already integrated in the refrigeration system and more cost efficient than entirely relying on district heating. Additionally, as mentioned earlier, the reference system layout for propane is not ideal, which means the system has great potential to adapt improvements and be optimized. Thus, heat recovery will also be used for propane.

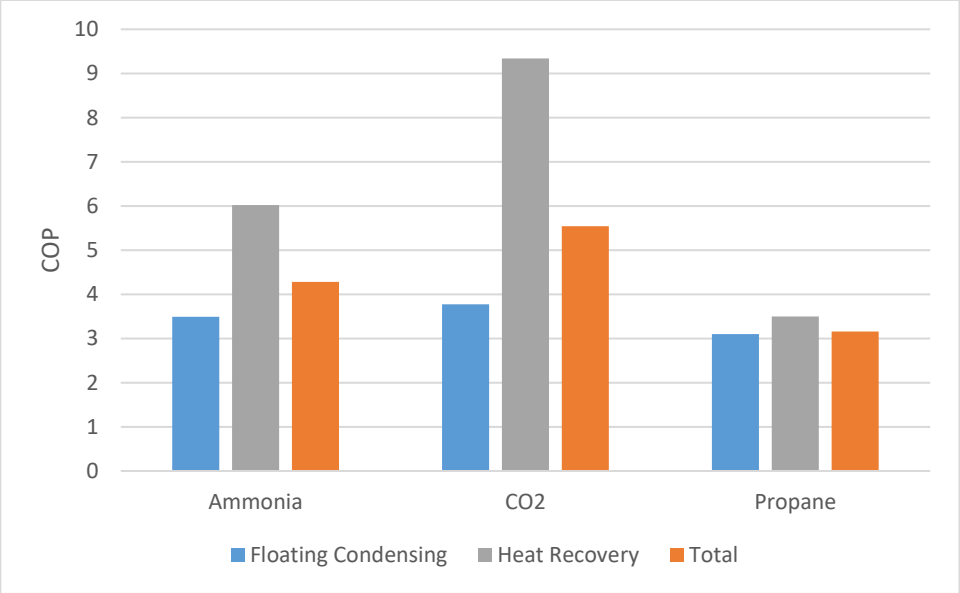

Figure 46: COP comparison between different operating modes

5.2.2 Ammonia

The modifications for the ammonia system, e.g. the addition of an internal heat exchanger, parallel compression, switching the secondary fluid and different auxiliary heat pumps and their effect on the system performance are presented as follows.

5.2.2.1 IHX

The addition of an internal heat exchanger for the ammonia system only has a minor effect on the system performance. Given to the superheat from the IHX, higher discharge temperatures can be achieved leading to more available heat in the superheater, while on the other hand the higher discharge temperatures are detrimental to the equipment and more compressor work is needed. In

the best case, the energy consumption can be decreased by 0.26% for an IHX with an efficiency of 10%, and the system performance starts to decrease for IHX efficiencies of 33% and above, as seen in Figure 47. For the specified operating conditions of the reference system in this work, an IHX does not have a significant positive effect, since a flooded evaporator is used and superheat is not necessarily needed.

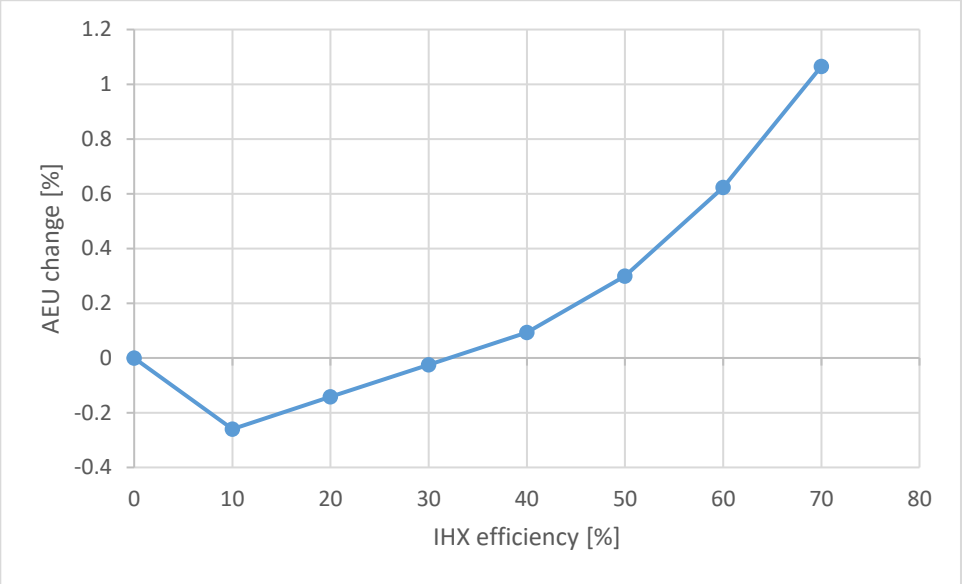

Figure 47:AEU change against IHX efficiency

5.2.2.2 Parallel Compression

Parallel compression has a considerable positive effect on the performance of the vapor compression cycle, and a minor effect on the performance of the system when including the heating demands. Depending on the pressure of the receiver, PC can lead to energy savings of approximately 6%. However, when taking the heating demands into account which need to be covered by the auxiliary heat source, the AEU energy savings hover around 1% for all intermediate pressures (see Figure 48). PC reduces the compressor work, but also reduces the amount of superheat that the desuperheater can recover for the high-grade heating demands, which leads to an increase of heat supplied by the auxiliary heater.

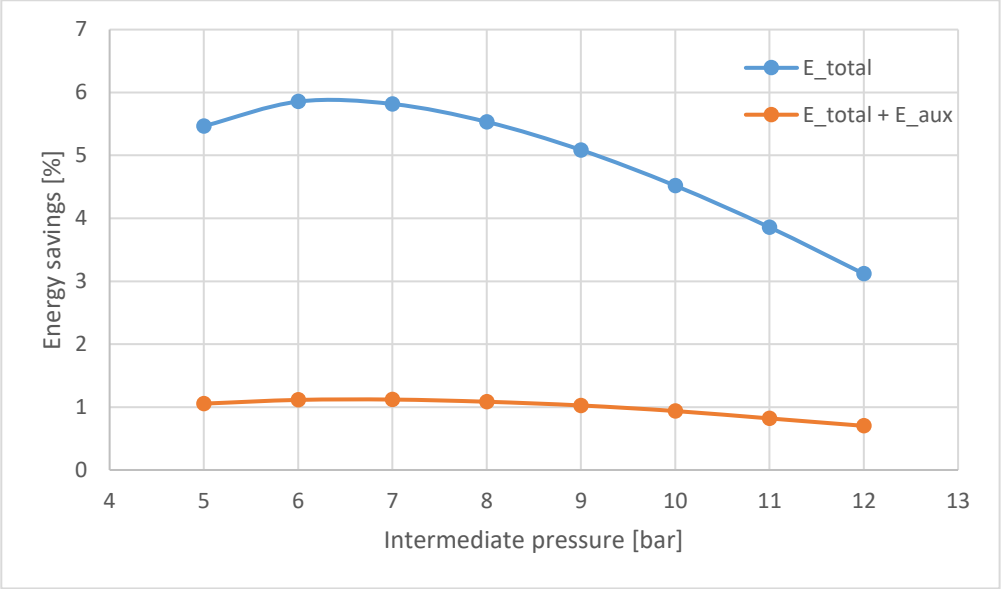

Figure 48: Ammonia parallel compression energy savings against intermediate pressure

5.2.2.3 Secondary Fluid

Switching from calcium chloride to ammonia water as the secondary fluid reduces the required annual pumping energy from 29.2 MWh to 16.6 MWh, which is a 43% reduction (see Table 11). It is an easy to implement and cost-effective measure and therefore recommended to do indirect ice rink systems. Since the same assumptions regarding the secondary fluid for all systems are used, the results for switching to aqua ammonia are the same for CO_2 and propane. As a simplification, fixed-speed pumps are assumed for all systems and a lower energy consumption can be achieved with variable-speed pumps.

Table 11: Comparison secondary fluids

	Calcium Chloride	**Aqua Ammonia**
Pump capacity	5 kW	2.85 kW
AEU pump	29.2 MWh	16.6 MWh
Energy savings	-	43%

5.2.2.4 Auxiliary Heat Pump

The effects of the different auxiliary heat pump configurations (see Chapter 4.4.8) compared to the reference system are found in Figure 49. By using a propane heat pump to cover the low-grade heating demands and lowering the condensing temperature of the main ammonia cycle, the annual energy consumption of the vapor compression cycle can be lowered by about 35 MWh, at the expense of lower high-grade heat in the available in the desuperheater. The additional heat required to cover the high-grade demands is higher than the energy savings in the main cycle, which leads to

an overall higher energy consumption than the reference system. R717 performs slightly better in the auxiliary heat pump than R290 for the same configuration, however, still no significant savings can be achieved. Adding an IHX to the arrangement allows for higher discharge temperatures and more superheat, resulting in 10 MWh energy savings compared to the reference system. The HT R290 heat pump arrangement combined with subcooling can cover all of the heating demands with the exception of a small part of high-grade heat in August and lowers the energy consumption by 14 MWh. Finally, the cascade solution with R744 in the upper cycle achieves the best results and energy savings of roughly 68 MWh.

Given their poor performances and limited possibilities to improve the efficiency, as well as high heat pump capacities, the LT HP configurations are deemed as not worth implementing. Even though the CO_2 heat pump shows the best results, the auxiliary heat pump capacity would be greater than that of the main ammonia cycle. In that case, it would be more beneficial to replace the ammonia system entirely with a new CO_2 system, saving on energy, costs and system complexity. The only option worth pursuing is the HT HP configuration. Since it is used to only upgrade part of the heat of condensation from the main cycle, the heat pump size stays within limits. Further, since the main ammonia cycle only requires additional heat to cover the heat demands during the warmer months, a control strategy can be applied to reduce the energy consumption in the winter months. It also offers more flexibility when used in ice rinks with deviating heating demands and demands different to the one defined in this work. The mass flow to the auxiliary heat pump as well as the condensing temperature can be adjusted to meet individual needs. Thus, the HT HP will be used in the SotA system.

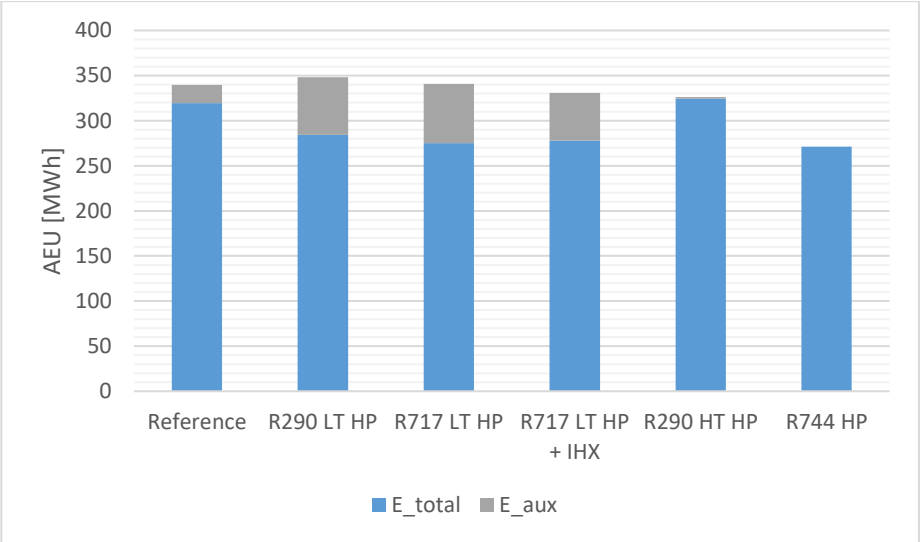

Figure 49: Ammonia AEU against different auxiliary heat pump configurations

5.2.2.5 Summary

Figure 50 summarizes the AEU changes of the different modifications with regards to the reference ammonia system. Adding an IHX to the reference system has virtually no effect and PC only a minor one. Changing the secondary fluid from calcium chloride to ammonia water leads to energy savings of 4% and is easy to implement. Of all the different heat pump configurations, the HT HP one is the most promising. The auxiliary CO_2 heat pump configuration is the most energy efficient one, but the large system capacity does not make it worth considering. PC has also been evaluated in combination

with the auxiliary HP configurations, however, due to lower condensation temperatures and therefore lower pressure lift in the main cycle, PC does not provide any additional savings. Finally, the State-of-the-Art ammonia system will use aqua ammonia as the secondary fluid and a HT HP to aid with covering the high-grade temperature demands.

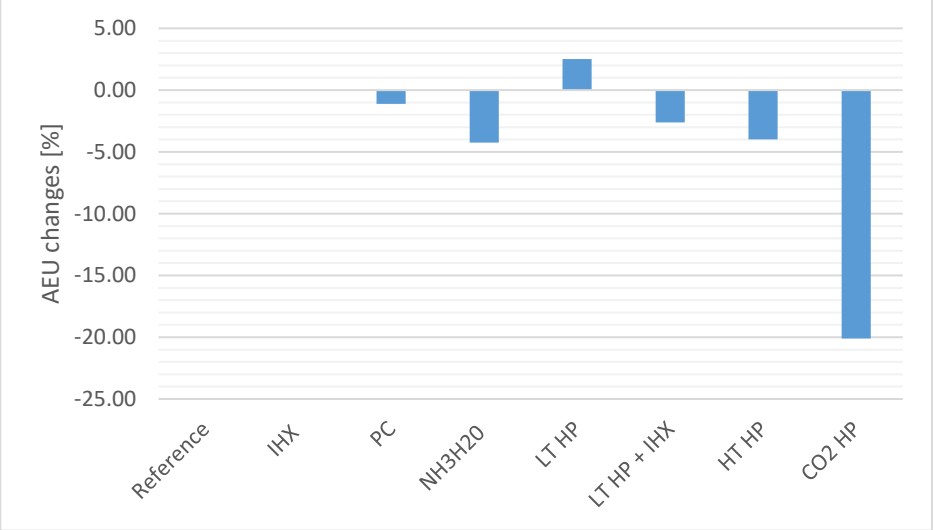

Figure 50: Evaluation of state-of-the-art modifications for ammonia system

5.2.3 Carbon Dioxide

The modifications for the carbon dioxide system, e.g. changing from an indirect to a direct system, the addition of an internal heat exchanger (and flash-gas bypass valve), parallel compression, subcooling, and ejectors and their effect on the system performance are presented as follows.

5.2.3.1 Direct System

Field data from two Swedish ice rinks using flooded evaporation show an average evaporation temperature of-8°C, which is three Kelvin higher than the evaporation temperature for the reference indirect CO_2 system. Further, the CO_2 circulation pump requires about 88% less energy than the brine pump. Together, the direct system manages to reduce the AEU by roughly 47 MWh, which equals about 18% (see Figure 51). Even though the switch to a direct CO_2 system requires the use of metal pipes which are more expensive than regular plastic pipes used to circulate brines under the ice rink, the energy savings that come with it are extensive and justified.

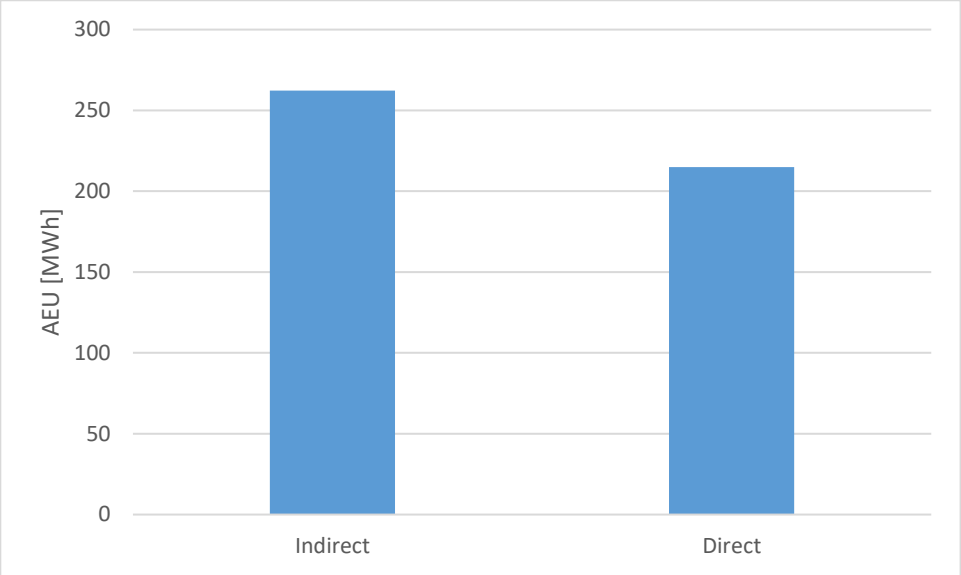

Figure 51: AEU comparison between indirect and direct operation

5.2.3.2 Internal Heat Exchanger

The addition of an IHX to the reference CO_2 system does not benefit the system performance with regards to the here specified operating conditions. Since the system is already able to cover all the heating demands, the additional heat caused by higher discharge temperature due to the IHX does not contribute useful heat. On the contrary, the increased compressor work caused by the higher suction temperatures outweighs the benefit of the introduced subcooling and increases the overall energy consumption of the system, for any amount of superheat by the IHX. Figure 52 shows the increase of the AEU when introducing an IHX for different IHX efficiencies. However, an IHX can still be useful. Under different circumstances, the additional heat might allow for lower discharge pressures, potentially increasing the efficiency of the system.

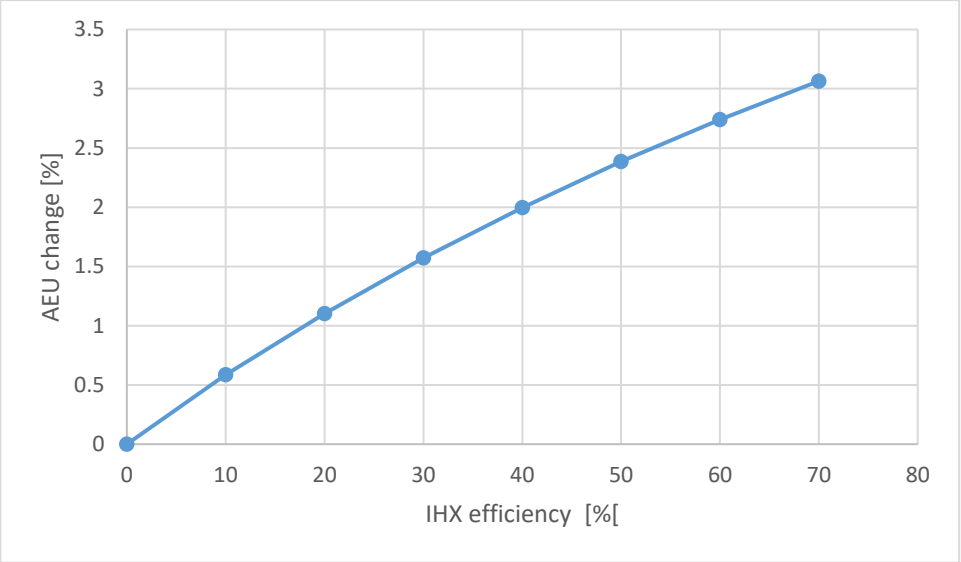

Figure 52: AEU change by IHX compared to reference system

5.2.3.3 Flash-gas Bypass + Internal Heat Exchanger

The FGB should be accompanied by an IHX. Mixing the saturated refrigerant at the evaporator outlet with the expanded vapor from the intermediate pressure level results in two-phase refrigerant, which cannot be fed to the compressor. Superheat is therefore necessary for safe operation, which the IHX can provide. The practical advantages of a FGB, e.g. improved flow distribution in the evaporator, are outside of the scope of the used modelling tool and not included in this work. The specified intermediate pressure level of the FGB receiver does not have any effect on the simulation results either, since the refrigerant mass flow that is compressed remains the same and is independent of the FGB. Thus, the results of adding a FGB to the reference system are identical to the ones of adding an IHX.

5.2.3.4 Parallel Compression

There is a tradeoff when choosing the intermediate pressure level between evaporator inlet quality and the amount/pressure ratio of the compressed flash gas when using parallel compression. A lower intermediate pressure means a lower evaporator inlet quality and more flash gas being compressed in the parallel compressor, which are both beneficial, however, it also means that the pressure ratio in the parallel compressor is higher. Therefore, there is an optimum that can be found, and it can be seen in Figure 53 in the form of the AEU change. An intermediate pressure of 38 bar is the most efficient, yielding AEU savings of 6% compared to the reference system while still covering all the heating demands. PC leads to notable energy savings and is thus a favorable modification in CO_2 ice rinks.

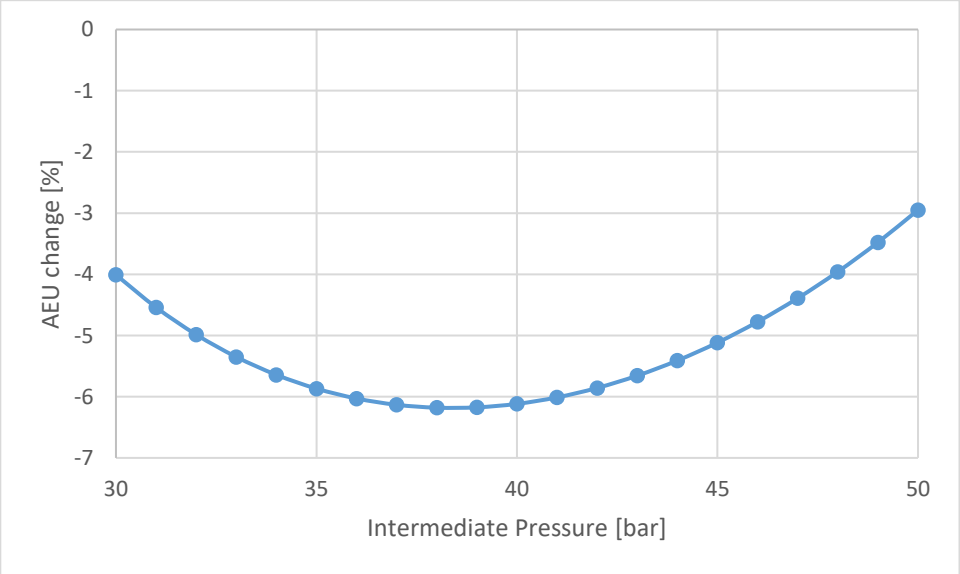

Figure 53: CO2 AEU change against PC intermediate pressure

5.2.3.5 Subcooling

Subcooling is evaluated in the form of dedicated mechanical subcooling using the refrigerants R290 and R717, both with and without heat recovery for different amounts of subcooling. The results can

be seen in Figure 54. In the case of no heat recovery, the condensing temperature is controlled in floating condensing operation rejecting heat to the ambient, keeping a minimum pressure ratio of 1.5 between the suction and discharge pressure. Evaluating the total COP shows that high degrees of subcooling reduce the overall performance of the system substantially. Even though subcooling reduces the energy consumption of the main cycle by reducing the refrigerant mass flow, it also reduces the amount of recoverable heat, which worsens the performance of the system by introducing the need for auxiliary heat. The difference between using ammonia and propane as the refrigerant is only marginal. Subcooling without heat recovery is therefore not an advantageous solution in ice rinks.

When running the subcooling system in heat recovery mode, i.e. increasing the condensing temperature and coupling it to the heat recovery system, subcooling achieves positive results. The thermal demands are still met, and the benefit of reducing the refrigerant mass flow in the main cycle is greater than the additional energy consumption by the subcooling heat pump. Ammonia performs slightly better than propane as the refrigerant, and an optimum amount of subcooling is found at around 15 K, increasing the total COP by about 7%, which makes it worth considering.

Subcooling could be a useful solution in warmer climates, where higher ambient temperatures cause higher discharge pressures and higher gas cooler exit temperatures. Heat which cannot be rejected to the ambient can be rejected by the subcooling system, potentially increasing the overall efficiency of the system.

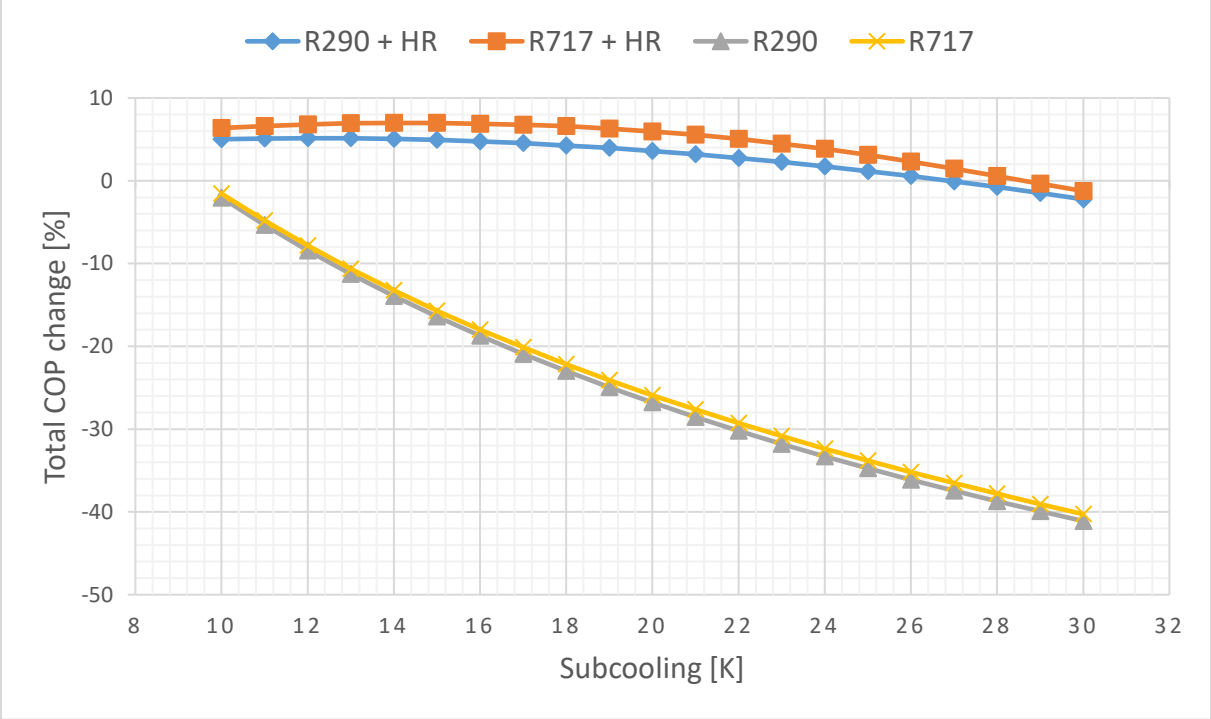

Figure 54: Total COP for different dedicated mechanical subcooling operation strategies

5.2.3.6 Ejector

The ejector is integrated into the system with an ejector efficiency of 30% and a pressure lift of 2 bar. This leads to energy savings of about 17 MWh (see Figure 55) or about 6.5%. However, it must be

mentioned that the results are based on the assumption that a constant ejector efficiency of 30%, which is on the higher end of ejector efficiencies, and pressure lift of 2 bar is used for the entire operation period. Field data [46] shows that ejector operation fluctuates and a constantly high ejector efficiency of 30% are very difficult to achieve, which would lower the performance. Detailed control strategies are necessary to ensure good operation.

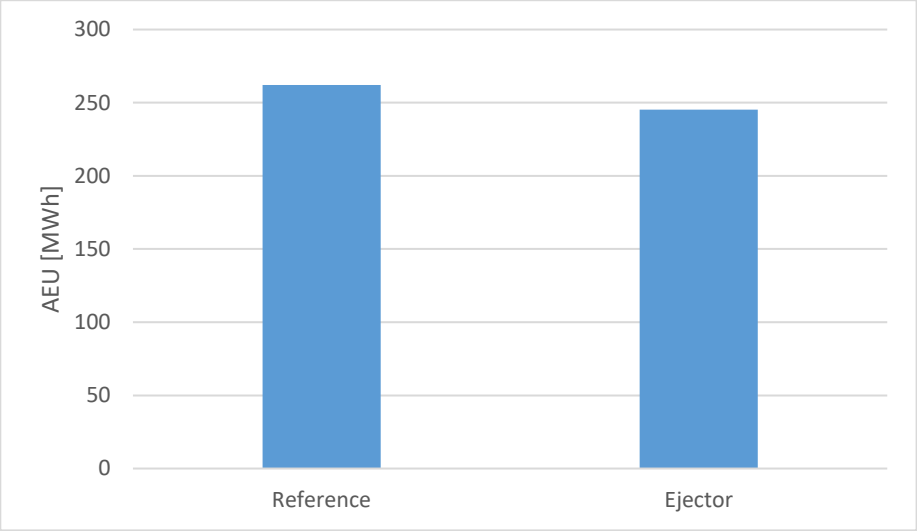

Figure 55: AEU comparison reference system and system with ejector

5.2.3.7 Summary

A summary of the different features for a CO_2 system can be found in Figure 56. Switching from an indirect to a direct system yields energy savings of about 18% compared to the reference system. Where such a retrofit is not possible and the indirect CO_2 stays in operation, it is worth changing the secondary fluid to aqua ammonia, which saves about 4.8% of energy every year. Adding an IHX/FGB+IHX slightly worsens the performance of the system and is worth considering in DX CO_2 systems, where superheat is required to ensure safe operation. Subcooling in combination with HR can lower the AEU by about 6.5%. Assuming idealized operating conditions, an ejector can also save up to 6.5% of energy annually. PC can achieve energy savings of 5.9% without adding much complexity to the system and easy operation. Even though SC + HR and ejectors achieve higher energy savings in this analysis than PC, the savings are only marginally higher. In the case of SC + HR, the savings come at the expense of adding an additional heat pump, increasing both system complexity and cost. In the case of ejectors, real operation differs from idealized conditions and the energy savings in a real installation will most likely be lower than the here presented results. Finally, the State-of-the-Art CO_2 system will be a direct system in combination with parallel compression.

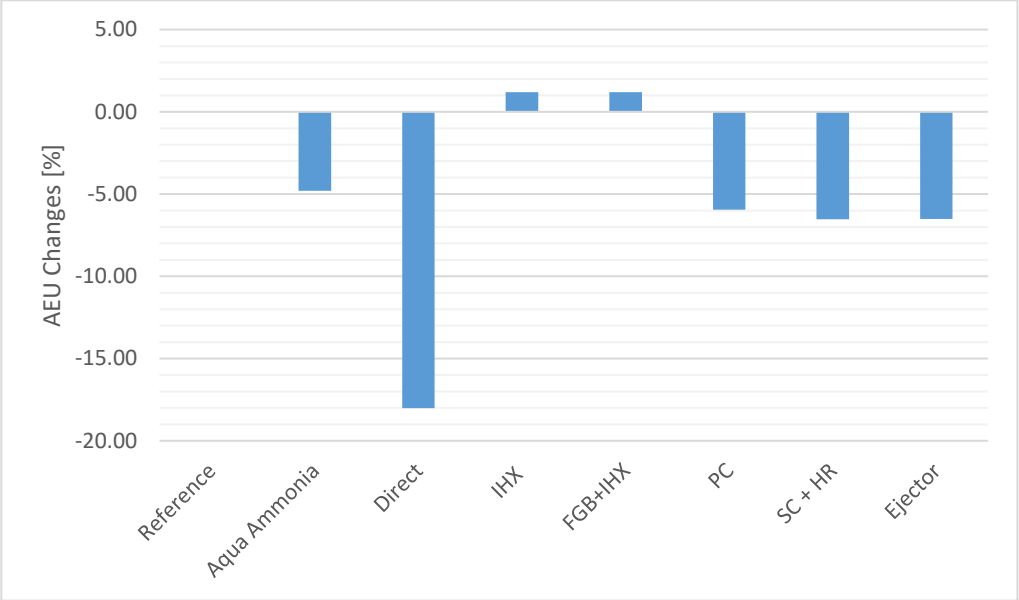

Figure 56: Evaluation of state-of-the-art modifications for CO_2 system

5.2.4 Propane

The modifications for the propane system, e.g. the addition of an internal heat exchanger, parallel compression and different auxiliary heat pumps and their effect on the system performance are presented as follows.

5.2.4.1 Internal Heat Exchanger

Adding an IHX to the reference propane system significantly improves the performance, as can be seen in Figure 57. For an IHX efficiency of 30%, energy savings of 7.4% can be achieved. Additionally, propane compressors often require suction gas superheat in the range of 20-30 K or higher to minimize the risk of refrigerant solution in the oil, which can be provided by the addition of an IHX.

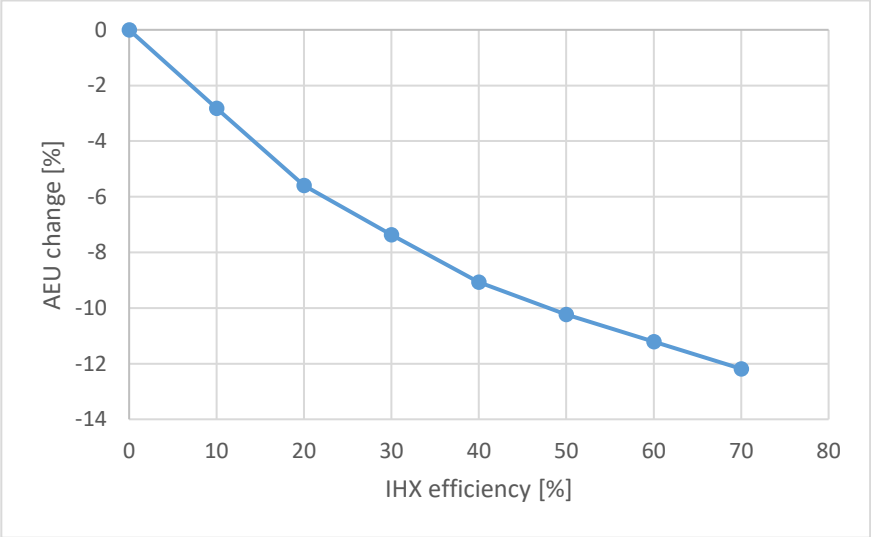

Figure 57: Propane AEU change against IHX efficiency compared to reference system

5.2.4.2 Parallel Compression

The high pressure difference between the condensing and evaporating temperature in the reference propane system allows PC to have a positive influence on the performance. Figure 58 shows the AEU change against the intermediate pressure, and an optimum is found at around 9 bar suction pressure for the parallel compressor, yielding energy savings of around 6.7%. Nonetheless, the system still largely relies on the auxiliary heating source to cover the high-grade heating demands.

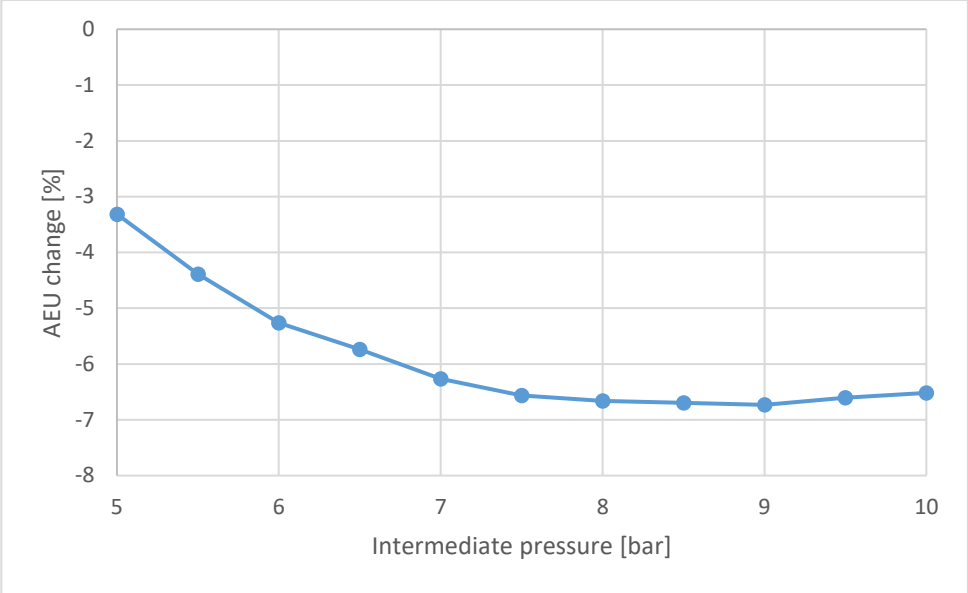

Figure 58: Propane AEU change against PC intermediate pressure

5.2.4.3 Auxiliary Heat Pump

The results of the different heat pump configurations for propane are found in Figure 59.The HT HP configurations using R290 and R717 in the auxiliary cycle led to energy savings of 45 and 67 MWh, respectively and eliminate the need for auxiliary heating. Similar to ammonia, the CO2 HP configuration is able to achieve the highest energy savings with 180 MWh, at the expense of requiring a large CO2 heat pump on top of the main propane cycle.

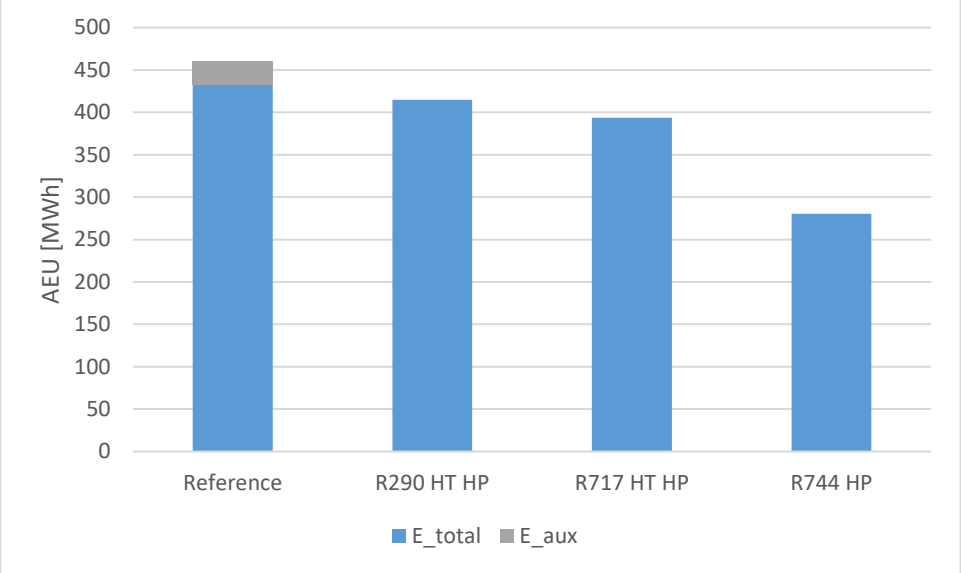

Figure 59: Propane AEU against different heat pump configurations

5.2.4.4 Summary

A summary of all the different modifications is displayed in Figure 60. Every modification is able to reduce the energy consumption, which makes combination of different features interesting to investigate. Replacing the secondary fluid with aqua ammonia is an easy and cost-effective measure and will be used in the final system. Adding an IHX and PC save 7.4% and 6.7%, respectively and together they achieve an energy reduction of 8.2%. Subcooling lowers the vapor quality of the receiver, reducing the amount of vapor entering the parallel compressor and making parallel compression less effective. Similarly, PC used together with the HT HP configuration does not simply add up the energy savings. The auxiliary heat pump achieves energy savings of 14.5% and when used together with PC, the savings amount to 19.1%. The CO_2 heat pump saves the most energy with 39% compared to the reference system. Despite this, the cascade heat pump configuration is not worth considering since two large vapor compressions systems are required. A single trans-critical CO_2 system providing both heating and cooling is both more energy and cost efficient than having an even larger CO_2 that only provides heating, and having a similarly large propane system to provide cooling. The most promising feature for propane is the HT HP configuration with R717 in the auxiliary cycle, in combination with aqua ammonia as the secondary fluid, which will be used in the final system.

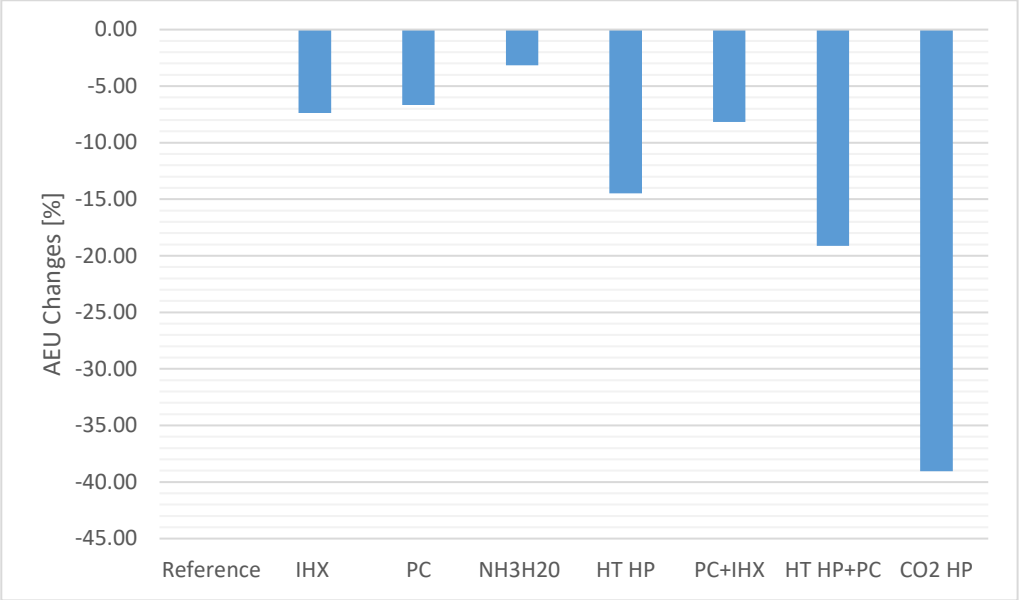

Figure 60: Evaluation of state-of-the-art modifications for propane

5.2.5 Final systems

The final system configurations, their control strategy and finally their energy performance are presented in this chapter. The systems are compared against the reference ammonia system, which is the most common ice rink refrigeration system found today.

5.2.5.1 Ammonia

The final configuration of the ammonia system can be seen in Figure 61. It is an indirect system operating with ammonia water as the secondary fluid and it covers the heating demands partly from the available superheat in the primary ammonia cycle and from its heat of condensation. An auxiliary heat pump operating with R290 is used to cover the remaining heating demands, drawing heat from the coolant cycle/condensation heat and additional heat is rejected via a dry cooler.

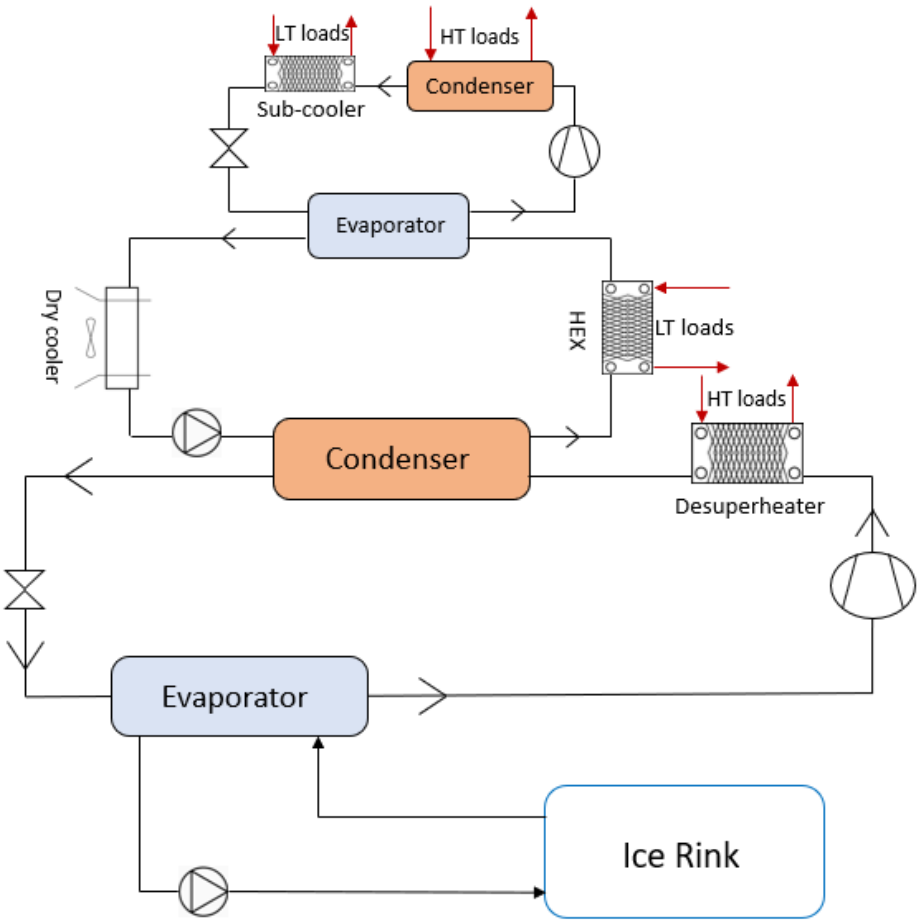

Figure 61: Ammonia State of the Art System

A control strategy is applied to match the available heat to the heating demands. In the warmer months of August, September and October the auxiliary heat pump operates at a condensation temperature of 65°C to supply high-grade heat in the form of condensation heat and enough low-grade heat in the sub-cooler to cover the remaining demands. The mass flow through the auxiliary heat pumps evaporator can be adjusted to match the demands. In the months following November, the desuperheater in the main cycle is able to cover all of the high-grade demands. Therefore, the auxiliary heat pump runs at a lower condensation temperature of 35°C to cover the remaining low-grade heating demands. This is a simplified control strategy, however, it offers flexibility in operation and allows demand-based control. The heat recovery performance of the system with the applied control can be seen in Figure 62. The system is able to cover all the demands in every month during the operating season.

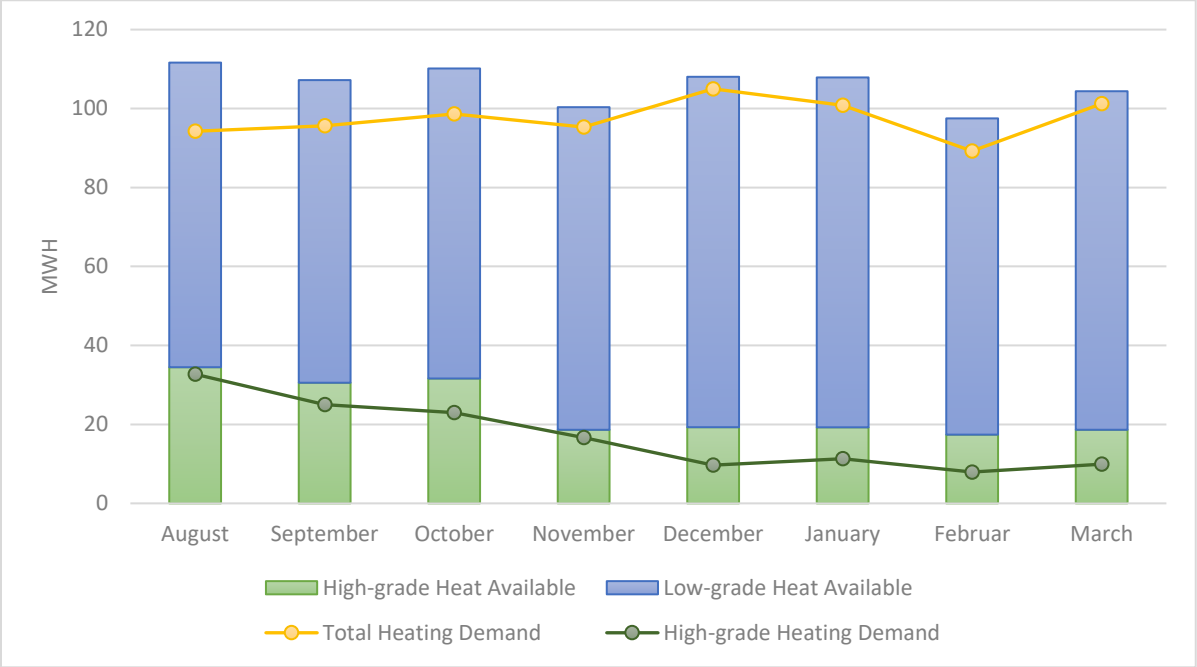

Figure 62: Ammonia State-of-the-Art system heat recovery performance

5.2.5.2 CO_2

The final CO_2 system configuration is seen in Figure 63. It is a direct system using pump circulated CO_2 to cool down the ice sheet. Parallel compression is used to lift the pressure to trans-critical levels and two desuperheaters are used to recover heat. Additional heat is rejected via a gas cooler, which is controlled to achieve the most efficient system performance.

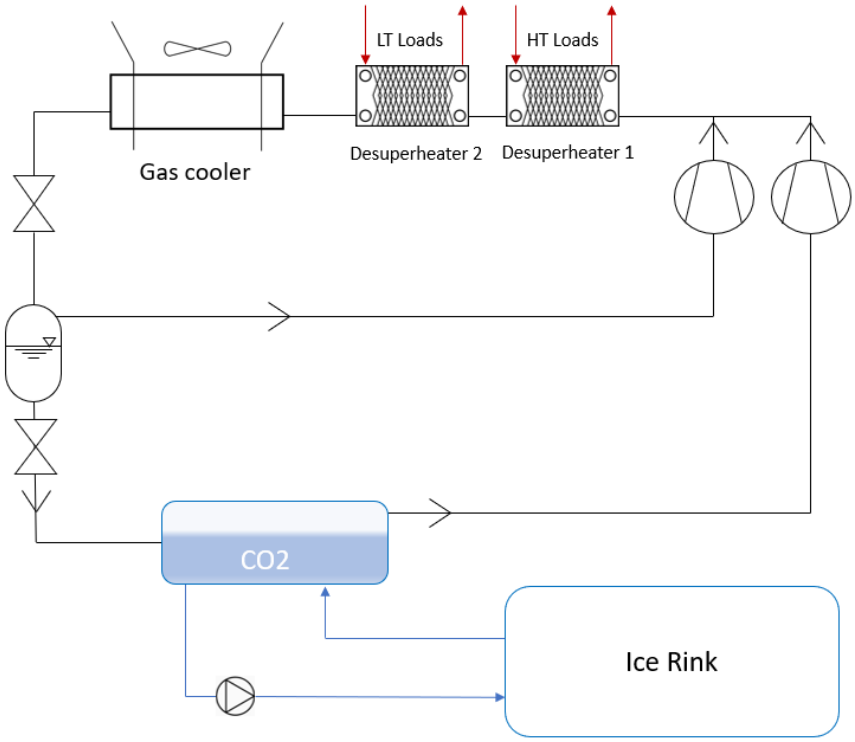

Figure 63: CO_2 State-of-the-Art system

The variable parameters for controlling the CO_2 system are the gas cooler pressure and outlet temperature. Their influence on the total COP can be observed in Figure 64. The general trend to achieve a higher system efficiency is lowering gas cooler pressure close to the critical point while still staying in trans-critical operation and lowering the gas cooler outlet temperature down to 18°C. The highest efficiency can be achieved using a gas cooler pressure of 74 bar and a gas cooler exit temperature of 18°C, which can still manage to cover all the heating demands, leading to a total COP increase of 43.4% compared to the CO_2 reference system. Operation with gas cooler exit temperatures of 16°C and 14°C can only cover the heating demands with gas cooler pressures of minimum 77 and 83 bar respectively, which explains the drop in the total COP once the gas cooler pressure drops lower due to the required use of the auxiliary heat source. The total COP increase drops for all gas cooler pressures when reaching sub-critical operating conditions which increase the approach temperature in the desuperheaters and gas cooler, and thus reduce the amount of recoverable heat. The system is set to a gas cooler pressure of 75 bar and a minimum gas cooler exit temperature of 18°C to have the highest possible efficiency and safe operating conditions, not too close to the critical point. Further, the changes in evaporation temperature and gas cooler outlet temperatures compared to the reference system affect the optimal intermediate pressure for parallel compression as well, which now shows the best performance at 40 bar.

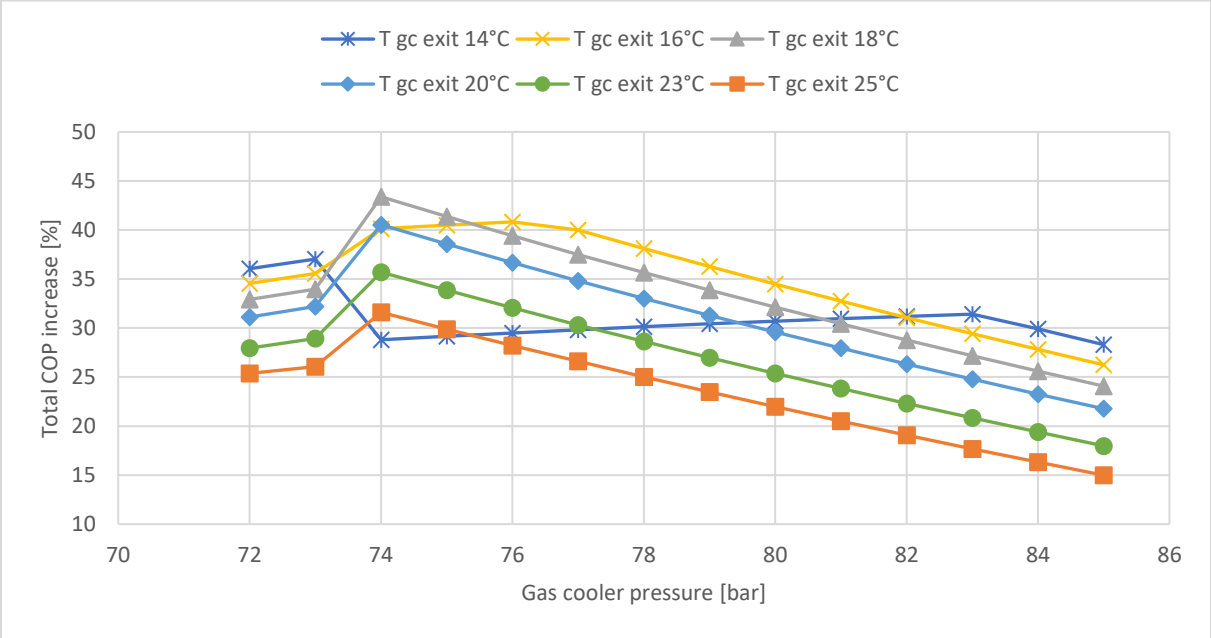

Figure 64: Total COP increase against gas cooler pressure and gas cooler exit temperature compared to reference system

The heat recovery performance for the system over one season can be found in Figure 65. The system is able to cover all demands, however, during the coldest month of December it might be useful to increase the gas cooler outlet temperature to increase the mass flow and have more recoverable heat available.

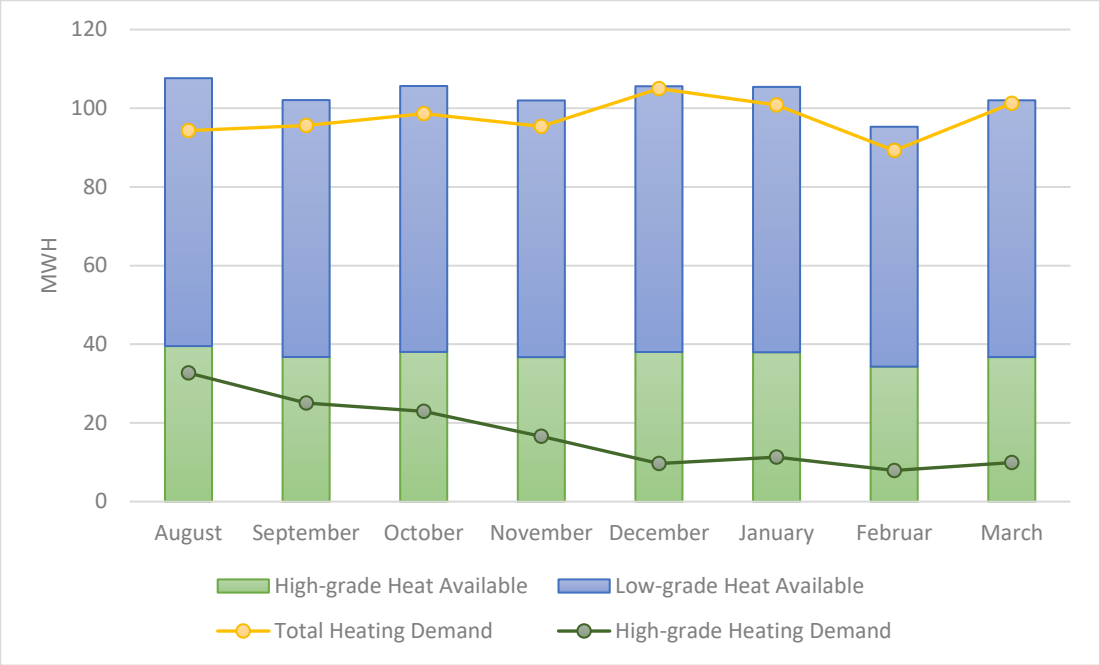

Figure 65: CO2 State-of-the-Art heat recovery performance

5.2.5.3 Propane

The final propane system is depicted in Figure 66. It is an indirect system using aqua ammonia as the secondary fluid and parallel compression to lift the pressure to the required pressure level. The heat of condensation is rejected to a coolant cycle, which is connected to the heat recovery system. Low-grade heating demands are extracted from the coolant via the HRHE, while high-grade heating demands are covered by upgraded heat from the coolant cycle through an auxiliary heat pump. Extra heat can be rejected by a dry cooler.

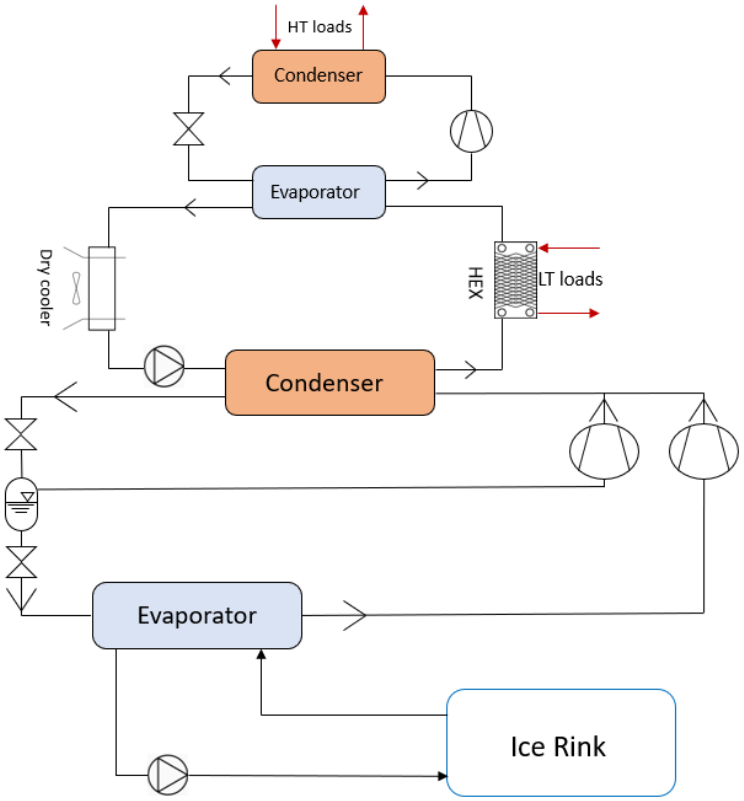

Figure 66: Propane State-of-the-Art System

The system operates at a condensing temperature of 40°C, which is required to ensure supply temperatures of 35°C for the low-grade demands. The parallel compressor uses an optimum intermediate suction pressure of 7 bar to achieve the highest efficiency. The mass flow passing through the auxiliary heat pump evaporator is controlled to match the high-grade heating demand, and additional heat is rejected via a dry cooler. The heat recovery performance is found in Figure 67. The system can cover all the heating demands without relying on an additional heat source and the auxiliary heat pump provides much operation flexibility.

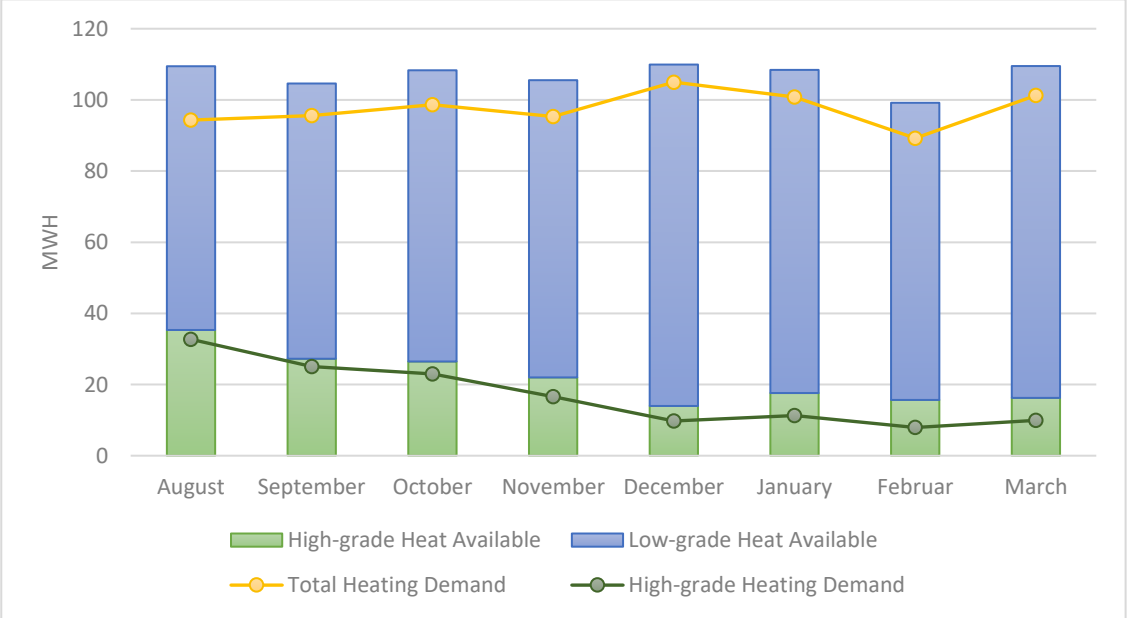

Figure 67: Propane State-of-the-Art system heat recovery performance

5.2.5.4 Comparison

Figure 68 displays the amount of annual energy that the reference systems and the final systems consume. Compared to their respective refence systems, the State-of-the-Art ammonia system requires 40 MWh of energy less annually, the CO2 system 69 MWh and the propane system 140 MWh. The high energy savings for the propane system show that the initial assumption that the reference design was not ideal is true. With a proper design the propane system even manages to consume less energy than the reference ammonia system, which theoretically makes it a viable ice rink solution. CO_2 has the lowest AEU with 195 MWh, followed by ammonia with 300 MWh and propane consumes the most amount of energy with 320 MWh.

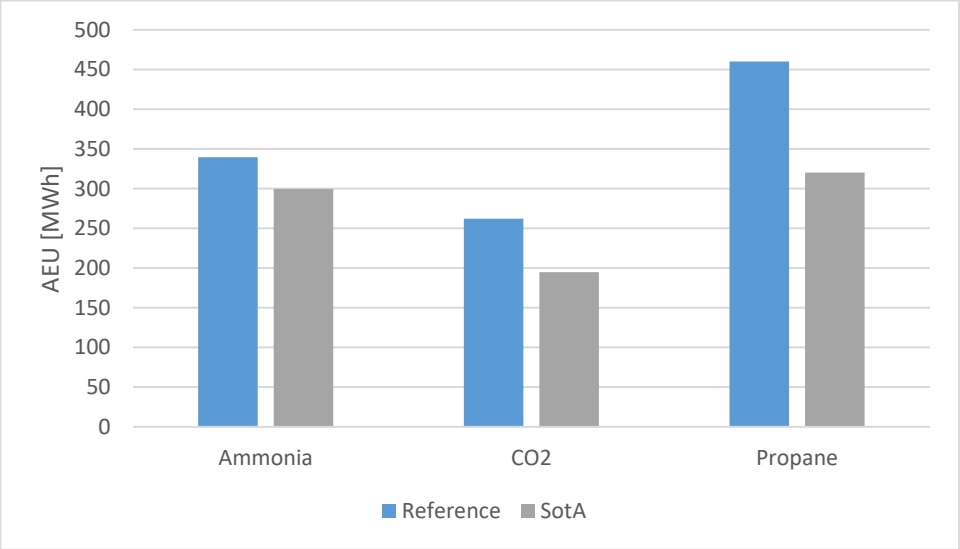

Figure 68: AEU of reference systems compared to State-of-the-Art systems

A comparison of energy consumption the state-of-the-art systems compared to the reference ammonia system is found in Figure 69. The implemented features allow the modern ammonia system to consume 12.9% less energy than the reference system. A modern CO_2 system displays outstanding energy performance and consumes 42.3% less energy than typical ammonia systems of today. A modern propane system achieves 5.7% energy savings compared to the reference ammonia system.

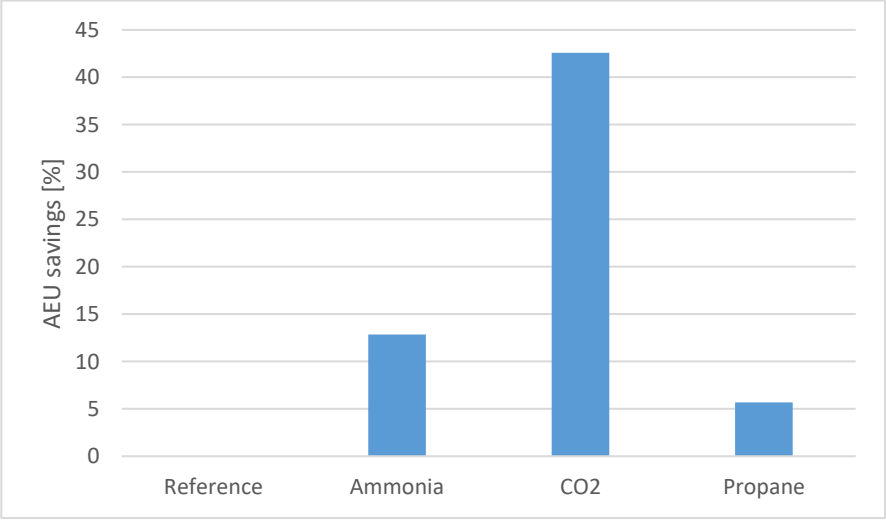

Figure 69: Energy savings of final systems compared to reference ammonia system

The SPFs of the final systems and the reference ammonia system are displayed in Figure 70. The SPFs of the reference ammonia, modern ammonia and propane system are in the range of 4.3-4.9, which is higher than well-performing heat pump systems today. By providing both heating and cooling with a single system at a high efficiency, all of the systems are worth considering. On the other hand, the CO_2 system displays an exceptional performance with an SPF of 7.5, surpassing any other method of heating/cooling and covering all the demands with the least amount of energy input.

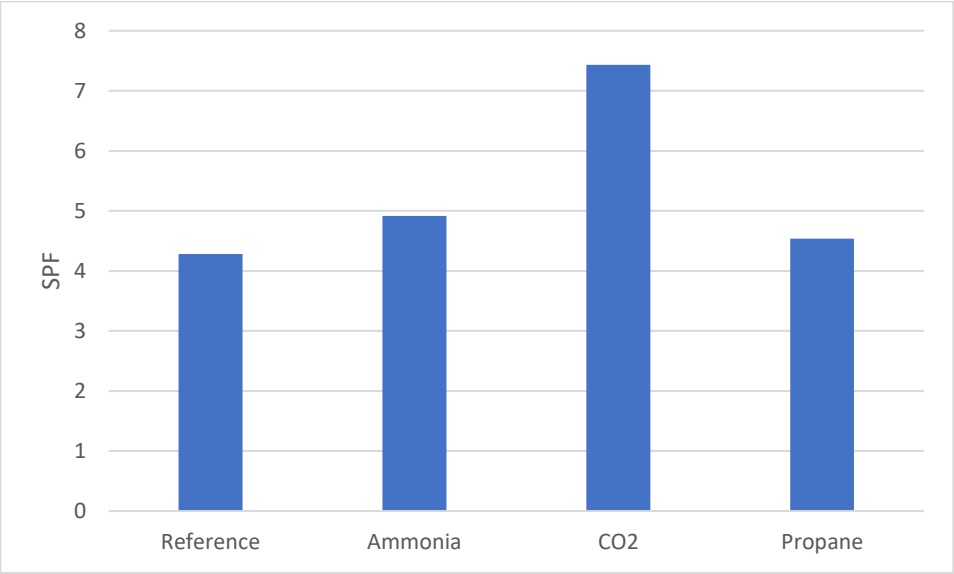

Figure 70: SPF of reference ammonia system and final systems

Lastly, the energy consumption distribution within the systems is shown in Figure 71. The auxiliary equipment in the fully indirect propane and ammonia systems, e.g. brine pumps, coolant pumps, dry coolers, etc. account for roughly 17% of the total energy consumption in both systems while the auxiliary equipment in the direct CO_2 system, i.e. the CO_2 circulation pump and gas cooler only account for roughly 2.5% of the total energy consumption. The low energy consumption for CO_2 is due to the fact that a CO_2 circulation pump requires significantly less energy than a brine pump, and the high amounts of recovered heat allow for a small gas cooler size, which reduces the gas cooler energy consumption. On the other hand, due to the constraints of operating as indirect systems, the brine and coolant parts are major energy consumers and among the main reasons why a direct CO_2 system performs better. For comparison, an indirect CO_2 system is added as well. While it also requires more auxiliary energy consumption than the direct CO_2 system due to the brine pump, the gas cooler requires less energy than the coolant pump and dry cooler of the fully indirect systems. Auxiliary equipment accounts for approximately 8% of the energy consumption in the indirect CO_2 system. Compared to operation in FC mode, all systems require less energy proportionally for auxiliaries in HR mode, which is another indicator of the increased efficiency.

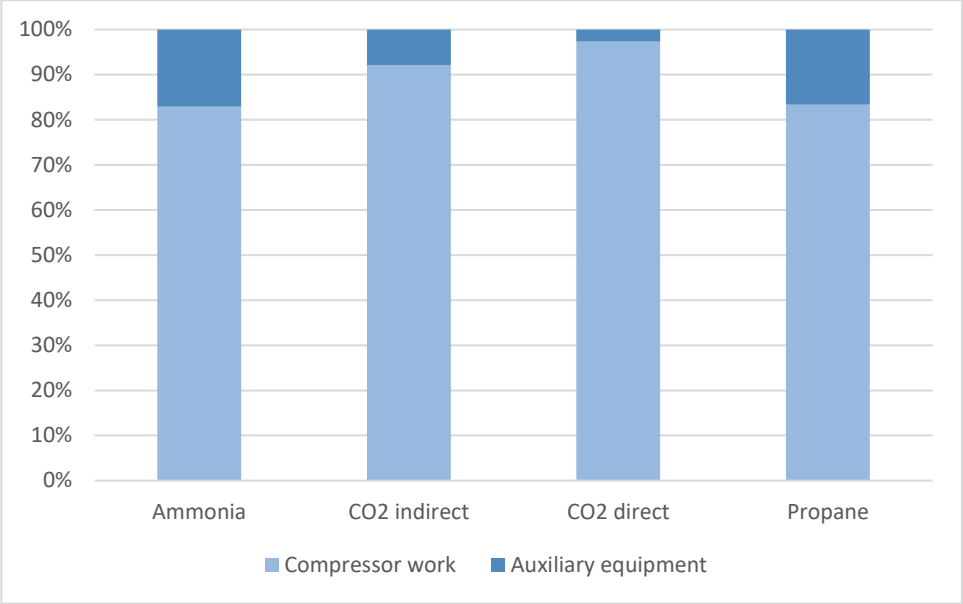

Figure 71: Energy distribution

To summarize, CO_2 is undoubtedly the most energy efficient solution for ice rinks available today. Trans-critical operation allows for great heat recovery potential, which can cover all the heating demands of the here specified reference ice rink. The possibility of being able to operate CO_2 in the form of a direct system, eliminating the need for a coolant cycle and energy intensive brine pumps, is advantageous compared to the necessary indirect operation requirements of ammonia and propane systems.

Ammonia is the second most efficient solution for ice rinks. Being the most common ice rink energy system, the reference design has difficulties covering the high-grade heating demands. A relatively easy to implement modification that can help with the high-temperature demands is the addition of an auxiliary heat pump, allowing the system to be self-sufficient by covering all the demands and lowering the condensation temperature, increasing the longevity of the equipment. Replacing the most popular secondary fluid calcium chloride with aqua ammonia is a very cost-effective and efficient measure to reduce energy consumption.

Compared to the ammonia and CO_2 systems, propane shows the lowest performance. Nonetheless, it is theoretically a feasible solution for ice rinks and able to cover all the energy demands without relying on auxiliary heating sources. The here proposed design is more efficient than the refence ammonia system and comparable to the State-of-the-Art ammonia system, however, the flammability and explosivity of propane are a still a safety concern, especially in large systems with high amounts of refrigerant charge like ice rink applications.

5.3 Economic Performance

The justified costs of each modification, calculated based on the difference in annual operation costs compared to the system without the modification over the lifetime of 20 years are seen in Figure 72 for ammonia and Figure 73 for CO_2. The IHX and LT HP modifications show negative justified costs, which means that these investments are not worth considering. The cascade CO_2 HP configuration is for reasons mentioned in the previous section also deemed not worth considering and not included

in the economic analysis. Selecting aqua ammonia as the secondary fluid is worth an investment of up to 27,100 € over the system lifetime. The real investment cost is very likely much lower than that, making it a cost-effective investment. PC is worth an investment of up to 12,700 €, however, other modifications are preferred. The LT HP + IHX configuration allows for higher justified costs (29,000 €) than the HT HP configuration (23,500 €). The reason for that is because even though the LT HP + IHX consumes slightly more energy than the HT HP configuration, a substantial amount of it comes from district heating which is cheaper than electricity. The drawbacks of the LT HP + IHX configuration, e.g. significantly higher investment costs due to a bigger heat pump size, reliance on district heating and less flexibility during operation outweigh the slightly lower annual energy expenses, which is why the HT HP configuration is selected for the final system.

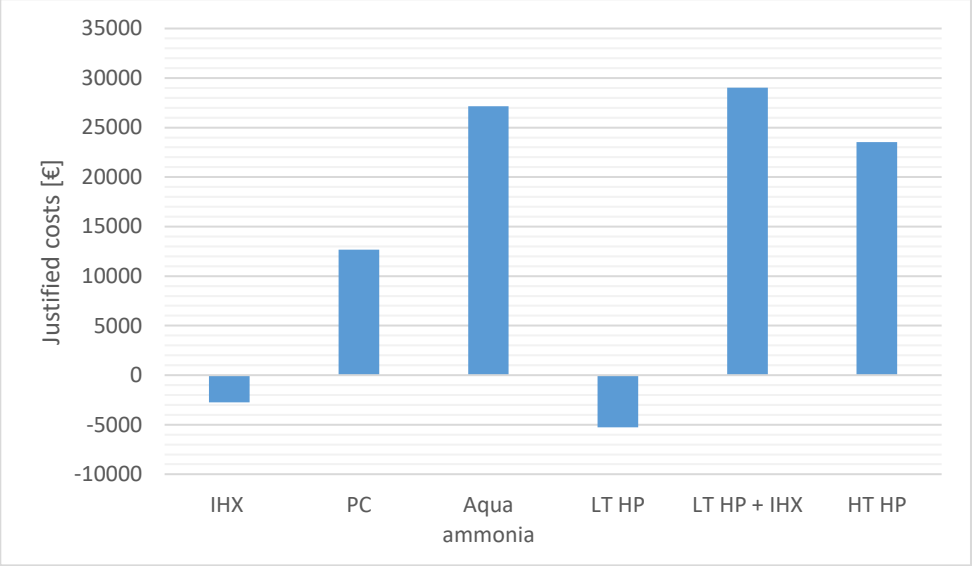

Figure 72: Justified costs for ammonia modifications

Similar to the ammonia system, the addition of an IHX/FGB+IHX worsens the performance of the CO_2 system, leading to an increase in annual energy costs and negative justified investment costs. Replacing the secondary fluid in the reference indirect system with aqua ammonia leads to the same energy savings as the replacement in the ammonia system. The most significant and cost-effective modification is switching from an indirect to a direct system, which is worth an investment of up to 101,000 € and very much justified. The justified costs of PC, SC + HR and ejectors are in the range of 33,600 € to 41,000 € for an expected lifetime of 20 years, and for the reasons mentioned in the energy performance analysis, PC will be selected for the final system.

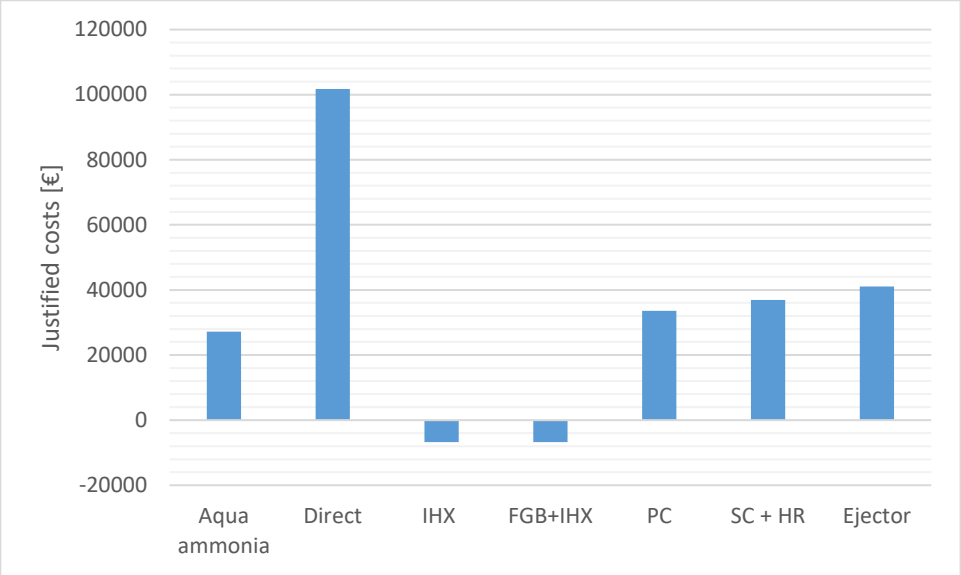

Figure 73: Justified costs for CO2 system

The annual operation costs for the final systems and the reference ammonia system operating in FC and HR mode are found in Figure 74. The reference system requires about 33,700 € annually for covering the energy demands, of which about 6% can be attributed to district heating. On the other hand, all of the state-of-the-art systems can operate self-sufficiently and do not rely on district heating. The modern ammonia system can save approximately 4,100 € on energy costs annually, the CO_2 system 14,200 € and the propane system 1,600 € compared to the reference system.

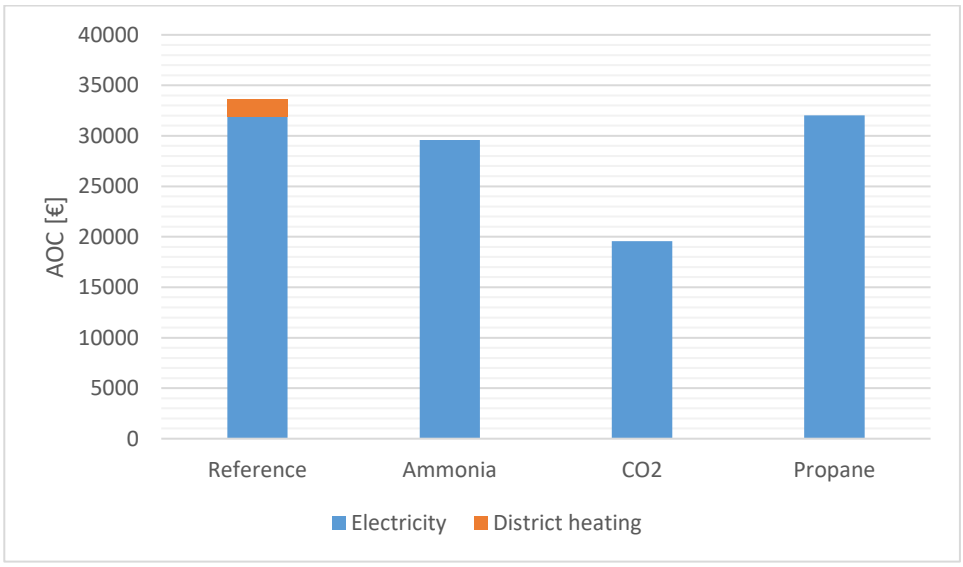

Figure 74: Annual operation costs

In conclusion, the modifications worth an investment and that can be considered as retrofit measures in ammonia ice rink systems are PC, replacing the secondary, as well as LT and HT auxiliary heat pump configurations, as long as the investment costs do not surpass the justified costs. Similarly, for CO_2, the modifications worth considering are replacing the secondary fluid, switching to a direct system, PC, SC + HR and/or ejectors, while the switch to a direct system is by far the most lucrative modification.

It must be mentioned at this point that the results are largely dependent on the selected inflation and discount rates and are accompanied by uncertainty. Further, the selected lifetime of 20 years is in the upper range of system lifespans, meaning that modifications with a lower lifetime would have lower justifiable costs.

5.4 Environmental Performance

The environmental performance of the systems in the form of CO_2-equivalent GHG emissions over the system lifetime is found in Figure 75. Since all refrigerants are natural refrigerants with GWP values of 0 (ammonia), 1 (carbon dioxide) and 3 (propane), the major contributor to CO_2 emissions is the system electricity usage and the related carbon footprint stemming from electricity generation processes. Over its lifetime, an ammonia ice rink emits approximately 266, CO_2 178 and propane 289 tCO_2-equivalent, making R744 environmentally friendliest solution thanks to its low energy consumption.

To exemplify the favorable properties of natural refrigerants with regards to their environmental impact, the TEWI of a system operating with R404A, the most common synthetic HFC refrigerant used in ice rinks is displayed as well. The same assumptions for the charge and leakage rate as for the indirect systems are used. With a GWP of 3,922, an indirect R404A system consuming the same amount of electricity as the reference ammonia system emits approximately 1,300 tons of CO_2 equivalent emissions over its lifetime, caused primarily by refrigerant leakage.

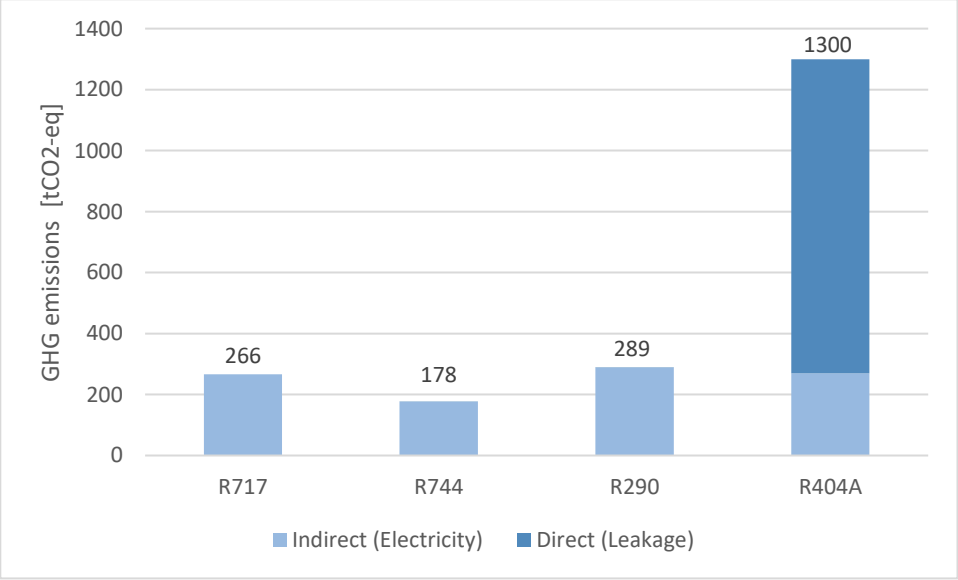

Figure 75: Lifetime TEWI comparison

6 CONCLUSION

A comparative analysis of energy systems for ice rinks using natural refrigerants has been conducted. Based on field data and literature, a reference ice rink representative for northern climates has been defined, including heating and cooling demands. Baseline energy systems for ice rinks operating with R717 and R744 as they are in use today have been modelled. Additionally, the suitability of R290 in ice rinks, which does not see any application today, has been investigated. Different state-of-the-art modifications are evaluated to find the most energy-efficient ice rink solution.

Integrated system solutions, i.e. covering both cooling and heating demands with the vapor compression system and waste heat recovery, are beneficial for all systems, both from an energetic and especially from an economic point of view.

A traditional ammonia ice rink consumes about 340 MWh of energy annually and relies on auxiliary heating sources to cover all the demands. An improved system design using aqua ammonia and an auxiliary R290 heat pump that aids in providing both high- and low-grade heating demands can lower the energy consumption down to 300 MWh, which amounts to energy cost savings of about 4,100 € annually. With an SPF 4.9, the modern integrated ammonia system is an efficient solution for ice rinks.

Trans-critical CO_2 systems in ice rinks have gained popularity over the last years for obvious reasons. A state-of-the-art direct CO_2 system using parallel compression can achieve an exceptional SPF of 7.5, consuming about 42.6% less energy than a traditional ammonia system, which corresponds to roughly 14,200 € lower energy costs annually. The drawback of using R744 as a refrigerant lies in the high operating pressure and higher investment costs, which are however most likely justified given the high energy and cost savings.

For the first time, an extensive energy analysis of propane and its suitability for ice rink applications has been conducted. A modern indirect propane system with heat recovery, parallel compression, aqua ammonia as the secondary fluid and an auxiliary heat pump to cover high-grade temperature demands is found to perform better than currently widespread ammonia ice rink energy systems, using about 5.7% less energy annually, but it is still less energy efficient than modern ammonia or CO_2 systems.

Given to the use of natural refrigerants with no-/low GWPs, the environmental impact of the systems is almost exclusively caused by indirect emissions related to their energy consumption and ranges from 178 (R744) to 289 (R290) tCO_2-equivalent emissions over their lifetime. A life cycle assessment of the systems would provide more detailed results. Additionally, a complimentary life cycle cost analysis for all systems could prove their economic feasibility and complement this energy analysis.

To conclude, CO_2 systems are the most efficient and environmentally friendly solution for ice rinks today. Existing ammonia systems can benefit from retrofits in the form of replacing the secondary fluid and adding auxiliary heat pumps to improve overall performance. There are no strong arguments that would favor a propane system over ammonia or CO_2 systems, however, it is still a feasible option.

7 FUTURE WORK

A more holistic view of ice rink energy systems could be provided by potential future works on these subjects:

- This study was limited to conditions representative for northern climates. Ambient conditions have a great influence on the performance, which is why investigations in other climates would provide useful insight in how the most efficient ice rink energy system in other climates could look like.
- This work primarily focused on the energy performance of the systems and did not go into detailed economic and environmental analyses. Life cycle cost (LCC) and life cycle assessment (LCA) investigations would complement the energy analysis of this work and provide greater detail about the costs and environmental impacts of ice rink energy systems.
- The control strategy of the systems is based on simplified assumptions. An optimized demand-based control strategy would allow for improved performance.
- An analysis regarding the potential of thermal exports to nearby facilities such as residential buildings, swimming pools, etc. could be interesting.
- Great emphasis was put into using realistic assumptions from field data and literature to increase the credibility of the results. Nevertheless, validation with real data remains the most definitive method to be certain about the outcomes. Future field measurement analyses of real systems could validate the findings of this work.

REFERENCES

[1] K. Calvin *et al.*, “IPCC, 2023: Climate Change 2023: Synthesis Report. Contribution of Working Groups I, II and III to the Sixth Assessment Report of the Intergovernmental Panel on Climate Change [Core Writing Team, H. Lee and J. Romero (eds.)]. IPCC, Geneva, Switzerland.,” Intergovernmental Panel on Climate Change (IPCC), Jul. 2023. doi: 10.59327/IPCC/AR6-9789291691647.

[2] IEA, “How Energy Efficiency Will Power Net Zero Climate Goals – Analysis - IEA,” 2021. https://www.iea.org/commentaries/how-energy-efficiency-will-power-net-zero-climate-goals (accessed Aug. 14, 2023).

[3] “Heating and cooling.” https://energy.ec.europa.eu/topics/energy-efficiency/heating-and-cooling_en (accessed Aug. 14, 2023).

[4] B. K. Sovacool, S. Griffiths, J. Kim, and M. Bazilian, “Climate change and industrial F-gases: A critical and systematic review of developments, sociotechnical systems and policy options for reducing synthetic greenhouse gas emissions,” *Renewable and Sustainable Energy Reviews*, vol. 141, p. 110759, May 2021, doi: 10.1016/j.rser.2021.110759.

[5] J. Rogstam, C. Beaini, and J. Hjert, “Stoppsladd - slutrapport fas 4,” Älvsjö, 2014.

[6] J. Rogstam, “Energy usage statistics and saving potential in ice rinks,” presented at the IIR Sustainable Refrigeration and Heat Pump Technology, Stockholm, 2010.

[7] T. Martin, “Evolution of ice rinks,” *ASHRAE JOURNAL*, vol. 46, pp. S24–S30, 2004.

[8] American Society of Heating, Refrigerating and Air-Conditioning Engineers, *ASHRAE Handbook: Refrigeration*, SI edition. Atlanta: ASHRAE, 2018.

[9] Svenska Ishockeyförbundet, “Energieffektivisering Ishaller,” Stockholm, 2023.

[10] International Ice Hockey Federation, “IIHF Ice Rink Guide,” Zurich, 2016.

[11] “Ice Rinks: Refrigeration On A Big Scale | Howden.” https://www.howden.com/en-us/articles/refrigeration/ice-rinks-refrigeration-on-a-big-scale (accessed May 20, 2023).

[12] C. Borgnakke and S. Richard E., *Fundamentals of Thermodynamics*, 8th ed. Ann Arbor, Michigan: Wiley, 2012.

[13] J. Pomerancevs, J. Rogstam, and A. Līckrastiņa, “Moisture handling mechanisms in ice rinks,” presented at the E3S Web of Conferences, 2020.

[14] J. Rogstam and W. Mazzotti, “Ice Rink Dehumidification Systems Energy Usage and Saving Measures,” presented at the 11th IEA Heat Pump Conference 2014, Montreal, 2014.

[15] J. Rogstam and J. Pomerancevs, “Comparison of refrigeration and sorption-based dehumidification in ice rinks NERIS – Part 5,” EKA - Energi & Kylanalys AB, 1916, 2019.

[16] E. Brągoszewska, A. Palmowska, and I. Biedroń, “Investigation of indoor air quality in the ventilated ice rink arena,” *Atmospheric Pollution Research*, vol. 11, no. 5, pp. 903–908, 2020, doi: https://doi.org/10.1016/j.apr.2020.02.002.

[17] M. Karampour, “Measurement and modelling of ice rink heat loads,” KTH Royal Institute of Technology, Stockholm, 2011.

[18] M. Karampour and J. Rogstam, “Measurement and Modelling of Ice Rink Heat Loads,” presented at the 10th IIR Gustav Lorentzen Conference on Natural Refrigerants, Delft, 2012.

[19] P. Makhnatch, “Technology and Energy Inventory of Ice Rinks,” KTH Royal Institute of Technology, Stockholm, 2011.

[20] S. Bolteau, J. Rogstam, and M. Tazi, “Evaluation of the Heat Recovery Performance in a CO2 Ice rink,” presented at the 12th IIR Gustav Lorentzen Natural Working Fluids Conference, Edinburgh, 2016.

[21] Å. Melinder and E. Granryd, “IIR handbook on indirect refrigeration and heat pump systems,” in *Refrigeration Science and Technology :*, KTH, Energy Technology, 2015, pp. 2240–2247. doi: 10.18462/iir.icr.2015.0892.

[22] T. Ngyuen, “Carbon dioxide in ice rink refrigeration,” Master’s Thesis, KTH, Applied Thermodynamics and Refrigeration, 2013.

[23] J. Rogstam, “Ice rinks using carbon dioxide as secondary refrigerant,” presented at the IIR Sustainable Refrigeration and Heat Pump Technology, Stockholm, 2010.

[24] B. O. Bolaji and Z. Huan, “Ozone depletion and global warming: Case for the use of natural refrigerant – a review,” *Renewable and Sustainable Energy Reviews*, vol. 18, pp. 49–54, 2013, doi: https://doi.org/10.1016/j.rser.2012.10.008.

[25] S. Sawalha, “Carbon Dioxide in Supermarket Refrigeration,” PhD Thesis, KTH, Applied Thermodynamics and Refrigeration, 2008.

[26] J. Rogstam, S. Bolteau, and C. Grönqvist, “Cooling and Heating Ice Rinks With CO2,” *ASHRAE JOURNAL*, vol. 57, pp. 48–56, 2017.

[27] G. Lorentzen, “Revival of carbon dioxide as a refrigerant,” *International Journal of Refrigeration*, vol. 17, no. 5, pp. 292–301, 1994, doi: https://doi.org/10.1016/0140-7007(94)90059-0.

[28] International Ice Hockey Federation, “IIHF Guide to Sustainable Ice Arenas,” Zurich, 2023.

[29] “General chemical and physical properties of R717 - General chemical and physical properties of R717.” https://www.bitzer.de/shared_media/html/at-640/en-GB/103563787103609611.html (accessed Aug. 15, 2023).

[30] A. Grzebielec, A. Rusowicz, and A. Szelągowski, “Safety aspects for the R290 (propane) as working medium in small air conditioning installations,” *Inżynieria Bezpieczeństwa Obiektów Antropogenicznych*, pp. 22–29, Jun. 2021, doi: 10.37105/iboa.110.

[31] J. Rogstam, A. Abdi, and S. Sawalha, “CARBON DIOXIDE IN ICE RINK REFRIGERATION,” presented at the 11th IIR Gustav Lorentzen Conference on Natural Refrigerants, Hangzhou, 2014.

[32] S. Thanasoulas, “Evaluation of CO2 Ice rink heat recovery system performance,” KTH Royal Institute of Technology, 2018.

[33] J. Pomerancevs, J. Rogstam, and A. Līckrastiņa, “Utilisation of Ice Rink Waste Heat by Aid of Heat Pumps,” in *Cold Climate HVAC 2018*, D. Johansson, H. Bagge, and Å. Wahlström, Eds., in Springer Proceedings in Energy. Cham: Springer International Publishing, 2019, pp. 453–463. doi: 10.1007/978-3-030-00662-4_38.

[34] B. Yu, J. Yang, D. Wang, J. Shi, and J. Chen, “An updated review of recent advances on modified technologies in transcritical CO2 refrigeration cycle,” *Energy*, vol. 189, p. 116147, Dec. 2019, doi: 10.1016/j.energy.2019.116147.

[35] F. Cao, Y. Wang, and Z. Ye, “Theoretical analysis of internal heat exchanger in transcritical CO2 heat pump systems and its experimental verification,” *International Journal of Refrigeration*, vol. 106, pp. 506–516, Oct. 2019, doi: 10.1016/j.ijrefrig.2019.05.022.

[36] R. Cabello, D. Sánchez, R. Llopis, A. Andreu-Nacher, and D. Calleja-Anta, “Energy impact of the Internal Heat Exchanger in a horizontal freezing cabinet. Experimental evaluation with the R404A low-GWP alternatives R454C, R455A, R468A, R290 and R1270,” *International Journal of Refrigeration*, vol. 137, pp. 22–33, May 2022, doi: 10.1016/j.ijrefrig.2022.02.007.

[37] S. Elbel and P. Hrnjak, “Flash gas bypass for improving the performance of transcritical R744 systems that use microchannel evaporators,” *International Journal of Refrigeration*, vol. 27, no. 7, pp. 724–735, Nov. 2004, doi: 10.1016/j.ijrefrig.2004.07.019.

[38] H. Tuo and P. Hrnjak, “Flash gas bypass in mobile air conditioning system with R134a,” *International Journal of Refrigeration*, vol. 35, no. 7, pp. 1869–1877, Nov. 2012, doi: 10.1016/j.ijrefrig.2012.05.013.

[39] Z. Wang, F. Han, and B. Sundén, “Parametric evaluation and performance comparison of a modified CO2 transcritical refrigeration cycle in air-conditioning applications,” *Chemical Engineering Research and Design*, vol. 131, pp. 617–625, Mar. 2018, doi: 10.1016/j.cherd.2017.08.003.

[40] A. Chesi, F. Esposito, G. Ferrara, and L. Ferrari, “Experimental analysis of R744 parallel compression cycle,” *Applied Energy*, vol. 135, pp. 274–285, Dec. 2014, doi: 10.1016/j.apenergy.2014.08.087.

[41] M. Karampour and S. Sawalha, “State-of-the-art integrated CO2 refrigeration system for supermarkets: A comparative analysis,” *International Journal of Refrigeration*, vol. 86, pp. 239–257, Feb. 2018, doi: 10.1016/j.ijrefrig.2017.11.006.

[42] E. Torrella, D. Sánchez, R. Llopis, and R. Cabello, “Energetic evaluation of an internal heat exchanger in a CO2 transcritical refrigeration plant using experimental data,” *International Journal of Refrigeration*, vol. 34, no. 1, pp. 40–49, Jan. 2011, doi: 10.1016/j.ijrefrig.2010.07.006.

[43] Danfoss, “Low pressure lift ejector system - Application Guide,” Aug. 2020. Accessed: Jun. 18, 2023. [Online]. Available: https://assets.danfoss.com/documents/90444/AB322920563002en-000103.pdf

[44] K. E. Ringstad, Y. Allouche, P. Gullo, Å. Ervik, K. Banasiak, and A. Hafner, “A detailed review on CO 2 two-phase ejector flow modeling,” *Thermal Science and Engineering Progress*, vol. 20, p. 100647, Dec. 2020, doi: 10.1016/j.tsep.2020.100647.

[45] A. Hafner, S. Försterling, and K. Banasiak, “Multi-ejector concept for R-744 supermarket refrigeration,” *International Journal of Refrigeration*, vol. 43, pp. 1–13, Jul. 2014, doi: 10.1016/j.ijrefrig.2013.10.015.

[46] S. Fehling, “CO2 Refrigeration with Integrated Ejectors: Modelling and Field Data Analysis ofTwo Ice Rinks and Two Supermarket Systems,” KTH Royal Institute of Technology, Stockholm, 2021.

[47] R. Llopis, L. Nebot-Andrés, D. Sánchez, J. Catalán-Gil, and R. Cabello, “Subcooling methods for CO2 refrigeration cycles: A review,” *International Journal of Refrigeration*, vol. 93, pp. 85–107, Sep. 2018, doi: 10.1016/j.ijrefrig.2018.06.010.

[48] R. Llopis, R. Cabello, D. Sánchez, and E. Torrella, “Energy improvements of CO 2 transcritical refrigeration cycles using dedicated mechanical subcooling,” *International Journal of Refrigeration*, vol. 55, pp. 129–141, Jul. 2015, doi: 10.1016/j.ijrefrig.2015.03.016.

[49] L. Nebot-Andrés, D. Calleja-Anta, D. Sánchez, R. Cabello, and R. Llopis, “Experimental assessment of dedicated and integrated mechanical subcooling systems vs parallel compression in

transcritical CO2 refrigeration plants," *Energy Conversion and Management*, vol. 252, p. 115051, Jan. 2022, doi: 10.1016/j.enconman.2021.115051.

[50] S. Minetto, R. Brignoli, C. Zilio, and S. Marinetti, "Experimental analysis of a new method for overfeeding multiple evaporators in refrigeration systems," *International Journal of Refrigeration*, vol. 38, pp. 1–9, Feb. 2014, doi: 10.1016/j.ijrefrig.2013.09.044.

[51] M. Ignatowicz, W. Mazzotti, J. Rogstam, K. Ab, and Å. Melinder, "SECONDARY FLUID IMPACT ON ICE RINK REFRIGERATION SYSTEM PERFORMANCE," presented at the 11th IEA Heat Pump Conference, Québec, 2014.

[52] B. Kilberg, "Aqua Ammonia as Secondary Fluid in Ice Rink Applications," KTH Royal Institute of Technology, Stockholm, 2020.

[53] "IWMAC - Kiona - Our most complete SCADA system yet." https://kiona.com/products/iwmac (accessed Jul. 01, 2023).

[54] "ClimaCheck online - ClimaCheck." https://home.climacheck.com/solutions/climacheck-online/ (accessed Jul. 09, 2023).

[55] K. Berglöf, "Methods and potential for on-site performance validation of air conditioning, refrigeration and heat pump systems," presented at the 8th IEA Heat Pump Conference, Las Vegas, NV, United States, 2005.

[56] J. Pomerancevs, "Geothermal function integration in ice rinks with CO2 refrigeration system," KTH Royal Institute of Technology, Stockholm, 2019.

[57] "Guidance on flow rates for taps, showers and baths," *Harwood and Associates*. https://www.harwoodandassociates.co.uk/faqs/guidance-on-flow-rates-for-taps-showers-and-baths/ (accessed Jul. 15, 2023).

[58] "EES: Engineering Equation Solver | F-Chart Software : Engineering Software." https://fchartsoftware.com/ees/ (accessed Jul. 20, 2023).

[59] A. Hughes and B. Drury, *Electric motors and drives: fundamentals, types and applications*. Newnes, 2019.

[60] "Statistics | Eurostat." https://ec.europa.eu/eurostat/databrowser/view/nrg_pc_205/default/table?lang=en (accessed Jul. 22, 2023).

[61] S. Thanasoulas, J. Arias, and S. Sawalha, "Investigating the heating and air conditioning provision capability of a supermarket to neighboring buildings: Field measurement analysis and economic evaluation," *Applied Thermal Engineering*, vol. 230, p. 120782, Jul. 2023, doi: 10.1016/j.applthermaleng.2023.120782.

[62] Y. Boussaa, A. Dodoo, T. Nguyen, and K. Rupar-Gadd, "Comprehensive renovation of a multi-apartment building in Sweden: techno-economic analysis with respect to different economic scenarios," *Building Research & Information*, pp. 1–16, Jul. 2023, doi: 10.1080/09613218.2023.2240442.

[63] "Sweden: power sector carbon intensity 2022 | Statista." https://www.statista.com/statistics/1290491/carbon-intensity-power-sector-sweden/ (accessed Jul. 17, 2023).

[64] IPU, "Pack Calculation Pro User's Guide," Dec. 2022. https://www.ipu.dk/wp-content/uploads/2018/09/packcalculationpro-4.pdf (accessed Aug. 12, 2023).

APPENDIX

Climate Data

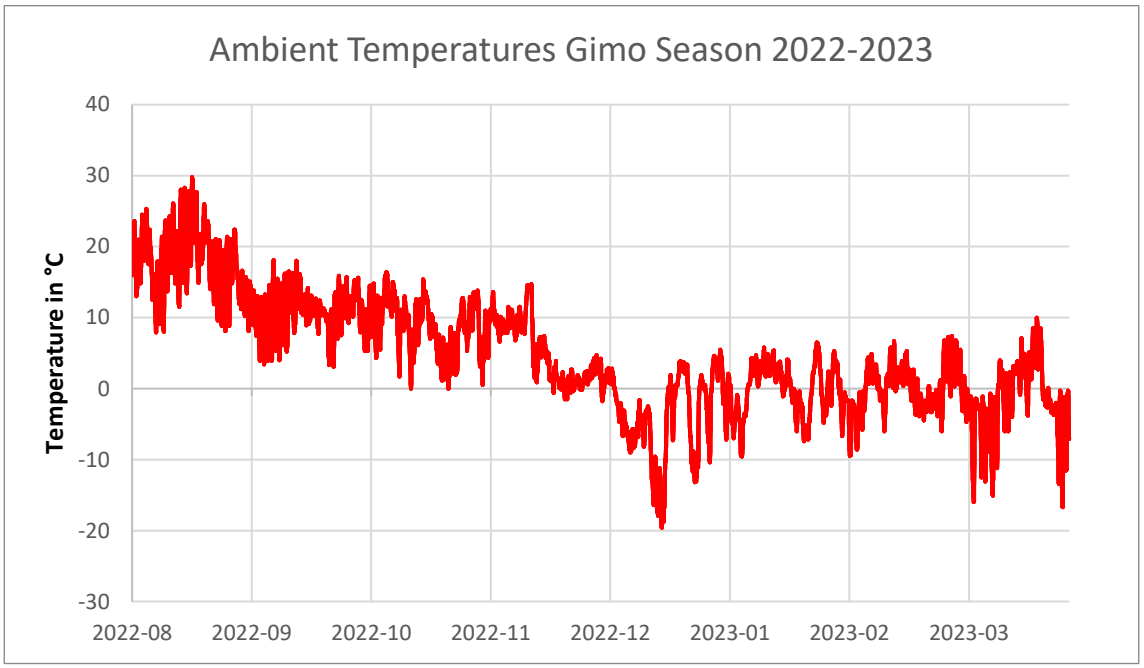

Appendix a: Ambient Temperatures

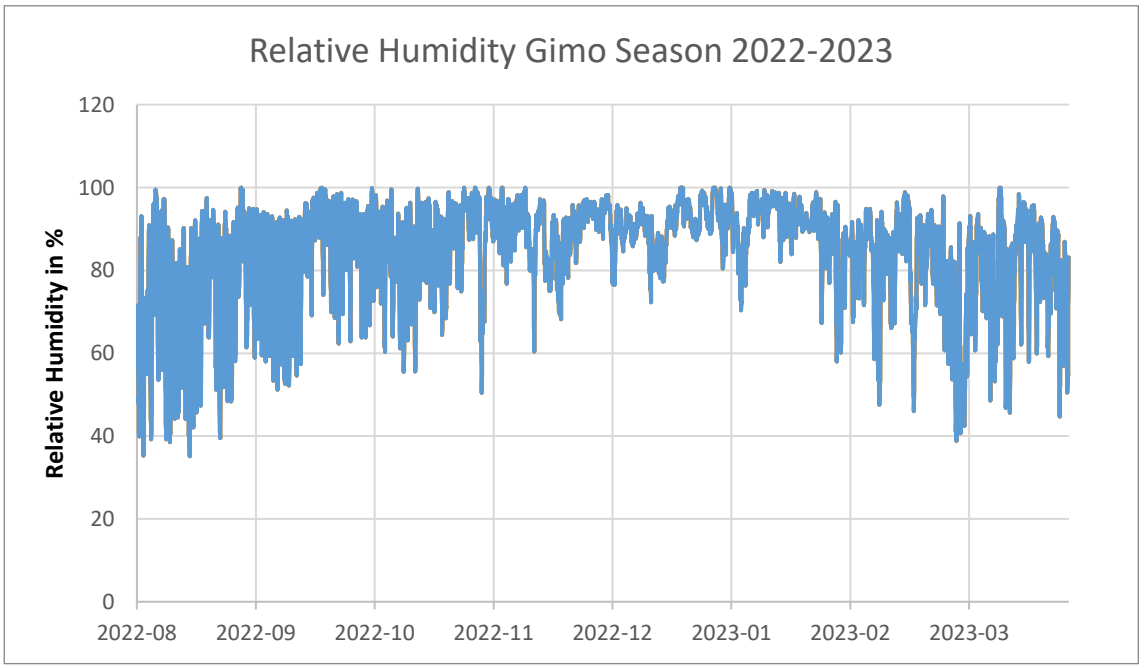

Appendix b: Relative Humidity

Compressor Efficiencies

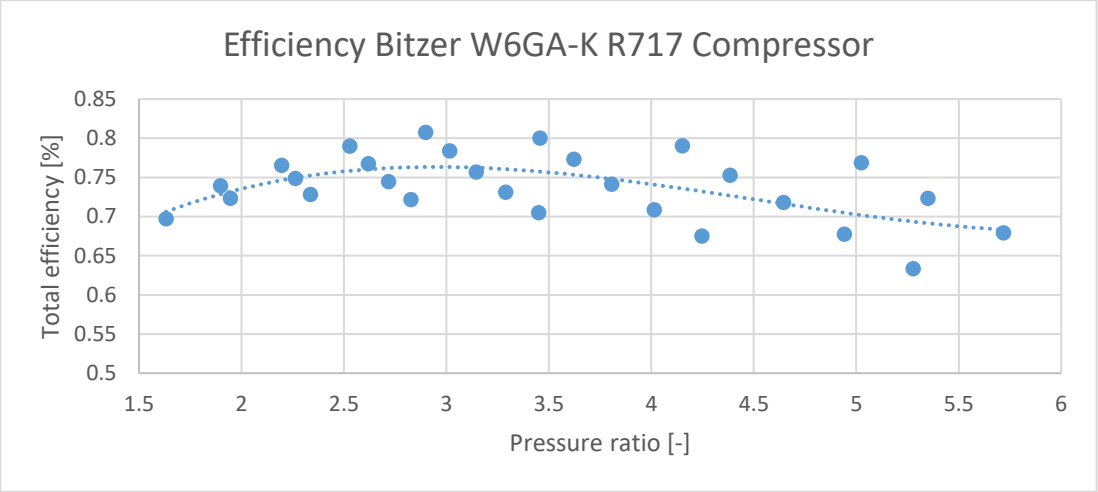

Appendix c: Ammonia Compressor Efficiency

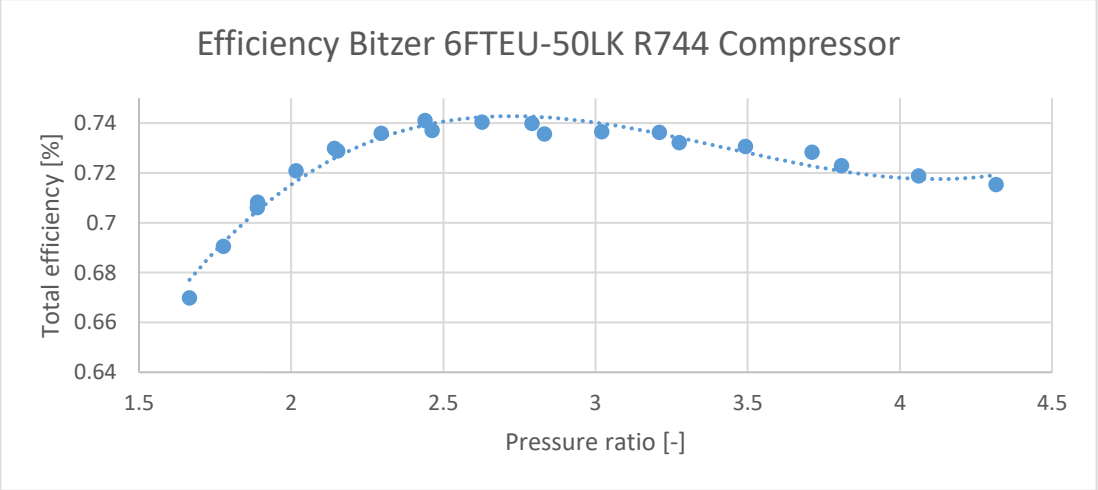

Appendix d: Carbon Dioxide Compressor Efficiency

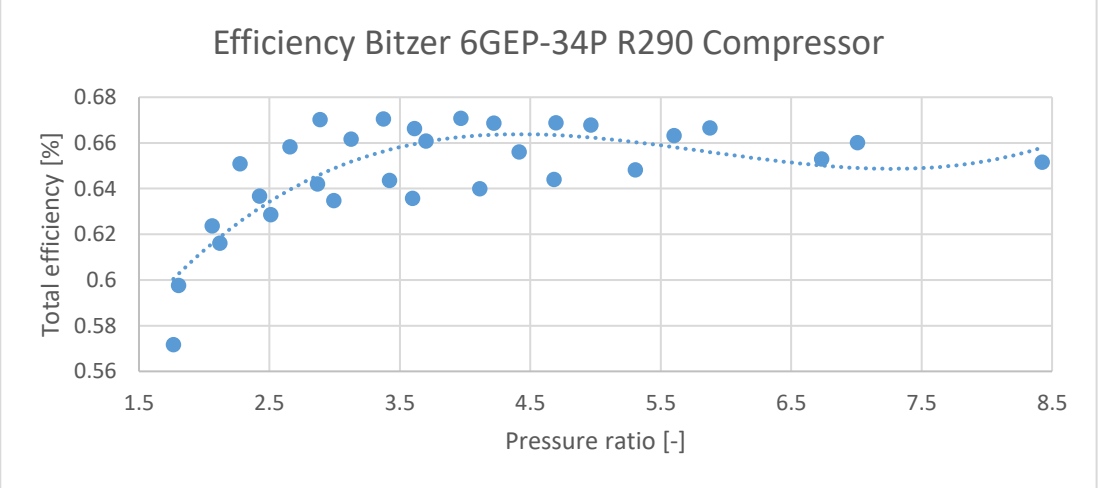

Appendix e: Propane Compressor Efficiency

Assumptions and Boundary Conditions

		Ammonia		Carbon Dioxide		Propane	
Variable	Unit	Value	Note/Source	Value	Note/Source	Value	Note/Source
Demands							
Cooling Demands	-	Cooling profile from Gimo ice rink (23.01.2023-29.01.2023)					
Heating Demands	-	See Chapter 5.1: Reference Ice Rink					
Vapor Compression Cycle							
Evaporator							
Type		Flooded, indirect		Flooded, indirect		Flooded, indirect	
Evaporation temperature	°C	-11	Field data (Järfalla ice rink)	-11	Assumed	-11	Field data (Valbo ice rink)
Internal/external superheat	K	0		0		0	
Compressor							
Model	-	Bitzer 6FTEU-50LK	https://www.bitzer.de/gb/en/reciprocating-compressors/w...a-series/	Bitzer W6GA-K	https://www.bitzer.de/gb/en/reciprocating-compressors/ecoline-1-transcritical/	Bitzer 6GEP-34P	https://www.bitzer.de/gb/en/reciprocating-compressors/ecoline-p-series/index-2.jsp
Type	-	Open-type reciprocating		Semi-hermetic reciprocating		Semi-hermetic reciprocating	
Total efficiency	%	See Appendix c	Extracted from manufacturer data	See Appendix d	Extracted from manufacturer data	See Appendix e	Extracted from manufacturer data
Motor efficiency	%	95	Permanent-magnet motor, [59]				
Efficiency at design conditions (HR)	%	68.6	Calculated	73.8	Calculated	66.3	Calculated
Compressor heat losses	%	7	[55]	7	[55]	7	[55]
Condenser/Gas cooler							
Minimum condensation temperature	°C	15	[41]	10	[41]	15	[41]
Condensation temperature HR mode	°C	40				50	
Gas cooler pressure HR mode	bar			80	Field data (Gimo ice rink)		
Subcooling	K	0		0		0	
Gas cooler approach temperature	K			3 in trans-critical region 7 in sub-critical region	[41]		
Gas cooler exit temperature HR mode	°C			20	Field data (Gimo ice rink)		
Gas cooler fan capacity	kW			2% of gas cooler capacity	[64]		
Indirect Cycle							
Heat transfer fluid	-	Calcium chloride		Calcium chloride		Calcium chloride	
Concentration	%	24		24		24	
Inlet temperature	°C	-7		-7		-7	
Outlet temperature	°C	-9		-9		-9	
Pump capacity	kW	5	Calculated	5	Calculated	5	Calculated
Coolant Cycle							
Coolant	-	Ethylene glycol				Ethylene glycol	
Concentration	%	38				38	
Temperature increase in condenser	K	5	[31]			5	[31]
Condenser approach temperature	K	2	[31]			2	[31]
Dry cooler approach temperature	K	5	[31]			5	[31]
Coolant pump capacity	kW	15% of total power (compressor, brine pump, fans)	[64]			15% of total power (compressor, brine pump, fans)	[64]
Dry cooler fan capacity	kW	3% of dry cooler capacity	[64]			3% of dry cooler capacity	[64]
Heat Recovery							
Approach temperature desuperheater	K	5		2 in trans-critical region		5	
Approach temperature HRHE	K	3				3	
High-grade supply/return temperature	°C	65/35		65/35		65/35	
Low-grade supply/return temperature	°C	35/20		35/20		35/20	

Modifications							
Internal Heat Exchanger							
Efficiency	%	30		30		30	
Parallel Compression							
Intermediate pressure	bar	7		38		9	
Secondary Fluid							
Heat transfer fluid	-	Aqua ammonia		Aqua ammonia		Aqua ammonia	
Concentration	%	13.5		13.5		13.5	
Pump capacity	kW	2.85	Calculated	2.85	Calculated	2.85	Calculated
Direct							
Heat transfer fluid	-			Carbon dioxide			
Pump capacity	kW			0.6	Field data (Gimo ice rink)		
Evaporation temperature	°C			-8	Field data (Gimo ice rink)		
Subcooling							
Type	-			Mechanical subcooling			
Refrigerant				R717			
Condensation temperature	°C			35			
Subcooling	K			15			
Ejector							
Efficiency	%			30	[46]		
Pressure lift	bar			2	[46]		
Auxiliary Heat Pump							
LT HP							
Refrigerant	-	R717					
Condensation temperature	°C	35					
HT HP							
Refrigerant	-	R290				R717	
Condensation temperature	°C	65/35				65	
Subcooling	K	25				0	
Cascade Configuration							
Refrigerant	-	R744				R744	
Gas cooler pressure	bar	80				80	
Gas cooler exit temperature	°C	20				20	
Cascade HE temperature difference	K	5				5	

Appendix f: Assumptions and Boundary Conditions